National Center for Computational Hydroscience and Engineering (NCCHE)

The University of Mississippi

Science and Technology

FEMA

DSS-WISE™ Lite

Flood Modeling and Simulation Capability Enhancements for Dam Safety

TECHNICAL REPORT

Current NCCHE Team Members:
Dr. Mohammad Al-Hamdan
Marcus McGrath
Dr. Nuttita Pophet
Paul Smith
Dr. Hazem Shatnawi

Former NCCHE Team Members:
Dr. Mustafa S. Altinakar
Dr. Vijay P. Ramalingam
Dr. Greg Easson

Electronic copy of this report can be downloaded from:
https://dsswiseweb.ncche.olemiss.edu/documentation/index.php

June 29, 2021

Acknowledgments

We gratefully acknowledge the funding from the U.S. Department of Homeland Security (USDHS) Science and Technology Directorate and the Federal Emergency Management Agency (FEMA) National Dam Safety Program, which have supported the original development of the DSS-WISE™ Lite and DSS-WISE™ Web since 2011, and its subsequent improvements and operations and maintenance.

We also acknowledge the Division of Safety of Dams (DSOD) of the California Department of Water Resources for the support and funding for the enhancements of some components of DSS-WISE Lite including modeling dams in series and levees.

We would also like to acknowledge the support and funding from Argonne National Laboratory (ANL) for the development of the Human Consequences Module (HCOM). LandScan data layers used by HCOM were provided by the ANL. LandScan USA data is developed by Oak Ridge National Laboratory (ORNL).

The authors gratefully acknowledge the permission given by the Dam Safety and Stormwater Permitting Division, S.C. Dept. of Health & Environmental Control (DHEC) and CDM Smith to use the example of Saluda Dam for the demonstration of DSS-WISE HCOM.

We would like to extend our special thanks to the following partners for their feedback and support:

- Mr. James Demby, Dr. Gokhan Inci, and Mr. Preston Wilson from the National Dam Safety Program at FEMA.
- Dr. David Alexander and Mr. Ronald Langhelm from the Science & Technology Directorate at USDHS.
- Dr. Christian Carleton from the Office of Water Programs at California State University, Sacramento.
- Mr. Kyle Pfeiffer from the National Preparedness Analytics Group, Decision and Infrastructure Sciences Division at ANL.
- Dr. Olufemi Omitaomu and Dr. Amy Rose from the Geographic Information Science and Technology Group, Computational Sciences and Engineering Division at ORNL.
- All the active users of DSS-WISE™ Lite for their valuable feedback and support.

LIST OF ABBREVIATIONS

A	Stands for Alpha channel in RGBA color system. Alpha is a number between 0 and 1 (corresponding to 0% to 100%) and defines the opacity of a pixel.
2D	Two-dimensional
2D SWE	Two-dimensional Shallow Water Equations
3D	Three-dimensional
ANL	Argonne National Laboratory of DOE https://www.anl.gov/
API	Application Programming Interface.
ASVD02	American Samoa Vertical Datum of 2002 (ASVD02) https://www.ngs.noaa.gov/datums/vertical/american-samoa-vertical-datum-2002.shtml
B	Stands for Blue color channel in RGBA color system. It can have a value from 0 to 255 corresponding to 0% to 100%.
BC	Breach Center (specified by the user for a DSS-WISE Lite simulation)
BC Hydro	Short form of BC Hydro and Power Authority, which is a Canadian electric utility in the province of British Columbia https://www.bchydro.com/index.html
BLM	Bureau of Land Management of DOI
BSCs	Breached-Structure Cells. Cells under the footprint of the breached impounding structure.
BW	Breach Width (specified by the user for a DSS-WISE Lite simulation)
CFL	Courant–Friedrichs–Lewy (CFL) condition is a necessary but insufficient condition for ensuring convergence while numerically solving hyperbolic partial differential equations using an explicit scheme. In the case of DSS-WISE Lite, it restricts the time step based on the cell size and the propagation speed of perturbations, which depends also on the flow depth.
CONUS	CONtiguous United States. It includes 48 states excluding Alaska and Hawaii. It is used as a technical term by the U.S. Department of Defense, and various federal agencies, such as NOAA.
DEM	Digital Elevation Model
DHS	Department of Homeland Security https://www.dhs.gov/
DMA	Defense Mapping Agency (folded into NIMA in 1996, which became NGA in 2003) See https://www.nga.mil/Pages/Default.aspx
DOD	Department of Defense https://www.defense.gov/
DOE	Department of Energy https://www.energy.gov/
DOI	Department of Interior https://www.doi.gov/
DOL	Department of Labor https://www.dol.gov/
d/s or D/S	Downstream
DSS-WISE	Decision Support System for Water Infrastructural Security

DSS-WISE Lite	Decision Support System for Water Infrastructural Security Lite, which is the web-based version of DSS-WISE dam-break and flood modeling tool
DSS-WISE HCOM	Decision Support System for Water Infrastructural Security Human COnsequence Module
DSS-WISE Web	Decision Support System for Water Infrastructural Security Web (https://dsswiseweb.ncche.olemiss.edu/index.php), which is the web-based system housing DSS-WISE Lite, DSS-WISE HCOM and other tools and services.
EAP	Emergency Action Plan
ESRI	Environmental Systems Research Institute https://www.esri.com/en-us/home
FEMA	Federal Emergency Management Agency, which is an agency under U.S. DHS https://www.fema.gov/
FERC	Federal Energy Regulatory Commission of DOE https://www.ferc.gov/
FIPS	Federal Information Processing Standard
FS	Forest Service of USDA https://www.fs.fed.us/
G	Stands for Green color channel in RGBA color system. It can have a value from 0 to 255 corresponding to 0% to 100%.
GDAL	Geospatial Data Abstraction Library. It is a computer software library for reading and writing raster and vector geospatial data formats. It is released under the permissive X/MIT style free software license by the Open Source Geospatial Foundation. https://www.gdal.org/
GNSS	Global Navigation Satellite System
GRACE	The Gravity Recovery and Climate Experiment. A joint mission of NASA and the German Aerospace Center for measuring Earth's gravity field anomalies. http://www2.csr.utexas.edu/grace/
GRS	Geodetic Reference System
GRS 80	Geodetic Reference System of 1980. It is a geodetic reference system which refers to a reference ellipsoid with following parameters: Semi-major axis (equatorial radius): $a = 6{,}378{,}137\ m$ Semi-minor axis (polar radius): $b = 6{,}356{,}752.314140347\ m$
GUI	Graphical User Interface
GUVD04	Guam Vertical Datum of 2004 https://www.ngs.noaa.gov/datums/vertical/guam-vertical-datum-2004.shtml
HCOM	Human COnsequence Module under DSS-WISE Web
ID	Identification Number Identification number of a feature in a shapefile
IERS	International Earth Rotation and Reference Systems Service https://www.iers.org/IERS/EN/Home/home_node.html
ITRF	International Terrestrial Reference Frame http://itrf.ensg.ign.fr/
IUGG	The International Union of Geodesy and Geophysics http://www.iugg.org/
JPL	Jet Propulsion Laboratory https://www.jpl.nasa.gov/

LBOUND	Lower bound for an interval
LSM	Life Safety Model (http://www.lifesafetymodel.net/). It was developed by BC Hydro in Canada as a dynamic model to simulate interaction of people with a flood. It is currently being operated jointly by BC Hydro and HR Wallingford (UK).
MHHW	Mean Higher High Water level
MLLW	Mean Lower Low Water level
MSHA	Mine Safety and Health Administration of DOL https://www.msha.gov/
MSL	Mean Sea Level
MTL	Mean Tide Level
NAD	North American (geodetic) Datum.
NAD 83	North American Datum of 83 is a reference datum for a latitude and longitude grid referring to GRS 80. This is the horizontal datum used for USGS DEM tiles.
NAVD 88	North American Vertical Datum of 1988. This is the vertical datum for orthometric heights (height along the local plumb line). It was established in 1991 by holding fixed the height of the primary tide gauge benchmark (surveying) referenced to the International Great Lakes Datum of 1985 local mean sea level (MSL) height value, at Rimouski, Quebec, Canada. NAVD 88 uses the Helmert orthometric height, which calculates the location of the geoid (which approximates MSL) from modeled local gravity. This is the vertical datum used for DEM tiles for CONUS and Alaska. https://www.ngs.noaa.gov/datums/vertical/north-american-vertical-datum-1988.shtml
NASA	National Aeronautics and Space Administration https://www.nasa.gov/
NCCHE	National Center for Computational Hydroscience and Engineering https://www.ncche.olemiss.edu/
NGA	National Geospatial-Intelligence Agency https://www.nga.mil/Pages/Default.aspx
NGVD 29	National Geodetic Vertical Datum of 1929 (originally Sea Level Datum of 1929)
NGS	The National Geodetic Survey under NOAA https://www.ngs.noaa.gov/
NIMA	National Imagery and Mapping Agency (became NGA in 2003) See https://www.nga.mil/Pages/Default.aspx
NLD	National Levee Database. The NLD is a congressionally authorized database that documents levees in the United States. The NLD is maintained and published by the U.S. Army Corps of Engineers (USACE). https://www.usace.army.mil/Missions/Civil-Works/Levee-Safety-Program/National-Levee-Database/
NMVD03	Northern Marianas Vertical Datum of 2003 https://www.ngs.noaa.gov/datums/vertical/northern-marianas-vertical-datum-2003.shtml
NOAA	National Oceanic and Atmospheric Administration, which is under U.S. Department of Commerce https://www.noaa.gov/

NO DATA	A special value assigned to a data field to represent, by convention, the absence of data.
NRCS	Natural Resources Conservation Service of USDA https://www.nrcs.usda.gov/wps/portal/nrcs/site/national/home/
NRMC	National Risk Management Center of DHS https://www.dhs.gov/cisa/national-risk-management-center
NWS	National Weather Service of NOAA https://www.weather.gov/
ORNL	Oak Ridge National Laboratory of DOE https://www.ornl.gov/
PAR	Population At Risk
PDB	Planning Database (PDB) provided by USCB https://www.census.gov/research/data/planning_database/
PLFZ	Potentially Lethal Flood Zone
PRVD02	Puerto Rico Vertical Datum of 2002 https://www.ngs.noaa.gov/datums/vertical/puerto-rico-vertical-datum-2002.shtml
R	Stands for Red color channel in RGBA color system. It can have a value from 0 to 255 corresponding to 0% to 100%.
RGBA	Stands for a color system with Red, Green, Blue, Alpha channels
SI	The International System of units
SWE	Shallow Water Equations. A system of partial differential equations obtained by integrating continuity equation and Navier Stokes equation over depth using certain assumptions.
TIGER	Topologically Integrated Geographic Encoding and Referencing. This is the database system through which the USCB makes geospatial census data available to the public and professionals. https://www.census.gov/geo/maps-data/data/tiger.html
UBOUND	Upper bound for an interval
UM	University of Mississippi https://olemiss.edu/
USCB	United States Census Bureau, or officially the Bureau of the Census https://www.census.gov/
US Custom.	U.S. Customary unit system
US or U.S.	United States
USA	United States of America
USACE	U.S. Army Corps of Engineers https://www.usace.army.mil/
USDS	U.S. Department of Agriculture https://www.usda.gov/
UTM	Universal Transverse Mercator projection.
VIVD09	Virgin Islands Vertical Datum of 2009 https://www.ngs.noaa.gov/datums/vertical/virgin-islands-vertical-datum-2009.shtml
VRT	VRT (Virtual Dataset) is a file type associated with GDAL. It is a mosaic of input GDAL-supported raster datasets with repositioning, and algorithms potentially applied as well as various kinds of metadata altered or added.

	https://www.gdal.org/gdal_vrttut.html
WGS 84	World Geodetic System of 1984 https://www.nga.mil/productsservices/geodesyandgeophysics/pages/worldgeodeticsystem.aspx

LIST OF SYMBOLS

Symbol	Units		Explanation
	US Custom.[1]	SI Units	
a	ft	m	Semi-major axis of the reference ellipsoid (also called spheroid)
b	ft	m	Semi-minor axis of the reference ellipsoid (also called spheroid). This is the axis about which the primary meridian (half ellipse) is revolved to generate the ellipsoid.
C	m^2/s^2 or J/kg	m^2/s^2 or J/kg	Geopotential number
c_1	-	-	The index number of the westmost column of the bounding box for the maximum inundation polygon
c_2	-	-	The index number of the eastmost column of the bounding box for the maximum inundation polygon
D	ft.	m	Flood depth (also denoted by H)
D_{max}	ft.	m	Maximum flood depth (also denoted by H_{max})
DV	ft^2/s	m^2/s	Depth times velocity magnitude. This is also called specific discharge and denoted by q.
DV_{max}	ft^2/s	m^2/s	Maximum value of depth times velocity magnitude. This is also called maximum specific discharge and denoted by q_{max}.
g	mgals	mgals	Surface gravity measurement
H_H	km	km	Helmet orthometric height
H_O	km	km	Approximate orthometric height
h , H	ft.	m	Flood depth (also denoted by D)
h_{final}	ft.	m	Final flow depth at the end of the simulation
h_{max} , H_{max}	ft.	m	Maximum flood depth (also denoted by D_{max})
i	-	-	A number identifying a computational grid cell along direction from west to east ($i = 1, \dots, M$).
j	-	-	A number identifying a computational grid cell along direction from north to south ($j = 1, \dots, N$).
M	-	-	Number of columns of the computational grid
N	-	-	Number of rows of the computational grid
q	ft^2/s	m^2/s	Magnitude of specific discharge in the horizontal plane (it is equivalent to depth times velocity magnitude by DV). For DSS-WISE Lite, the specific discharge is a vector quantity in the horizontal plane. It is denoted by $\vec{q}(u, v)$. Velocity magnitude is given by the expression $q = \sqrt{{q_x}^2 + {q_y}^2}$.
$q_x = hu$	ft^2/s	m^2/s	Component of the specific discharge (computed at the cell center) in the horizontal plane in the direction west to east.

[1] U.S. Customary Units

$q_y = hv$	ft²/s	m²/s	Component of the specific discharge (computed at the cell center) in the horizontal plane in the direction north to south.
r_1	-	-	The index number of the southernmost row of the bounding box for the maximum inundation polygon
r_2	-	-	The index number of the northernmost row of the bounding box for the maximum inundation polygon
q_{max}	ft²/s	m²/s	Maximum value of specific discharge magnitude. This is also called maximum value of the product of depth and velocity and denoted by DV_{max}.
u	ft/s	m/s	Component of the flow velocity (computed at the cell center) in the horizontal plane in the direction west to east.
t	s	s	Current time ($t = t_{old} + \Delta t$)
t_{old}	s	s	Previous time
T_{arr}	hrs	hrs	Flood arrival time
T_{end}	hrs	hrs	Time at the end of the simulation
$TBIG$	hrs	hrs	A large time value (greater than 1,440 hours) that is used to initialize the array for T_{arr}.
Tq_{arr}	hrs	hrs	Arrival time of q_{max} (or DV_{max})
v	ft/s	m/s	Component of the flow velocity (computed at the cell center) in the horizontal plane in the direction north to south.
V	ft/s	m/s	Flow velocity magnitude. For DSS-WISE Lite, the flow velocity is a vector quantity in the horizontal plane. It is denoted by $\vec{V}(u, v)$. Velocity magnitude is given by the expression $V = \sqrt{u^2 + v^2}$.
V_{max}	ft/s	m/s	Maximum flow velocity magnitude.
x	ft	m	Horizontal distance along west to east direction measured based on a specified projection. DSS-WISE Lite results are provided based on UTM projection.
y	ft	m	Horizontal distance along north to south direction measured based on a specified projection. DSS-WISE Lite results are provided based on UTM projection.
Z	ft	m	Elevation from a vertical datum with respect to a geoid. In DSS-WISE Lite, the default vertical datum is NAVD 88, which measures elevations with respect to GRS80 geoid. The units will be written as ft. NAVD 88 or m NAVD 88.
Z_b	ft	m	Elevation from a vertical datum with respect to a geoid. In DSS-WISE Lite, the default vertical datum is NAVD 88, which measures elevations with respect to GRS80 geoid. The units are ft. NAVD 88 or m NAVD 88.
Z_w	ft	m	Elevation from a vertical datum with respect to a geoid. In DSS-WISE Lite, the default vertical datum is NAVD 88, which measures elevations with respect to GRS80 geoid. The units are ft. NAVD 88 or m NAVD 88.

Δt	s	s	Time step
Δx	ft.	m	Computational grid spacing in x-direction
Δx	ft.	m	Computational grid spacing in y-direction

Table of Contents

Chapter 1 INTRODUCTION

DSS-WISE™ HCOM module a companion analytical module for the web-based, automated dam-break flood modeling and mapping tool DSS-WISE™ Lite. Both modules are part of the DSS-WISE™ Web system, which is a secure web portal including a map server and a user interface, and provides access to these analytical modules. DSS-WISE Lite provides web-based, automated, two dimensional (2D) dam-break flood modeling and mapping capability. DSS-WISE HCOM module relies on the results of the two-dimensional dam-break flood simulation provided by DSS-WISE Lite to create flood hazard maps and potentially lethal flood zones (PLFZ) for humans and to extract and analyze Population at Risk (PAR) numbers by interfacing population data with the flood simulation results.

National Center for Computational Hydroscience and Engineering (NCCHE), the University of Mississippi developed the DSS-WISE Lite and DSS-WISE Web with funding from FEMA through a five-year, sole source contract extending from the beginning of October 2015 to the end of September 2020. Since its release in November 8, 2016, DSS-WISE Lite has encountered great access. The system is handling on average 30-40 simulations per day submitted by more than 700 active users. The users are from FEMA and its regional offices, from state dam safety offices, local governments, and numerous federal agencies (FEMA-HQ, DHS-NRMC, USDA-NRCS, USDA-FS, NOAA-NWS, DOD-USACE, DOE-FERC, DOE-ANL, DOE-ORNL, DOI-BLM, DOL-MSHA).

In response to the needs expressed by the user community, FEMA and Argonne National Laboratory have decided to jointly support the development of a companion post-processing module for DSS-WISE Lite to evaluate the consequences of the floods resulting from the operation and/or failure of dams and levees. This new module is designed to assist dam safety engineers, emergency response planners, communities and private dam owners to establish emergency action plans (EAP) and flood risk maps, and to make informed decisions towards improving the safety and security of dams and levees and mitigating the consequences of floods resulting from their operation and/or failure. NCCHE received the funding for development of this new module, called HCOM (Human COnsequences Module), through a contract with ANL beginning in October 2017.

DSS-WISE HCOM module was also developed by NCCHE. Following a beta-testing period by the development team, it was officially released on January 24, 2019, under DSS-WISE Web. DSS-WISE HCOM analysis can be launched for all successful DSS-WISE Lite simulations launched on or after January 21, 2014.

Implementation of DSS-WISE HCOM required a redesign of the Status and Results page to add the features that would allow the user to launch DSS-WISE HCOM module following the termination of a DSS-WISE Lite simulation, to monitor to monitor the progress of the analysis and to view the highlights of the results. DSS-WISE HCOM uses some of the results generated by DSS-WISE Lite simulation and the population data to generate various types of results files, which include a PDF report of the results of HCOM, a Microsoft Excel file containing various tabular data, results and plots, and a series of geospatial results files in the form of ESRI shapefiles of polygon type.

In order to understand and efficiently use the results generated by HCOM module, the user needs to understand the methods and assumptions used in generating the output files. The present technical report first reviews the results file generated by DSS-WISE Lite simulations and provides detailed information on how HCOM uses these computed results of flood simulation and the population data from different sources to generate flood hazard maps and PLFZs for humans, evolution of inundation

areas by hazard classes, and analysis of PAR numbers. The manual gives detailed information on methodologies, structures of the results files, and briefly discusses how the results can be interpreted and used.

The Chapter 2 of the present technical manual introduces basic definitions and concepts of GIS data layers used by DSS-WISE Lite and DSS-WISE HCOM.

Chapter 2 UNDERSTANDING GEOSPATIAL DATA LAYERS

DSS-WISE Lite and DSS-WISE HCOM use and produce geospatial data layers in geographical coordinates or in projected coordinates. Understanding the material presented in this technical manual requires at least a basic understanding of the terminology and principles needed in creating and using geospatial data. This chapter briefly introduces some of the basic concepts and definitions.

2.1 Shape of the Earth and its Mathematical Representation

The earth is not a perfect sphere. It can be considered as a sphere flattened at the poles. The diameter in the equatorial plane is longer than the diameter along the axis of rotation, which can be approximately assumed as the line passing through north and south poles.

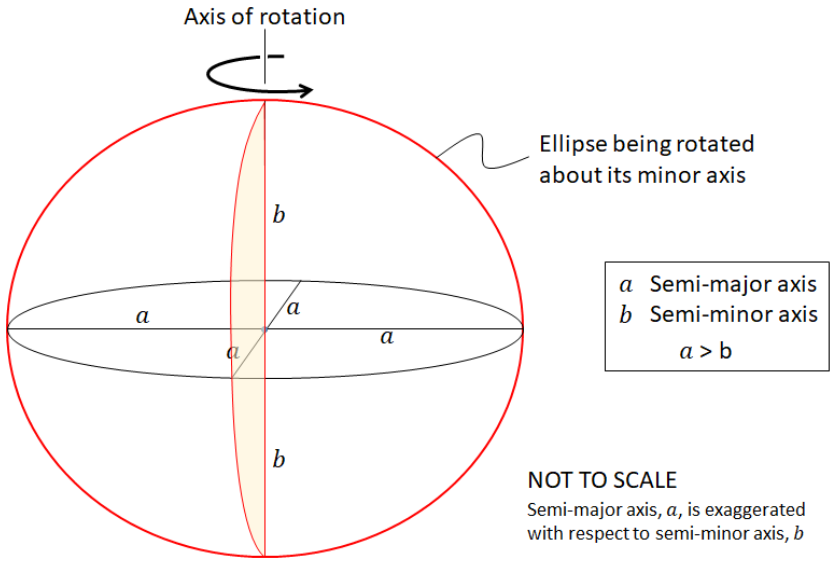

Figure 1 Oblate spheroid obtained by rotation of an ellipse about its minor axis.

In geodesy[2], the shape of the earth is mathematically approximated as an oblate ellipsoid (or oblate spheroid), which is the three dimensional shape obtained by rotating an ellipse about its minor axis as shown in Figure 1. The ellipsoid represents a defined smooth reference surface, which can be expressed mathematically. It is important to mention two important facts about the ellipsoid:

- The reference ellipsoid is a mathematical approximation of the shape of the Earth. It does not represent the real topography of the surface of the Earth. The real points on the surface of the Earth are located below or above this reference surface.
- The plumb line is not everywhere perpendicular to the surface of the ellipsoid. Thus, the reference ellipsoid does not represent the mean sea level.

[2] According to the definition given by NOAA, geodesy is the science of accurately measuring and understanding three fundamental properties of the Earth: its geometric shape, its orientation in space, and its gravity field — as well as the changes of these properties with time

A number of ellipsoids have been developed by geodesists since the 19th century. There were several national ellipsoids specifically developed for use in different countries. Earlier ellipsoids were developed based on high-precision surveys carried out on the surface of the Earth. With the help of satellites, it became possible to develop precise geocentric ellipsoids (centered at the center of the Earth) based on highly-precise measurements of the shape and mass of the Earth.

In this technical manual, we will refer to two ellipsoids:

- The GRS 80 (Geodetic Reference System of 1980), which was approved and adopted by the IUGG (International Union of Geodesy and Geophysics) at its 1979 annual meeting in Canberra, Australia.
- The WGS 84 (World Geodetic System of (1984) developed by NGA (aka NIMA aka DMA).

The reference ellipsoids are defined based on a set of four defining parameters and constants that define the approximated shape and size of the Earth, and its gravitational and electromagnetic fields:

- Defining parameters of GRS 80 ellipsoid are
    - the semi-major radius denoted by a,
    - the geocentric gravitational constant of the earth (including the mass of atmosphere) denoted by GM,
    - Dynamical form factor of the earth denoted by J_2, and
    - the angular velocity of the Earth, ω.
- Defining parameters of WGS 84 ellipsoid are
    - the semi-major radius denoted by a,
    - reciprocal (inverse) flattening of the earth denoted by f^{-1} (or $1/f$),
    - the geocentric gravitational constant of the earth (including the mass of atmosphere) denoted by GM, and
    - the angular velocity of the Earth, ω.

The values of the defining parameters and some of the derived parameters for the GRS 80 and WGS 84 reference ellipsoids are listed in Table 1. It is important to note that the values of the derived parameters in Table 1 have been rounded off.

In addition to the shape of the ellipsoid, which is defined mathematically, one should also define the location of the center of the ellipsoid with respect to the center of the Earth, which is defined as the center of mass of the Earth. WGS 84 is a truly geocentric ellipsoid and uses the ITRF (International Terrestrial Reference System) origin, whose position changes with time following the movement of the motion of the Earth's crust as the tectonic plates move with respect to one another. Referring to Figure 2, currently, there is an offset of 2.24 m between the origin of GRS 80 and the ITRF origin (center of mass of the Earth) used by WGS 84.

As it clearly stands out from the choice of the defining parameters, the reference ellipsoid should not be regarded as a simple geometric model of the Earth. The list of defining parameters for GRS 80 and WGS 84 ellipsoid listed above shows that only the semi-major radius is a geometrical parameter. The semi-minor axis is a derived parameter calculated using the flattening, f, or the first eccentricity, e, which in turn are defined based on the other defining parameters that take into account the gravitational field of the Earth.

Another important point to keep in mind is that the ellipsoid shape in Figure 1 is not to scale. For the purposes of illustration, the ellipsoid is deformed by making the semi-minor axis significantly shorter

than the semi-major axis. In reality, the difference between the axes is only 21,384.69 m (=$a - b$). This difference is very small compared to the $a = 6378137$ m, leading to a flattening of $f = a/(a - b) = 298.2572215$. This means that the difference between semi-major and semi-minor axes is about 1 in 300 and the true shape of the ellipsoid is very close to a circle. As seen in Figure 3, the scale plot the GRS 80 ellipsoid is very close to circle.

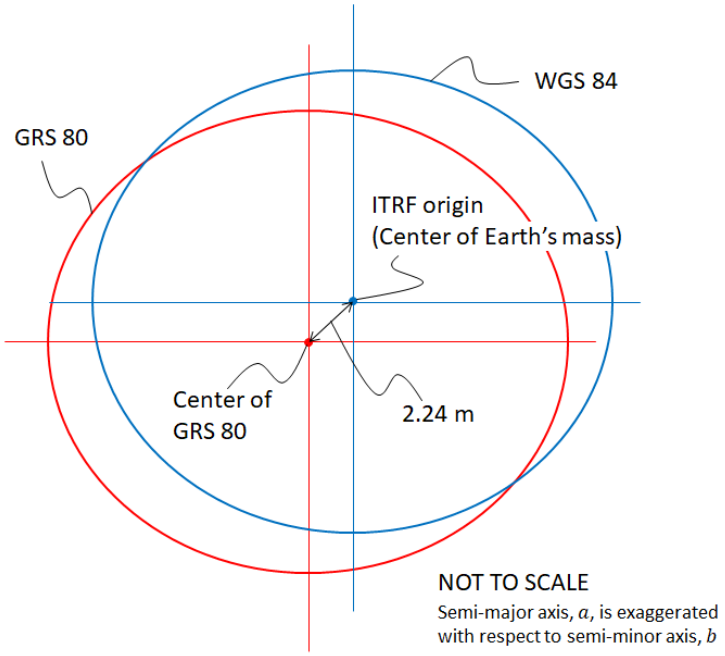

Figure 2 Offset between the centers of GRS 80 and WGS 84.

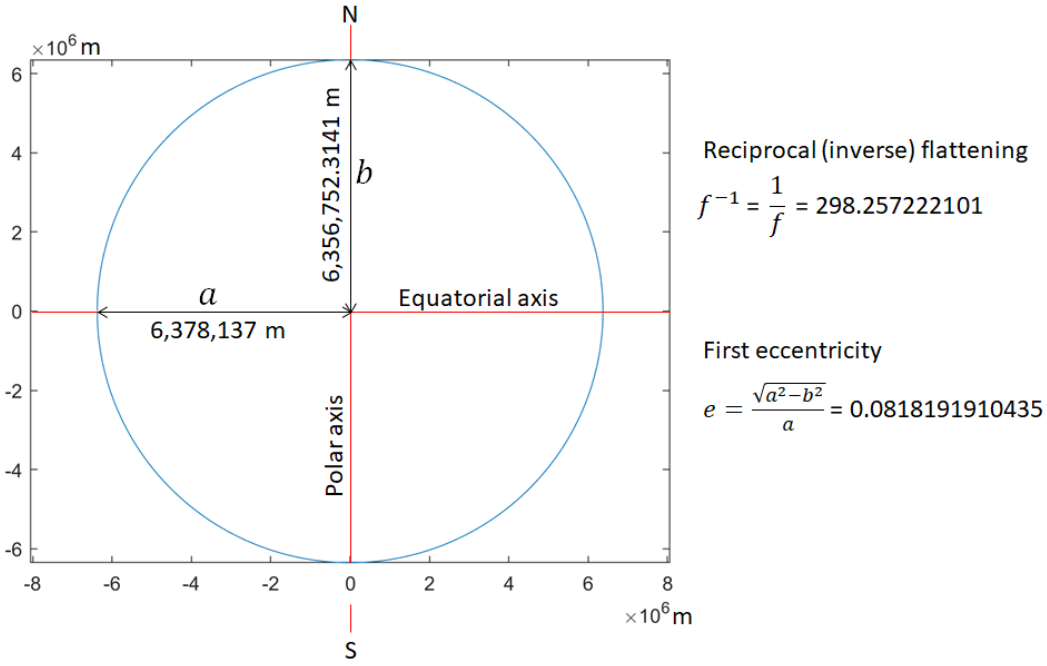

Figure 3 GRS 80 ellipsoid plotted to the scale.

Table 1 Parameters of the reference ellipsoids GRS 80 () and WGS 84 (NIMA 1997, Moritz 1980).

Symbol	Name	Formula and/or Explanation	Numerical Value*	
			GRS 80	WGS 84
a	Semi-major axis/radius (equatorial axis/radius)	Longer axis of the ellipse rotated about its shorter axis	6,378,137.0 m	6,378,137.0 m
GM	Geocentric gravitational constant of the Earth (including the mass of atmosphere)	Product of the Newtonian gravitational constant, G, and the total mass of the earth and the atmosphere, M_a	3,986,005×10^8 m^3/s^2	3,986,005×10^8 m^3/s^2
J_2	Dynamical form factor of the Earth	$J_2 = \frac{C - A}{M\ a^2}$ C and A are the polar and equatorial principal moments of inertia of the level ellipsoid, respectively	108,263×10^{-8}	108,187.4×10^{-8}
$\bar{C}_{2,0}$	Second degree (zero order) zonal harmonic coefficient of the geopotential	$\bar{C}_{2,0} = \frac{I_{zz} - I_{xx}}{M\ a^2}$ I_{zz} and I_{xx} moments of inertia of the Earth		-484.16685×10^{-6}
ω	Angular velocity of the earth	Calculated from astronomical and geophysical data	7,292,115×10^{-11} rad/s	7,292,115×10^{-11} rad/s
b	Semi-minor axis/radius (polar axis/radius)	$b = a\sqrt{1 - e^2}$ $b = a(1 - f)$	6,356,752.3141 m	6356752.3142 m
R_1	Mean radius (arithmetic mean)	$R_1 = \frac{(2a + b)}{3}$ $R_1 = a\left(1 - \frac{f}{3}\right)$	6,371,008.7714 m	6,371,008.7714 m
R_2	Radius of a sphere of the same surface	Eq. (23) or Eq. (25)	6,371,008.1810 m	6,371,007.1809 m
R_3	Radius of a sphere of the same volume	$R_3 = \sqrt[3]{a^2 b}$	6,371,000.7900	6,371,000.7900 m
E	Linear eccentricity	$E = \sqrt{a^2 - b^2}$	521,854.0097 m	521,854.00842339 m
c	Polar radius of curvature	$c = a^2/b$	6,399,593.6259 m	6,399,593.6258 m
Q	Meridian quadrant		10,001,965.7793 m	10,001,965.7793 m

f	Flattening	$f = \frac{(a-b)}{a}$	0.00335281068118	0.0033528106647
f^{-1}	Reciprocal (inverse) flattening	$f^{-1} = 1/f$	298.257222101	298.257223563
e	First eccentricity	$e = \frac{\sqrt{a^2 - b^2}}{a}$	0.0818191910435	0.0818191908426215
e'^2	Second eccentricity squared	$e'^2 = \frac{(a^2 - b^2)}{b^2}$ $e'^2 = \frac{e}{\sqrt{1 - e^2}}$	0.00673949677548	0.00673949674228

(*) Lines highlighted in grey have the same numerical value of the parameter for GRS 80 and WGS 84 reference ellipsoids.

GRS 80 ellipsoid is used by NAD 83 whereas WGS 84 ellipsoid is used by the Global Navigation Satellite System (GNSS). In fact, popular applications such as Google Maps, Google Earth, and Microsoft Visual Earth use a Mercator projection based on WGS 84 datum, which is developed for the entire world, rather than just the USA and Canada. Although, the ellipsoids GRS 80 and WGS 84 are almost the same, NAD 83 and WGS 84 coordinates are different due to different locations of the datum origins and due to reliance on surveyed data. The differences may be one meter or more. This explains small differences when DSS-WISE Lite results plotted using UTM based on NAD 83 are superposed on Google Earth images (Burkholder 2017).

2.2 Horizontal Datum and Geodetic Coordinate System

A horizontal datum is a geographic or geodetic coordinate system which is established to locate points of the Earth on the reference ellipsoid and to measure distances and directions on the surface of the Earth.

Since the ellipse is rotated about the rotation axis connecting north and south poles, the plane of the equator is a perfect circle. The so-called geodetic (or geographic) coordinate system defines any point on the surface of the earth with three components $P(\phi, \lambda, Z)$, where ϕ is the geodetic latitude, λ is the longitude and Z is the height with respect to a vertical reference datum.

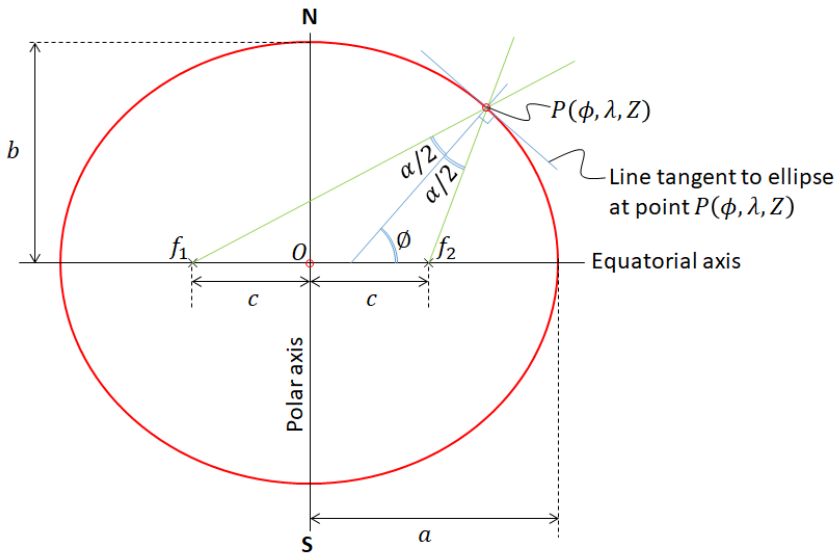

Figure 4 Definition of geodetic latitude on the reference ellipsoid.

Let us first define the geodetic latitude[3], ϕ, by referring to Figure 4. The reference ellipsoid has two generating focal points which are marked as f_1 and f_2. These focal points are located at a distance of

[3] In addition to the geodetic latitude there are six auxiliary latitude, which are useful for different purposes in geodesy: 1) geocentric latitude, 2) parametric (or reduced Latitude), 3) rectifying latitude, 4) authalic latitude, 5) conformal latitude, and 6) isometric latitude. The discussion of auxiliary latitudes are beyond the scope of their technical manual. However, we will be defining and using authalic latitude when discussing the use of LandScan gridded nighttime and daytime population data.

$c = \sqrt{a^2 - b^2}$ from the center of the ellipsoid O. The two green lines join the point $P(\phi, \lambda, Z)$ to the focal points f_1 and f_2. The blue line is the bissectrice of the angle formed by the two green lines at point $P(\phi, \lambda, Z)$. The bissectrice is perpendicular to the ellipse at point $P(\phi, \lambda, Z)$; thus, it is also perpendicular to the line tangent to the ellipse at point $P(\phi, \lambda, Z)$. The angle formed by the bissectrice and the equatorial plane is called geodetic latitude. The collection of points on the surface of the ellipsoid having the same latitude form a circle parallel to the Equator as shown in Figure 5. Thus, the lines joining the points of equal geodetic latitude are called "parallels".

The equatorial plane, which is a perfect circle. The equator serves as a natural origin for the latitude and is assigned as the zero latitude $\lambda = 0°$. In the direction of north, the value of geodetic latitude varies from $\lambda = 0°$ at the equator to $\lambda = +90°$ at the North Pole. In the direction of south, the value of geodetic latitude varies from $\lambda = 0°$ at the equator to $\lambda = -90°$ at the South Pole. It is also possible to denote the latitudes by the qualifier N and S. For example the latitude $\lambda = +40°$ can be written as $\lambda = 40°\text{N}$ and $\lambda = -40°$ can be written as $\lambda = 40°\text{S}$.

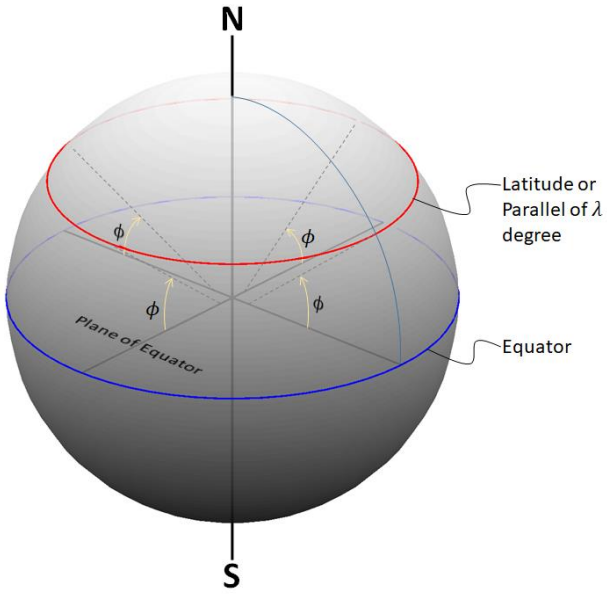

Figure 5 A parallel is a collection of points on the ellipsoid having the same geodetic latitude.

Longitudes, also called meridians, are imaginary lines on the surface of the reference ellipsoid. They run from North Pole to South Pole and intersect the equator at a right angle. In Figure 6, the longitudes are shown as red lines. The longitudes do not have a natural origin. In order to create a coordinate system, one longitude line is chosen by convention to be the prime longitude, or prime meridian. The prime longitude is the zero longitude, $\lambda = 0°$. In Figure 6, the prime longitude is highlighted in green. All other longitudes are referred by the central angle in the equatorial plane with respect to the zero longitude as shown in Figure 6. It should be noted that all longitudes converge at the poles.

As mentioned before, the latitudes are measured in degrees to the north and to the south. Similarly, the longitudes are measured in degrees of longitude to the east and west of the prime longitude/meridian, which serves as zero longitude/meridian. In either direction, the numerical value of the meridian varies from 0° to 180°. To the east of the prime longitude, the longitude varies from $\phi = 0°$ at the prime

longitude to $\phi = +180°\text{E}$ at the anti-longitude (or anti-meridian), which is exactly opposite of the prime longitude. To the west of the prime longitude, the longitude varies from $\phi = 0°$ at the prime longitude to $\phi = +180°\text{W}$ at the anti-longitude (or anti-meridian), which exactly is opposite of the prime longitude. Thus, $\phi = +180°\text{E}$ and $\phi = +180°\text{W}$ correspond to the same meridian, which is the anti-meridian.

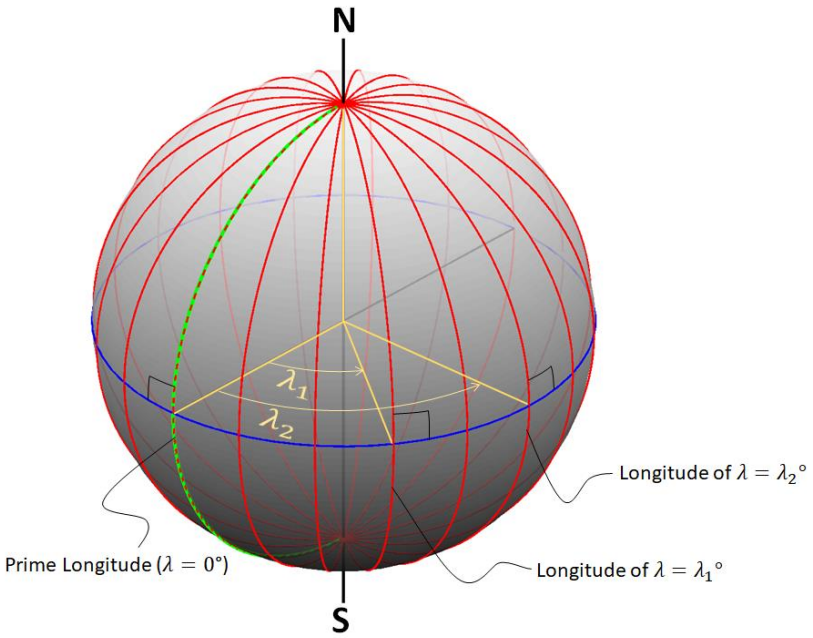

Figure 6 Definition of longitude.

As it will be discussed later, in mathematical models, sometimes the meridians are measured in degrees full circle to the east from the "initial meridian", which is the zero degree meridian. In this case, there is no need to label the meridian with the letter E or W. Thus, 0° and 360° correspond to the same meridian line.

Figure 7 shows a series of equally spaced latitudes (parallels) and longitudes (meridians) that form a grid on the surface of the ellipsoid. This grid is also called a "reticule'. Definition of a geographic or geodetic coordinate system, which will serve as horizontal datum, requires first attaching and orienting an ellipsoid with respect to the center of the earth. Then, it is necessary to define the origin of the geodetic latitude and longitude. Only then, one can define the location of any point $P(\phi, \lambda, \text{Z})$ on the surface of the ellipsoid.

In this technical manual we will be discussing and using only two horizontal datum systems:

1. North American Datum of 1983, which is abbreviated as NAD 83.
   NAD 83 uses GRS 80 ellipsoid. The center of the ellipsoid has a 2.24 m offset with respect to the the center of mass of the Earth. The zero latitude is defined by the Equator. The NAD 83 (GRS 80) meridian of zero longitude passes through the center of the transit instrument at the Royal Observatory of Greenwich, which is taken as the Reference Meridian.
2. World Geodetic System of 1984, which is abbreviated as WGS 84.

WGS 84 uses GRS 80 ellipsoid with some small differences (see Table 1). The center of the ellipsoid is located at the center of mass of the earth. The WGS 84 meridian of zero longitude is the IERS (International Earth Rotation and Reference Systems Service) Reference Meridian, which is 5.3 arc seconds or 102 m (335 ft) east of the Greenwich meridian at the latitude of the Royal Observatory of Greenwich (51° 28’ 40.1”N or 51.47780556° GPS coordinate).

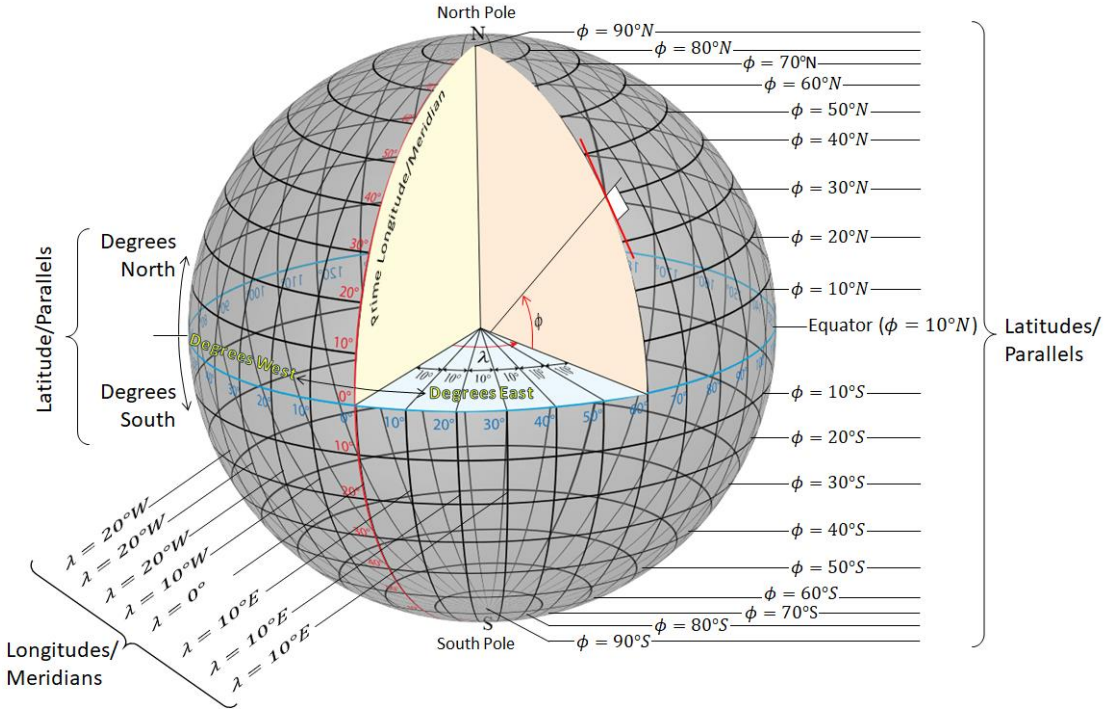

Figure 7 Grid formed by a series of equally spaced latitudes (parallels) and longitudes(meridians).

2.3 Mapping 3D Earth on a 2D Map Using UTM Projection

UTM projection stands for Universal Transverse Mercator projection. UTM is not a single projection system but a collection of a special type of transverse Mercator projections at 6° intervals of meridian.

Different types of Mercator projections are shown in Figure 8.

- Mercator projection, represented by the left illustration in Figure 8 (only half cylinder is shown), is a cylindrical map projection. The points on the surface of the earth are projected onto a cylinder which is tangent to the reference ellipsoid at the equator. The map is obtained by flattening the cylinder as a planar surface. The latitude and longitude lines on the reference ellipsoid appear as horizontal and vertical lines on the map. It is a conformal projection, meaning that it conserves the shapes of small features. The sizes of the features, however, become larger with increasing degree of latitude from the equator. It is the standard projection method for nautical navigation maps.
- Standard (or regular) transverse Mercator projection, represented by the middle illustration in Figure 8 (only half cylinder is shown), is also a cylindrical map projection. The points on the surface of the earth are projected onto a cylinder which is tangent to the reference ellipsoid along a meridian, which is called the central meridian. The map is obtained by flattening the

cylinder as a planar surface. The name transverse is due to the fact that the cylinder is rotated 90° with respect to the cylinder used for Mercator projection. Only the central meridian and equator appear as a straight lines on the map. All other lines of latitude and longitude lines appear as orthogonally intersecting curved lines on the map. Standard transverse Mercator projection is also a conformal projection. Small features retain their shape, however, the scale is true only along the central meridian. The distortion increases with east and west distance from the central.

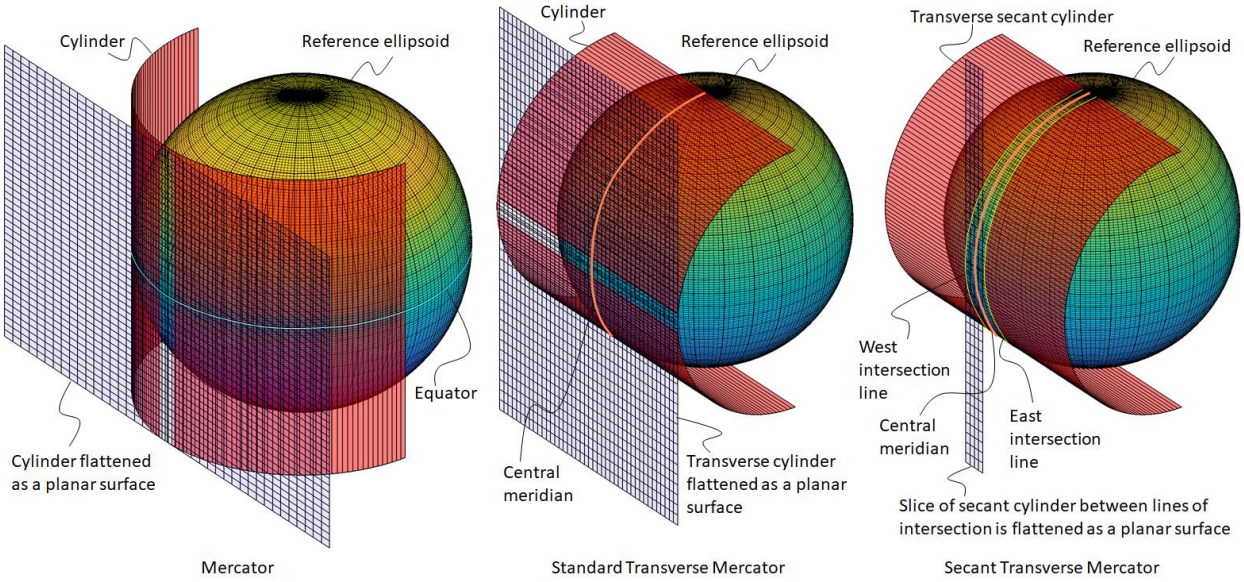

Figure 8 Illustrations of different Mercator projections.

- Secant transverse Mercator projection, represented by the right illustration in Figure 8, is an adaptation of the standard transverse Mercator projection. The points on the surface of the earth onto a cylinder having a slightly reduced diameter in such a way that it intersects the reference ellipsoid along two lines about 180 km to the west and to the east of the central meridian. The map is obtained by flattening the slice of the cylinder between cut lines as a planar surface. The use of secant cylinder for the projection of a slice reference ellipsoid with a meridional angle of 6° reduces the overall map distortion. The scale factor is equal to 1 along the west and east intersection circles, which are also called true-scale lines. The scale factor reduces to 0.9996 along the central meridian and increases to 1.0010 along the boundaries of the 6° meridional slice (about 668 km along the equator). This way, the amount of distortion is kept to be less than 1 part in 1,000 in the mapped area. Secant transverse Mercator projection maps large areas along south-north direction with low distortion. It is the projection method used by UTM coordinate system.

UTM coordinate system uses 60 secant transverse Mercator projections, which are generated by rotating the secant cylinder by 6° of meridian along the equator. Each projection forms a separate UTM zone representing a 6° slice of the earth as shown in Figure 9. Starting with the first UTM with the centerline meridian at 177° W, the subsequent UTM zones are numbered sequentially up to 60 while proceeding eastward at 6° intervals. Thus, the first zone extends from the meridian 180° W, which is the International Date Line, to the meridian 174° W.

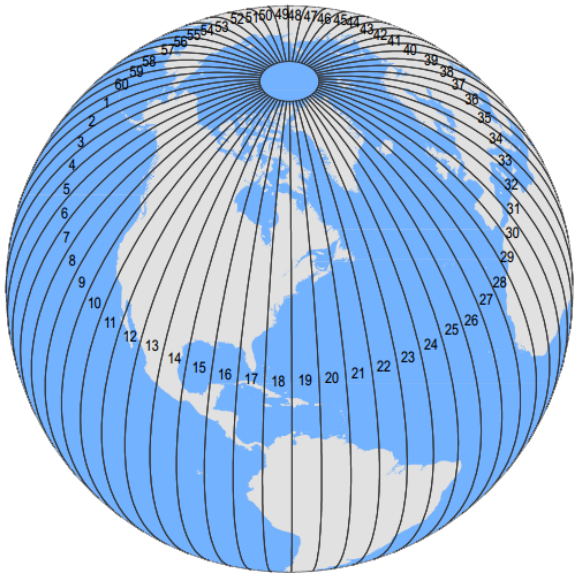

Figure 9 Positions of 6° slices forming the 60 UTM zones.

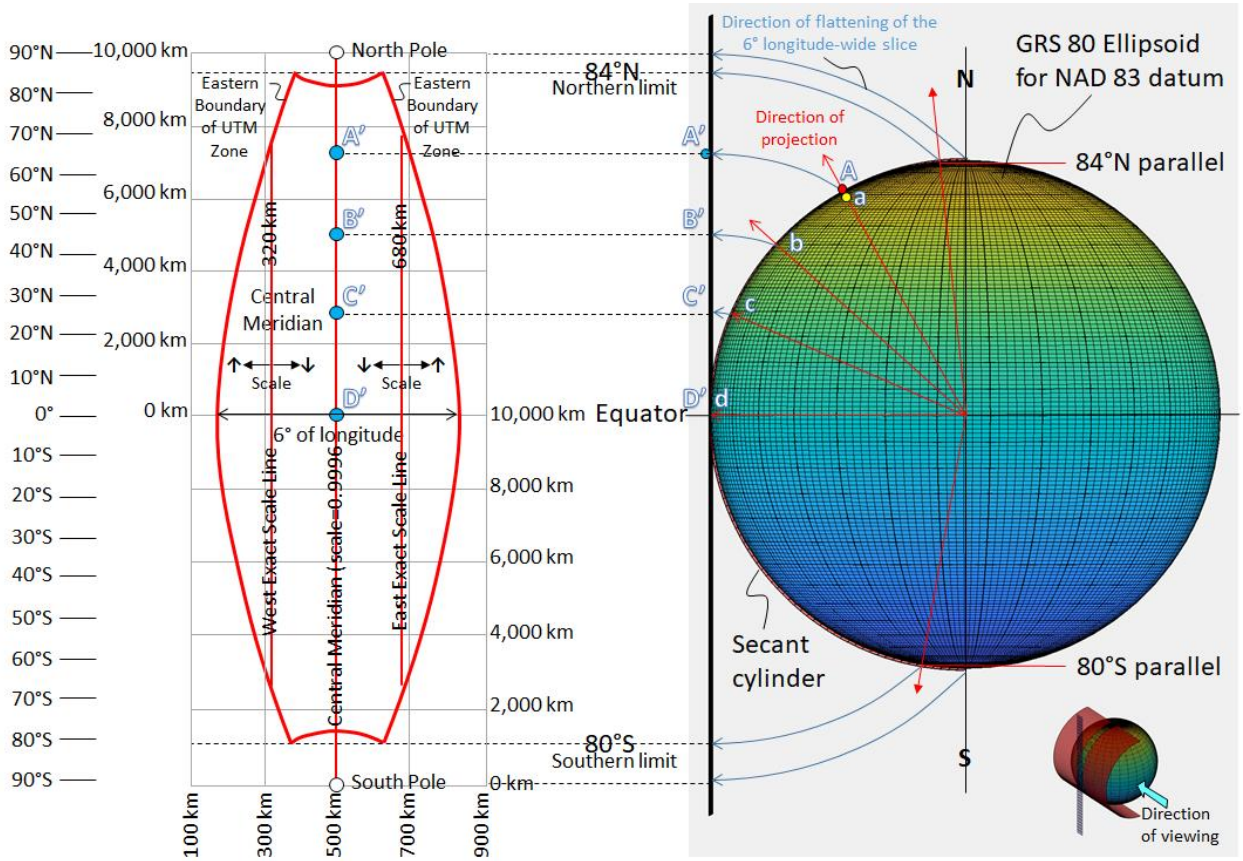

Figure 10 Schematic illustration of UTM projection.

Figure 10 illustrates the projection of a 6° slice of the earth onto the secant cylinder, which is then opened and flattened to a planar map with UTM coordinates. The meridians converge towards north and south poles. In order to limit the deformation, the projected area is restricted to the area between

the latitudes 80° S and 80° N. The polar caps (80° S to 90° S and 84° N to 90° N) are projected using a different projections. The projected planar map shown on the left side of Figure 10 has a Cartesian coordinate system whose origin is at the intersection of the central meridian with equator. The x coordinate, which points towards east, is called easting and y coordinate, which points towards north is called northing. Location of any point on the map is defined by its easting and northing.

In order to avoid negative easting and northing values, all zones are assigned local coordinates that are called false easting and northing. In UTM projection, the eastings and northings are always given in meters. Referring to Figure 10, the central meridian is always assigned the false easting of 500,000 m, regardless of the UTM zone. The west and east meridians, which are -3° and +3° from the central meridian appear as curved red lines. They delineate the western and eastern boundary of the projected region where the distortion is less than 1 part in 1,000. The circumference of the equator is about 40,075,000 m. When this length is divided into 60 slices, the maximum width of a UTM zone at the equator is found to be about 668,000 (=40,075,000)/60. Thus, in a UTM zone, easting values remain positive between 166,000 m (=500,000-668,000/2) to 834,000 m (=500,000+668,000/2). The northing for the south and north hemispheres are different. For the northern hemisphere, the northing runs from 0 m at the equator to 10,000 m at the North Pole. For the southern hemisphere, the northing runs from 0 m at the South Pole to 10,000 m at the equator. Since a northing value can be in either northern or southern hemisphere, it is necessary to add the letter N or S following the zone number when providing UTM coordinates.

2.4 Geoid

It is important to recall that the ellipsoid is a mathematical construct that facilitates establishment of a horizontal datum such as NAD 83 or WGS 84. Mount Everest has an altitude of 8,848 m whereas the deepest point in the Mariana Trench is at a depth of 11,034 m. Thus the amplitude of the topographic variation is 19,882, which is only 0.31% of the semi-major axis. Thus, GRS 80 or WGS 84 ellipsoids provide a good approximation for the surface of the world.

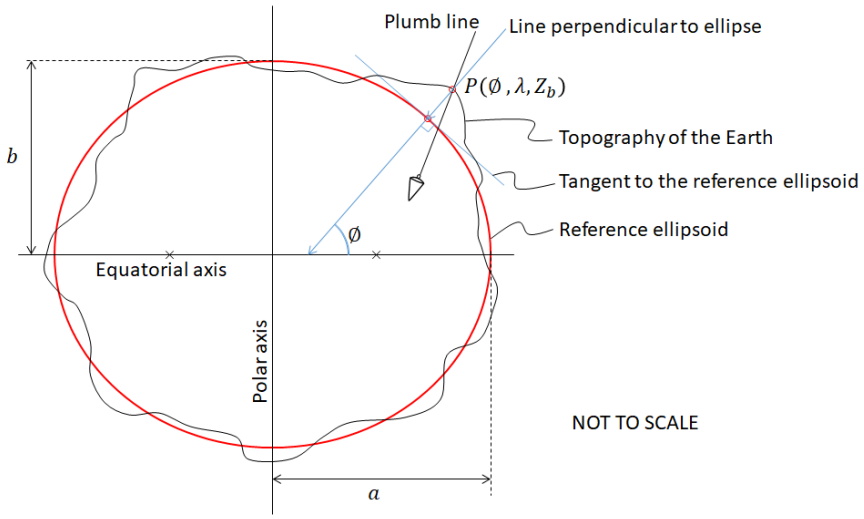

Figure 11 Reference ellipsoid, topography of the Earth and the plumb line.

Figure 11 shows the schematic representation of the reference ellipsoid and the topography of the Earth. As it can be seen, the topography of the Earth is at certain places above the reference ellipsoid and at other places below it. Consider the point $P(\phi, \lambda, Z_b)$ on the surface of the earth. As we have already discussed, the horizontal datum allows us to locate the point by the latitude ϕ and longitude λ. The latitude ϕ is obtained by projecting the point perpendicular to the reference ellipsoid, i.e. perpendicular to the tangent to the ellipsoid. We have not yet discussed, however, how the elevation Z_b should be determined.

In Figure 11, it is important to note that the plumb line passing through point $P(\phi, \lambda, Z_b)$ is not perpendicular to the ellipsoid. There is an angle between the plumb line and the line perpendicular to the ellipsoid, which was used to determine the latitude.

As we had to establish a horizontal datum to locate a point on the surface of the Earth, we need to establish a vertical datum to determine its elevation Z_b. The establishment of the vertical datum, requires the establishment of a so-called "geoid".

Before explaining what a geoid is, let us first define the concepts of geopotential and equipotential surface. Geopotential is the resultant of the gravitation which is the attraction force towards the center of mass of the Earth and the centrifugal force due to the rotation of the Earth. An equipotential surface is a virtual surface where the geopotential has the same value $W = constant$. Different equipotential surfaces can be defined by setting W to specific values. The gravity of the Earth is not uniformly distributed due to irregular distribution of the mass of the Earth. Therefore, the equipotential surface is an irregular surface, which ondulates under the effect of local irregularities of the distribution of mass in the Earth's crust. An equipotential surface having a higher value of geopotential W is closer to the center of the Earth than the one with a lower geopotential value.

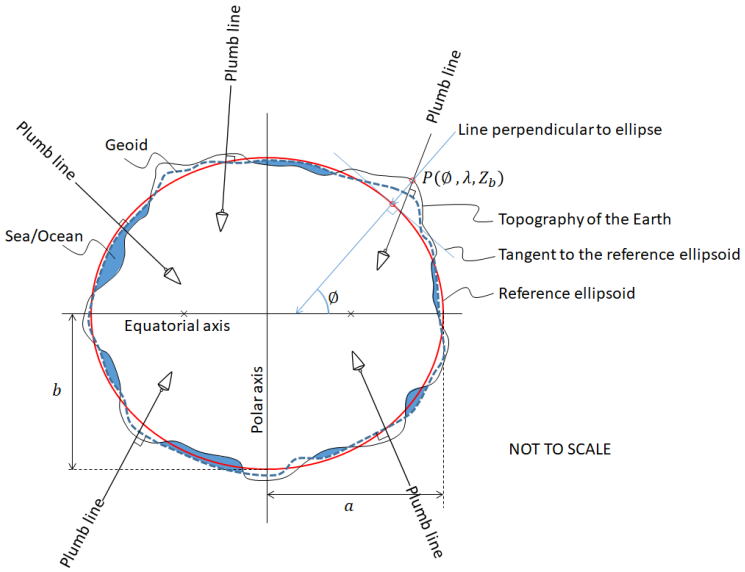

Figure 12 Schematic illustration of the ellipsoid, the topography of the Earth and the geoid.

A specific value of geopotential, we will call it W_o, corresponds to the theoretical global mean sea surface we would expect if only the effect of gravity (resultant of gravitation and centrifugal force) is

considered and the effect of the tides, currents, waves, density differences due to salinity and temperature are neglected. This specific equipotential surface with the geopotential value of W_o is called geoid. Figure 12 shows a schematic illustration of the geoid together with the ellipsoid and the natural topography of the Earth. As it can be seen, the direction of local gravity represented by the plumb line is everywhere perpendicular to the geoid because it is an equipotential surface.

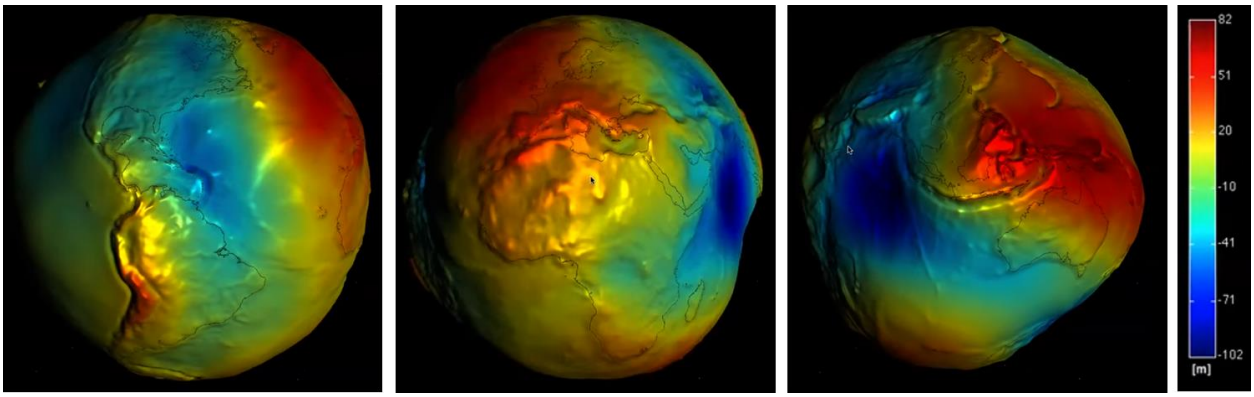

Figure 13 Views of the geoid computed from GOCE satellite data (created using images taken from Geoid Viewer[4] by Andrea Gatti, Politecnico di Milano, Italy, May 2011).

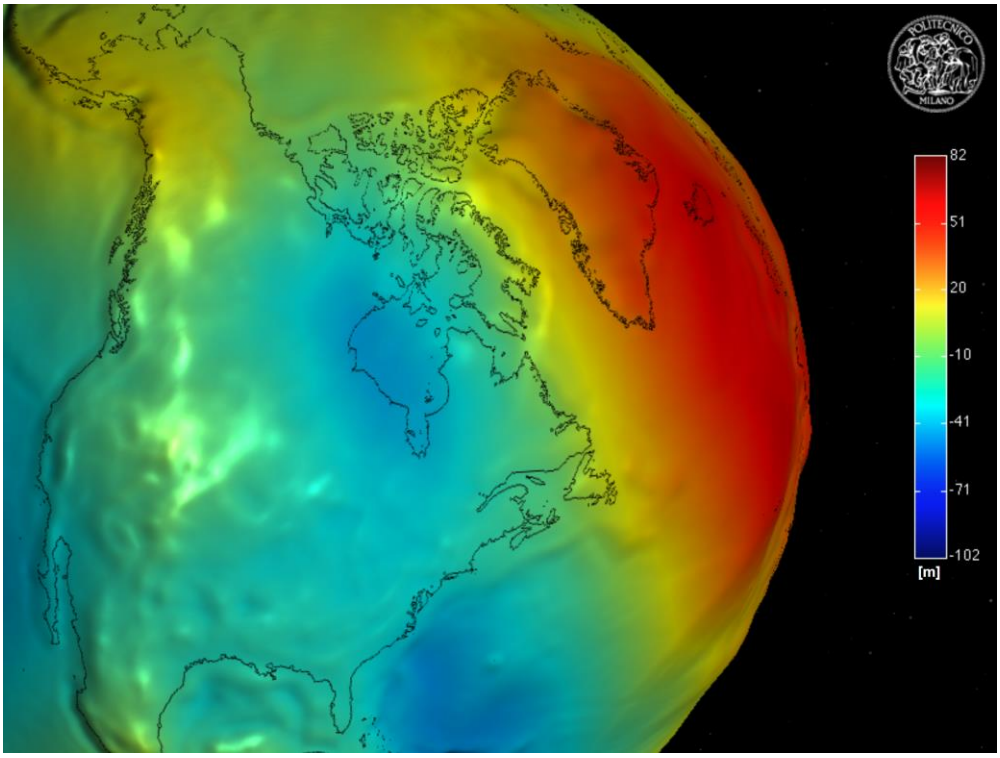

Figure 14 Enlarged view of the geoid from the geoid using Geoid Viewer by Andrea Gatti, Politecnico di Milano, Italy, May 2011.

It is important to understand that although it relates to the ideal mean sea level surface, the geoid does not represent the true mean sea level because of the lack of averaging of the effects of tides, currents,

[4] http://geomatica.como.polimi.it/elab/geoid/geoidViewer.html

water temperatures, salinity, etc. Moreover, the geoid is not a smooth surface because of the variations of the distribution of mass in Earth's crust.

Figure 13 shows the irregular shape of the geoid. The images are taken from the Geoid Viewer tool created by Andrea Gatti at Politecnico di Milani, Italy, using the GOCE satellite data. The tool allows viewing the geoid from any viewpoint and offers various types of controls for the rendering. It can be seen that the elevation difference between the geoid and the ellipsoid varies from +82 m to -102 m approximately. Areas above the ellipsoid are colored from light green to dark red passing through yellow whereas the areas below the ellipsoid are colored from light green to dark blue. The enlarged view of the geoid in Figure 14 shows that the geoid is below the ellipsoid in large areas of the eastern part of the CONUS.

Another way of illustrating the geoid is to map the gravity anomalies with respect to the standard gravity, which is defined as the gravity that would have resulted from an idealized Earth, which is perfectly smooth and homogenous. The gravity anomaly is defined as the deviation from this standard gravity. A joint mission of NASA and German Aerospace Center, which is called Gravity Recovery and Climate Change Experiment (GRACE)[56], made detailed measurements of Earth's gravity field anomalies using two satellites from 2001 to 2017. These measurements showed how mass is distributed and how it varies over time. Figure 15 shows a three dimensional representation of the undulating surface of gravity anomalies as measured by the GRACE program. Red and blue areas correspond to the strongest and weakest gravity anomalies, respectively.

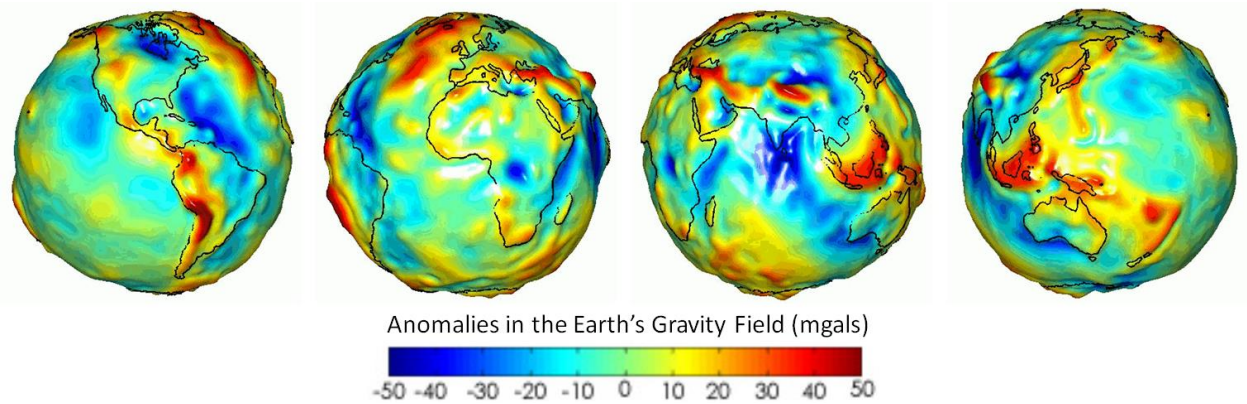

Figure 15 Anomalies of the Earth's gravity field based on the measurements made by the GRACE program. The figure was created using images from an animation provided by NASA/JPL/University of Texas Center for Space Research[7].

2.5 Vertical Datum, Orthometric Height and Helmert Orthometric Height

Measurement of the elevation or height requires the establishment of a datum that will serve as the zero elevation or height. Some of the available datums are

1. Ellipsoid

[5] http://www2.csr.utexas.edu/grace/
[6] https://grace.jpl.nasa.gov/
[7] https://grace.jpl.nasa.gov/resources/6/grace-global-gravity-animation/

2. Geoid
3. Local mean sea level (LMSL)
4. Tidal
    a. Mean Higher High Water (MHHW)
    b. Mean Tide Level (MTL)
    c. Mean Sea Level (MSL)
    d. Mean Lower Low Water (MLLW)

Historically, the mean sea level (MSL), which was believed to be the same everywhere was used as datum. This came from the belief that the sea level is in balance with the Earth's gravity. In 1929, a general adjustment of 1,000 bench marks was conducted to obtain a best fit of mean sea level observations at 26 tide stations in the U.S. and Canada. It involved a total of 106,724 km of leveling, consisting of 246 closed circuits and 25 circuits at sea level[8]. It was originally known as Sea Level Datum of 1929. It was neither an MSL, nor a geoid, nor an equipotential surface. Therefore, in 1973 it was named National Geodetic Vertical Datum of 1929, abbreviated as NGVD 29.

NGVD 29 was established based on the wrong belief that the sea surface is level. Later numerous surveys by National Geodetic Survey (NGS) showed that the sea surface is not level. The variations are caused by the variations in the Earth's gravity, currents, tides, wind, barometric pressures, temperature, the topography of the sea bed, and salinity differences. One of the problems with NGVD 29 was that, in order to be able to match the mean sea level at 26 selected gages the datum had to be warped.

In 1991, the North American Vertical Datum, abbreviated NAVD 88, was introduced to superseed NGVD 29. NAVD 88 is currently the official vertical control datum for Alaska, Canada and CONUS. It should be noted that NAVD 88 is also a tidal datum, but it only refers to the mean water level at only one tide gage, which is the tide gauge at Father Point (Point-au-Pere) in Rimouski, Quebec, Canada. The mean water level to serve as datum was computed based on the measurements carried out during a period of 18.6 years from 1960 to 1978.

NAVD 88 uses so called Helmert orthometric height, which is based on a geoid elevation obtained from modeled local gravity. Just like NGVD 29, NAVD 88 is not in conformance with MSL or a geoid that fits the equipotential surface. Nevertheless, NAVD 88 is a better realization of an orthometric datum based on a geopotential surface; however that geopotential is not the ideal global geoid. Later, better geoid models were developed based on satellite measurements. These geoids are adjusted from time to time to take into account the variations in the tectonic of the Earth. NAVD 88 geoid, however, is kept fixed. The basis for measuring orthometric heights based on a specified geoid elevation will be explained in what follows without going into the details.

The explanation of the orthometric height will be presented by referring to Figure 16, which shows the topography of the Earth together with the ellipsoid and various equipotential lines. The reference ellipsoid, say GRS 80, is shown as a red line.

The equipotential corresponding to the geopotential W_o corresponds to the geoid, which approximates the mean sea level. Other equipotential surfaces correspond to weaker geopotential levels as they are further from the geoid; i.e. $W_o > W_1 > W_2 > W_3$. It is important to note that due to irregularities in the

[8] https://www.ngs.noaa.gov/datums/vertical/national-geodetic-vertical-datum-1929.shtml

distribution of mass in the Earth's crust, the equipotential lines corresponding to different geopotential values are not necessarily parallel to one another.

Consider point P on the surface of the Earth. The equipotential $W = W_3$ passes through point P. Thus, the geopotential of point P is $W_P = W_3$. Each equipotential surface can be assigned a so-called geopotential number, which is defined as the potential energy difference between an equipotential surface and the geoid. Thus, the geopotential number of point P is given as

$$C_P = W_o - W_P \tag{1}$$

The concept of geopotential number is important. The points having the same geopotential number are at the same potential value. Thus, they are in hydrostatic equilibrium and the water will not flow between these two points.

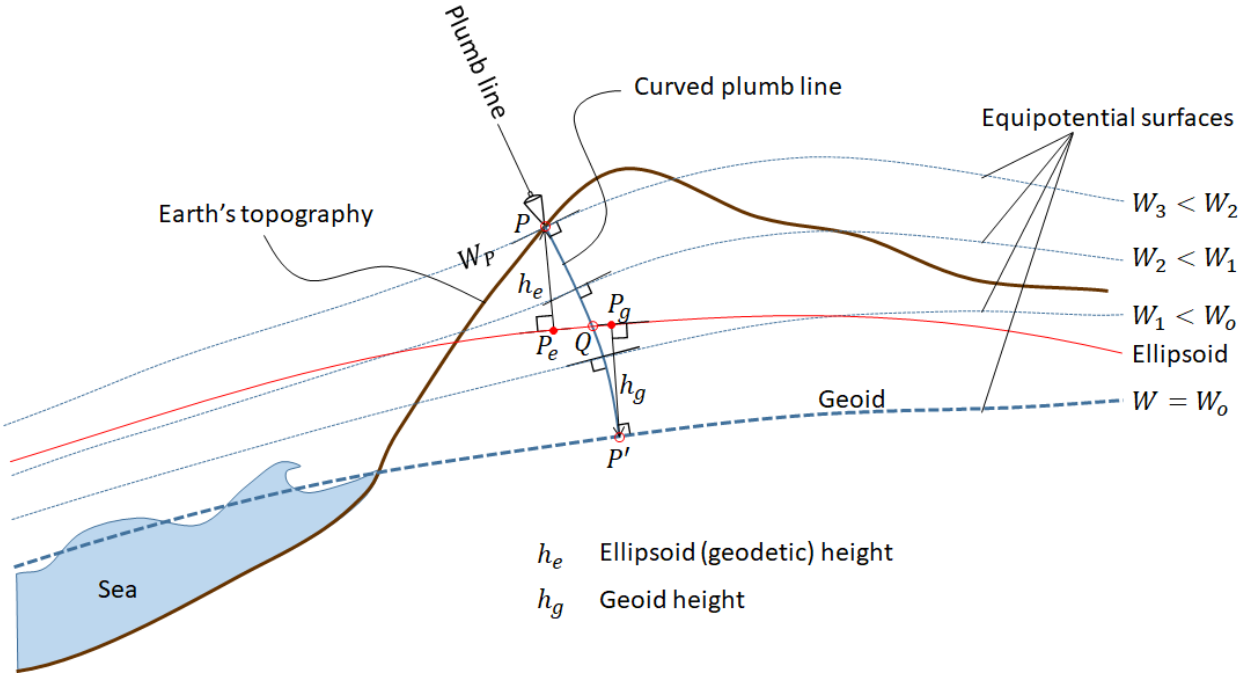

Figure 16 Definition of orthometric height.

The point P_e is the projection of point P on the surface of ellipsoid. The latitude and longitude of point P_e with respect to the horizontal datum NAD 83 gives the latitude and longitude of P. The point P is projected perpendicular to the surface of the ellipsoid. The distance between points P_e and P is called ellipsoid height (or geodetic height) and denoted by h_e.

The plumb line at point P makes an angle with the ellipsoid (line P-P_e). In fact, the plumb line follows a curved path, which intersects all equipotential lines orthogonally. The curved plumb line intersects the ellipsoid at point Q and the geoid at point P'. Consider now a line perpendicular to the ellipsoid from the point P' on the geoid. This normal line intersects the ellipsoid at point P_g. The distance between points P' and P_g is called geoid height (or geoid separation) and denoted by h_g.

The approximate orthometric height (in km) is given by the expression

$$H_O = h_e - h_g \tag{2}$$

USGS 1/3 arc-second DEM tiles are based on NAVD 88, which uses Helmert orthometric height system. Helmert orthometric height, H_H, for point is computed using the expression

$$H_H = \frac{C_P}{g + 0.024\, H_o} \tag{3}$$

where g is the surface gravity measurement in mgals[9], and H_O is the approximate orthometric height in km. The denominator in the above formula represents the correction. Note that $H_H = 0$ is nearly a level surface.

It is important to emphasize that NAVD 88 is based on a leveling network on the North America, which covers Alaska, Canada and CONUS. The only bias introduced is the fact that $H_H = 0$ is tied to the global mean sea level at Father Point (Point-au-Pere) in Rimouski, Quebec, Canada[10].

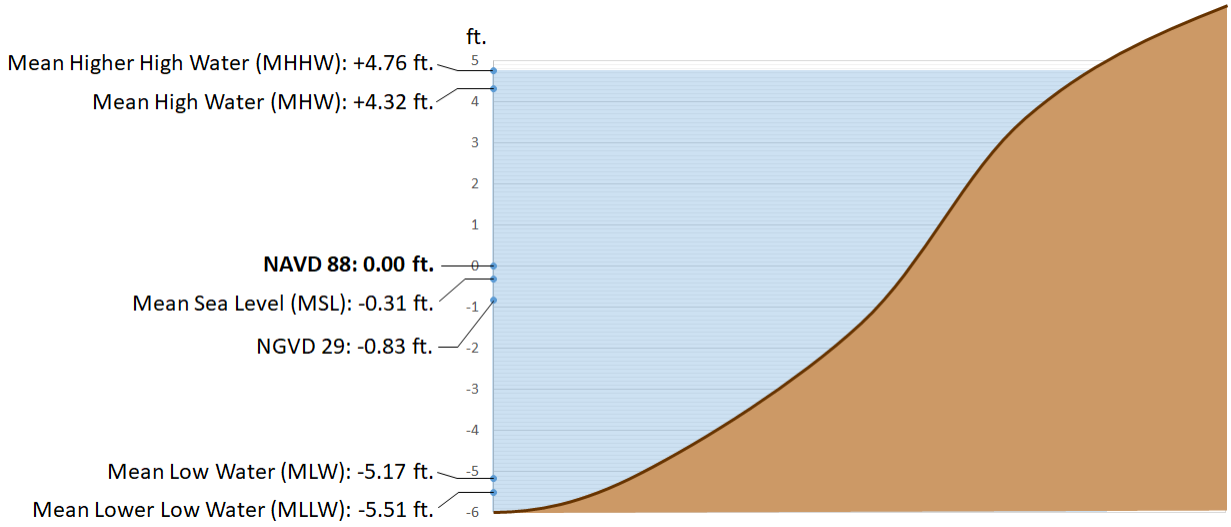

Figure 17 Comparison of different datums relative to NAVD 88 datum at the NOAA tide gauge in Boston (station ID 8443970)[11].

Current vertical datums of the U.S. and territories are Listed in Table 2. The USGS DEM tiles use the corresponding vertical datums.

[9] Units of gravitational acceleration. It is named galileo after Galileo Galilei. The gal is defined as 1 cm/s^2. The abbreviations mGal and µGal stand for milligal (one thousandth of a Gal) and microgal (one millionth of a Gal). The Gal is not part of the SI system, although its use was allowed by Comité international des poids et mesures (CIPM) in Paris, France. In 2006, ISO 80000-3:2006 deprecated the use of this unit. However, it still remains popular in the science of gravimetry.

[10] https://www.ngs.noaa.gov/datums/vertical/north-american-vertical-datum-1988.shtml

[11] https://www.mass.gov/service-details/north-american-vertical-datum-of-1988-navd-88

Table 2 List of vertical datums for the United States and Territories.

Datum Name	Date	Remarks
North American Vertical Datum of 1988 (NAVD 88)	1992 - present	https://www.ngs.noaa.gov/datums/vertical/north-american-vertical-datum-1988.shtml
American Samoa Vertical Datum of 2002 (ASVD02)	2002 - present	https://www.ngs.noaa.gov/datums/vertical/american-samoa-vertical-datum-2002.shtml
Guam Vertical Datum of 2004 (GUVD04)	2004 - present	https://www.ngs.noaa.gov/datums/vertical/guam-vertical-datum-2004.shtml
Northern Marianas Vertical Datum of 2003 (NMVD03)	2003 - present	https://www.ngs.noaa.gov/datums/vertical/northern-marianas-vertical-datum-2003.shtml
Puerto Rico Vertical Datum of 2002 (PRVD02)	2002 - present	https://www.ngs.noaa.gov/datums/vertical/puerto-rico-vertical-datum-2002.shtml
Virgin Islands Vertical Datum of 2009 (VIVD09)	2009 - present	https://www.ngs.noaa.gov/datums/vertical/virgin-islands-vertical-datum-2009.shtml
Hawaii		Under development

2.6 Geospatial Data Layers Used by DSS-WISE Lite and DSS-WISE HCOM

The USGS 1/3 arc-second DEM tiles used as base layer DEM refer to the horizontal datum and ellipsoid height of the North American Datum of 1983, abbreviated as NAD 83. The orthometric heights in DEM tiles for Alaska and CONUS are referenced to North American Vertical Datum of 1988, abbreviated as NAVD 88. Thus, during the simulation set up using DSS-WISE Lite Prep Tool the user is required to provide the elevations in ft. NAVD 88. The DEM tiles for Hawaii and U.S. territories refer to the respective datums listed in Table 2.

The 3 arc-second LandScan nighttime and daytime population data refers to the horizontal datum of the World Geodetic System of 1984, abbreviated as WGS 84. However, this data is internally used by the system and the population density maps produced by DSS-WISE HCOM are provided with UTM projection using the zone in which the breach point is located.

Chapter 3 REVIEW OF DSS-WISE™ LITE AND ITS RESULTS FILES

DSS-WISE Lite is a web-based, automated two-dimensional dam-break flood modeling and mapping tool provided under the secure web portal DSS-WISE Web hosted on a cluster at NCCHE. The user can quickly set up a simulation scenario by entering input data with the help of a specially designed graphical user interface (GUI) called DSS-WISE Prep Tool. Real-time error checking of the input data during the simulation set up process helps to minimize input errors. After the simulation request is submitted, the input data for the computational engine is automatically prepared based on the minimal information provided by the user. The computational engine performs the numerical computations and the results are made available on the status and results page for viewing and for downloading.

DSS-WISE™ computational engine solves the conservative form of two-dimensional shallow water equations (2D SWE) discretized over a regular Cartesian grid in the horizontal plane using finite volume method. The computational domain is automatically prepared using USGS 1/3 arc-second NED tiles that serve as the base layer DEM. These tiles are in geographic coordinates in units of decimal degrees with reference to the North American Datum of 1983 (NAD 83). The orthometric[12] elevations are in meters and, over the continental United States, are referenced to the North American Vertical Datum of 1988 (NAVD88). For Hawaii, Puerto Rico and other U.S. territories, the vertical reference datums are listed in Table 2.

The computational grid is first prepared in geographic coordinates (NAD 83) which are defined on the reference ellipsoid GRS 80 shown in Figure 18. The computational domain is defined as a square area on the reference ellipsoid centered at the coordinates of the user specified breach point (BP). The edges of the square computational domain extend a distance equal to the user-specified downstream distance, denoted as DD in Figure 18, in four cardinal directions. Referring to the special case depicted in Figure 18, the computational domain overlaps nine DEM tiles. DSS-WISE Lite system backend prepares the computational domain as a VRT file (virtual raster) based on the portions of the 9 DEM tiles that are needed to create the computational grid. At this point, the datasets reference by the VRT file are still in NAD 83 coordinates and have their original resolution of 1/3 arc-second.

The computational engine, however, is not designed to work with a computational grid defined on the reference ellipsoid. It requires a computational grid in the local horizontal plane with elevations defined perpendicular to the horizontal plane. Moreover, the computational grid must be created at the user specified cell size, which can have any value from 20 ft. to 200 ft. Therefore, DSS-WISE Lite system prepares a new warped[13] VRT file by projecting the computational domain onto a plane using UTM Projection (See Appendix B) with the appropriate UTM zone, which is the UTM zone of the breach point BP.

[12] Orthometric elevations are elevations that are measured along the local plum line with reference to the true mean sea level (MSL) represented by the geoid. Geoid represents an equipotential surface that takes into account variations in earth's gravitational field due to local variations in the mass. It is a virtual surface that continues under the continents. GPS (Global Positioning System), on the other hand measures the ellipsoid height, which is the elevation from the reference ellipsoid along a line perpendicular to the ellipsoid. Ellipsoid elevation is different from orthometric elevation. The differences between orthometric and ellipsoid elevations can be in the order of plus or minus tens of meters.

[13] Warping ensures systematic geometric correction.

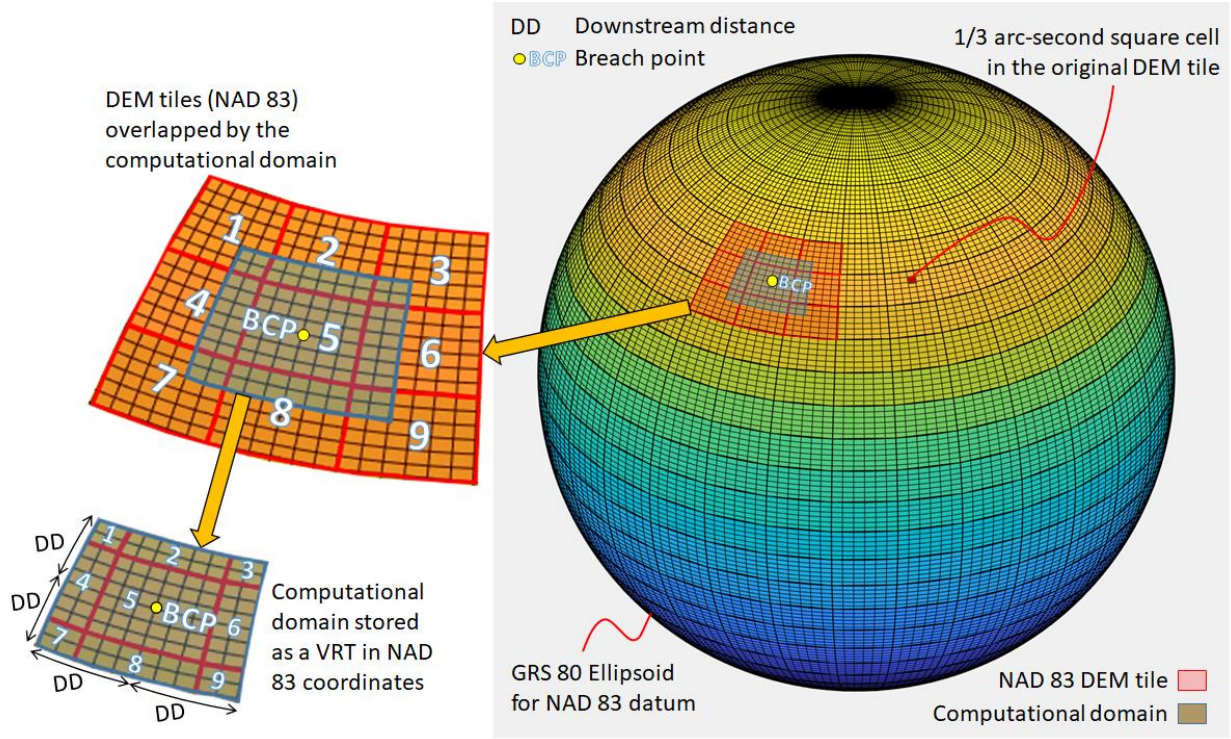

Figure 18 Identification of DEM tiles to be used to create the computational domain.

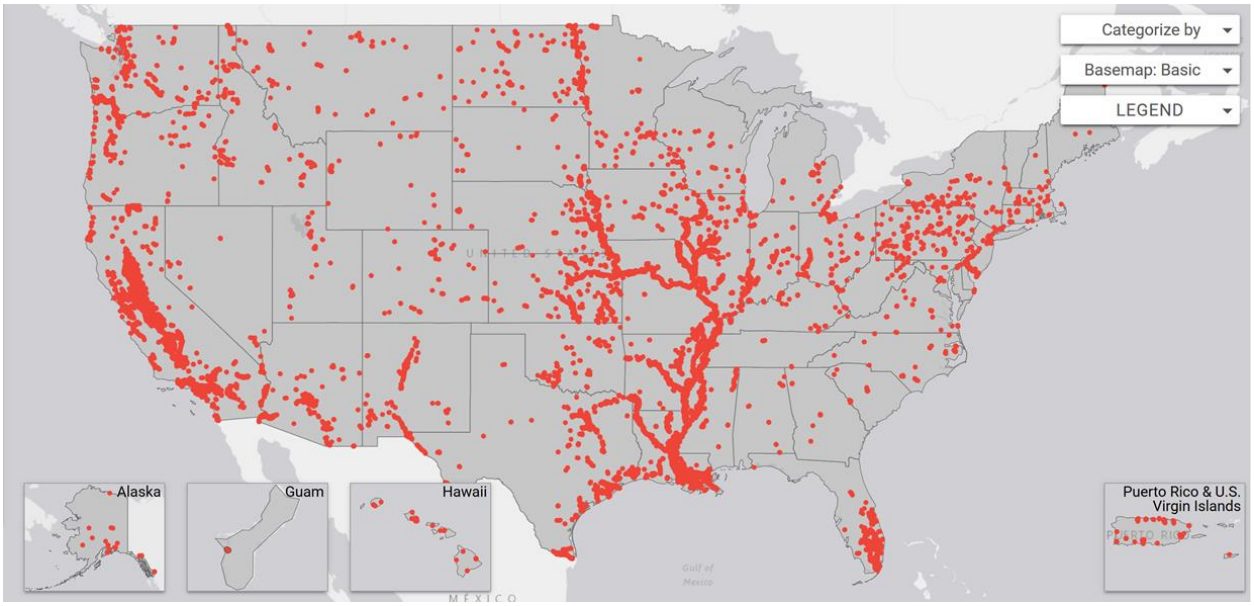

Figure 19 Map of the levees in the NLD (taken from https://levees.sec.usace.army.mil/#/).

A copy of the National Levee Database (NLD) was made available to DSS-WISE Lite system as an ESRI shapefile of three-dimensional 3D polyline type (see Figure 19). The features in the original NLD shapefile have been converted to a series of points at 1-m interval and stored as an ESRI shapefile of three-dimensional 3D point type. The features are indexed to DEM tiles. The levees in the computational domain are extracted and projected using the same UTM zone and cell size as the computational grid.

The levees, are burned into the projected computational domain at the correct user-defined cell size. Burning the levees into the DEM practically corresponds to setting the elevations of the cells along the levee path to the crest elevation of the levee. Since the levees are converted to a series of points with 1m-interval and the smallest cell size is 20 ft. (6.1 m), it is guaranteed that each computational cell along the levee polyline has at least one corresponding levee point.

The final version of the computational grid is obtained by burning in estimated unknown reservoir topography and by removing the user specified bridges. Figure 20 shows the final computational domain, which forms a nearly square domain in the horizontal plane defined by x- and y-coordinates. The x-coordinate points towards east and the y-coordinate points towards north. The breach point BP is at the center of the grid. The grid extends a distance of DD on four cardinal directions. The spacing between the gridlines is the same in both directions and equal to the user-specified resolution, which can vary from 20 ft. to 200 ft. Since the cell size is the same over the entire domain and the grid lines are orthogonal, the computational grid is said to be a regular Cartesian grid.

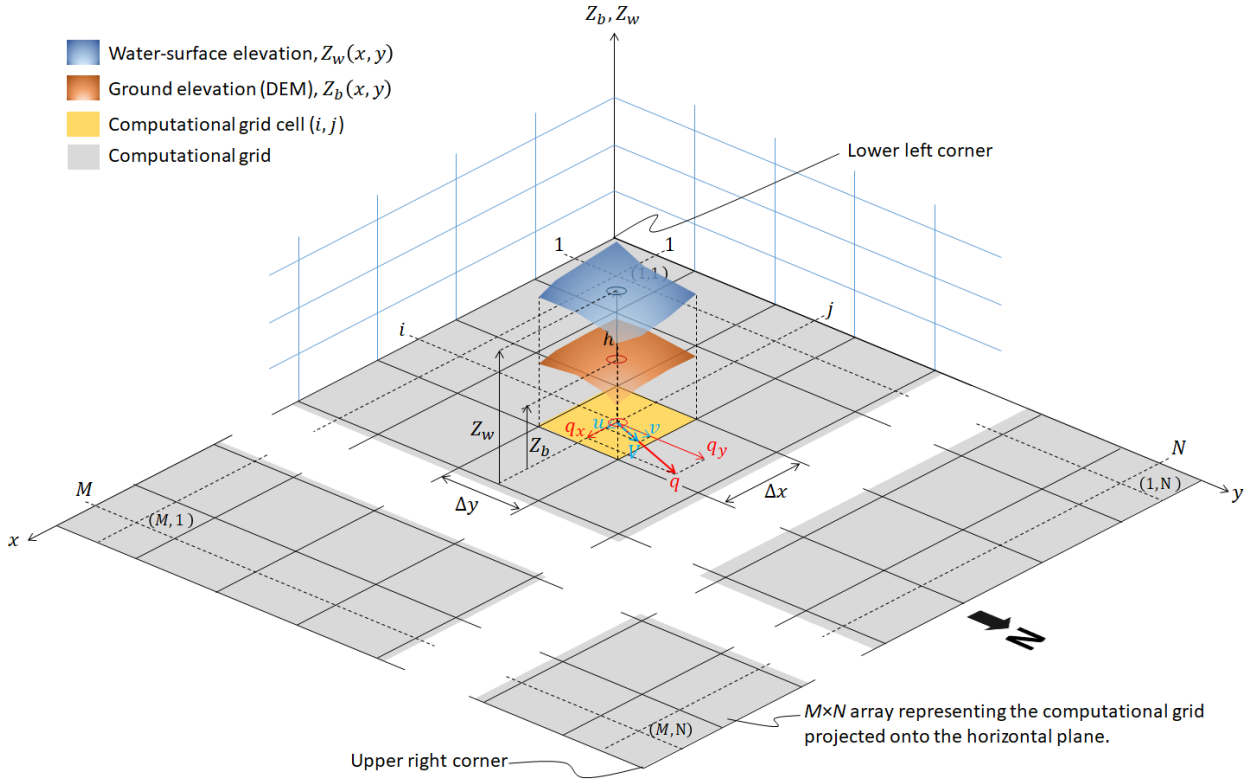

Figure 20 Definition sketch showing the computational domain, ground elevation (DEM), and the water surface elevation.

The computational grid is defined by x and y coordinates of the cell centers. The ground elevation at the center of each cell is the orthometric elevation Z_b. Grid coordinates and orthometric elevations are in meters. In fact, the computational engine carries out all computations in SI unit system. At the end of the simulation, the results are written into output files in U.S. Customary System units.

Referring to Figure 20, the computational grid can be considered as a two-dimensional array of size $M \times N$, where M is the number of columns of cells in x direction and N is the number of rows of cells in y direction. A computational cell is identified by i and j, where

- $i = 1, \dots, M$ is the column number (column number in x-direction starting from the lower left cell of the computational grid) and
- $j = 1, \dots, N$ is the row number (row number in y-direction starting from the lower left cell of the computational grid).

Using the notation with the column and row indexes i and j, respectively, the computational grid can be denoted as $Z_b(i,j)$ with $i = 1, \dots, M$ and $j = 1, \dots, N$. The size of the computational domain depends on the user-specified downstream distance. The largest computational domain would cover a 780×780 mile square area. The number of cells in the computational grid may range from tens of thousands to several hundreds of millions.

The propagation of flood on complex topography is described by 2D SWE. 2D SWE are a set of three partial differential equations. They are obtained by integrating three dimensional Navier-Stokes equations[14] over the depth by assuming that the horizontal extent of the flow is much greater than the vertical extent and the pressure is hydrostatic. The resulting set of three partial differential equations are hyperbolic. One equation represents the conservation of mass and the remaining two equations represent the conservation linear momentum in x and y directions.

Since they are obtained by integration over the depth, the discretized form of conservative SWE defines the flood flow condition at each cell center by three independent variables (see Figure 20):

1. Flood depth, h (ft.), which is the difference between water-surface elevation Z_w (ft. NAVD 88) and the ground elevation Z_b (ft. NAVD 88)

$$h = Z_w - Z_b \tag{4}$$

   Note that when the cell is dry, $Z_w = Z_b$, and $h = 0$. Flood depth is also denoted by D.

2. Specific discharge in x-direction, $q_x = hu$, which is the product of the flow depth h and the component of the flow velocity in x-direction, which is denoted u.

3. Specific discharge in y-direction, $q_y = hv$, which is the product of the flow depth h and the component of the flow velocity in y-direction, which is denoted v.

Simulation starts at time $t = 0$ with known initial values assigned to all independent variables and other variable that are computed from them. Starting with these initial conditions, the computational engine advances the time in sufficiently small increments, which is called "time step" and denoted Δt. Let the time at the previous time step to be t_{old}. The current time at the beginning of a new time step is then computed as $t = t_{old} + \Delta t$. At each new time, t, the computational engine solves for the three independent variables at the center of all computational cells[15]. The duration of the time step (which may have a value ranging from fractions of a second to a few seconds) is not constant but varies from one time step to another. Since, the computational engine uses an explicit scheme, the duration of the

[14] Navier-stokes equations are a set of partial differential equations describing the three dimensional flow of incompressible fluids.

[15] This is a simplification. In reality, the software tracks wet cells. Only wet cells and their neighbors are calculated.

time step is computed by the computational engine in a manner that satisfies the so-called CFL (Courant-Friedrichs-Levy) condition, which is a necessary but insufficient condition for the stability of the computations. All other variables describing flood flow are computed from the three independent variables (h, q_x, and q_y) that are computed directly by the computational engine at each time step.

Although, the computational engine uses different storage techniques to optimize computational efficiency, for the purposes of this manual, one may consider that the previous and current values for each variable are stored in separate two-dimensional arrays of size $M \times N$:

1. $(h)_{i,j}^{t_{old}}$ stores the current time values and $(h)_{i,j}^{t}$ stores the next time step values of flood depth
2. $(q_x)_{i,j}^{t_{old}}$ stores the current time values and $(q_x)_{i,j}^{t}$ stores the next time step values of x-component of specific discharge, and
3. $\left(q_y\right)_{i,j}^{t_{old}}$ stores the current time values and $\left(q_y\right)_{i,j}^{t}$ stores the next time step values of y-component of specific discharge.

The specific discharges q_x and q_y are conserved quantities across flow discontinuities, such as hydraulic jumps of traveling positive waves. Their use as independent variables allows the computational engine to solve the 2D SWE for mixed flow regimes (subcritical, transcritical and supercritical) using shock-capturing upwind computational schemes. At the end of each time step the components of velocity vector in x and y directions, which are denoted by u and v, are computed indirectly as follows:

$$(u)_{i,j}^{t} = \begin{cases} 0 & if \quad (h)_{i,j}^{t} = 0 \\ \frac{(q_x)_{i,j}^{t}}{(h)_{i,j}^{t}} & if \quad (h)_{i,j}^{t} > 0 \end{cases} \qquad \text{and} \qquad (v)_{i,j}^{t} = \begin{cases} 0 & if \quad (h)_{i,j}^{t} = 0 \\ \frac{(q_y)_{i,j}^{t}}{(h)_{i,j}^{t}} & if \quad (h)_{i,j}^{t} > 0 \end{cases} \tag{5}$$

The components of velocity are also stored in two-dimensional arrays of size $M \times N$:

1. $(u)_{i,j}^{t_{old}}$ stores the current time values and $(u)_{i,j}^{t}$ stores the next time step values of x-component of velocity, and
2. $(v)_{i,j}^{t_{old}}$ stores the current time values and $(v)_{i,j}^{t}$ stores the next time step values of y-component of velocity.\

DSS-WISE Lite simulation starts with known initial conditions that define the values of the three independent variables over the entire computational domain. The terrain is assumed to be dry everywhere except where there is a reservoir.

- The dry computational cells are assigned the initial values of $(u)_{i,j}^{t=0} = (v)_{i,j}^{t=0} = 0$ (which means $(q_x)_{i,j}^{t=0} = \left(q_y\right)_{i,j}^{t=0} = 0$) and $(h)_{i,j}^{t=0} = -9999$ (i.e. $(Z_w)_{i,j}^{t=0} = -9999$). It is important to note that the initial water surface elevation for dry cells is not zero but equal to -9999 m, which by convention corresponds to “no data”.
- The computational cells representing the impounded reservoir are assigned the following initial values of $(u)_{i,j}^{t=0} = (v)_{i,j}^{t=0} = 0$ (which means $(q_x)_{i,j}^{t=0} = \left(q_y\right)_{i,j}^{t=0} = 0$). This means that the impounded water is assumed to be stagnant. The reservoir cells that are initially wet are assigned the flow depth value of $(h)_{i,j}^{t=0} = Z_f - (Z_b)_{i,j}$, where Z_f is the failure pool elevation specified by the user.

At the end of the simulation, DSS-WISE™ Lite generates a series of raster files that are clipped to the extent of the bounding box of the maximum inundation extent polygon. Consider the computational domain depicted in Figure 21. The bounding box of the maximum inundation polygon is the rectangular area between columns $j = c_1$ and $j = c_2$ and rows $i = r_1$ and $i = r_2$. All raster output files are clipped using these column and row extents.

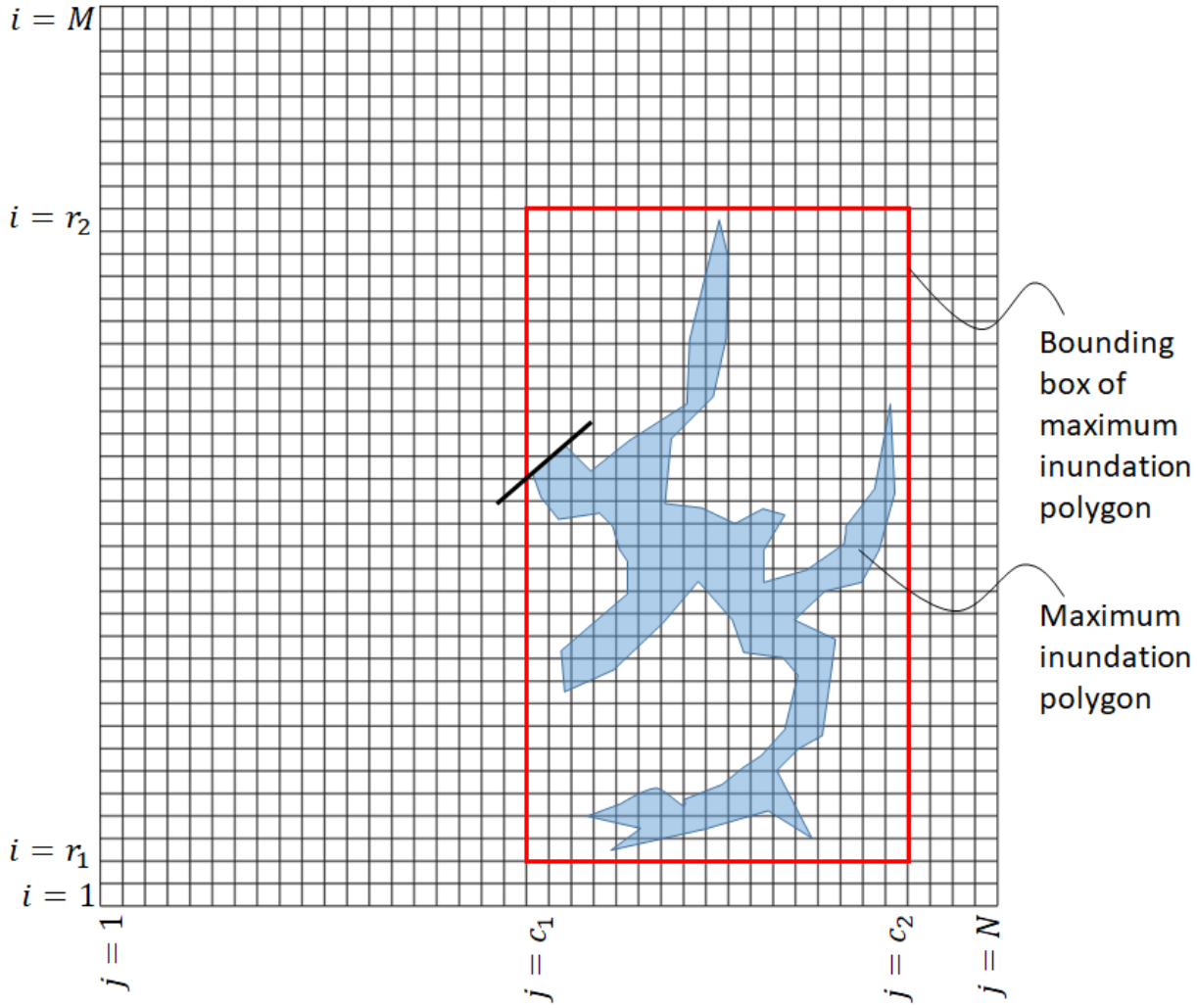

Figure 21 Definition of the bounding box of maximum inundation polygon.

The raster files output at the end of a simulation are briefly described as follows:

1. Raster file of ground elevations of the cells within the bounding box.

   Computational grid can be considered as a two dimensional array of ground elevations $(Z_b)_{i,j}$ (ft. NAVD 88) with $i = 1, \dots, M$ and $j = 1, \dots, N$.

   In reservoir type simulations, the user defines all structures (i.e. dams) impounding the reservoir. The computational cells in the footprint of these structures are initially raised to the crest elevation of the associated structure (Z_{cr}) while storing their original valley elevations in special arrays.

Although, it is allowed to define multiple structures, only one structure can be breached. Let us call the cells under the footprint of the breached structure as "breached-structure cells" (BSCs). During the simulation, the elevations of the breached-structure cells are modified based on the type of breach specified by the user.

- For simulations with sudden and complete failure of the dam, all BSCs are returned to their original valley elevation at the very first time step.
- For simulations with partial and gradual failure of the dam, starting with the very first time step, the elevations of BSCs in the footprint of the breach, which extends half of the breach width (BW) to each side of the breach center (BC), are lowered to the breach invert elevation (Z_{bi}) within the user-specified breach formation time (T_f).

At the end of the simulation, the array of computational grid cells in the bounding box, i.e. $(Z_b)_{i,j}$ with $i = r_1, \dots, r_2$ and $j = c_1, \dots, c_2$, is output as a raster file.

2. Raster file of the maximum flood depth achieved in each cell h_{max} (ft.).

The computational engine stores the maximum flood depths as a separate two-dimensional array $(h_{max})_{i,j}$ with $i = 1, \dots, M$ and $j = 1, \dots, N$.

- At time $t = 0$, i.e. the beginning of simulation, the initial values of depths are simply assigned as the maximum flood depths $(h_{max})_{i,j} = (h)_{i,j}^{t=0}$.
- The time is advanced to $t = t_{old} + \Delta t$ and the new depth values $(h)_{i,j}^{t}$ are computed from the known values of the independent variables at the previous time t_{old}. At the end of each time step, the maximum flood depth array is updated using the following method:

$$(h_{max})_{i,j} = \begin{cases} (h_{max})_{i,j} & if \quad (h)_{i,j}^{t} \leq (h_{max})_{i,j} \\ (h)_{i,j}^{t} & if \quad (h)_{i,j}^{t} > (h_{max})_{i,j} \end{cases} \tag{6}$$

Application of Eq. (6) at the end of each time step until the end of the simulation produces a two-dimensional array containing the maximum depth achieved in each cell during the duration of the simulation.

At the end of the simulation, the array of maximum flood depths within the bounding box, i.e. $(h_{max})_{i,j}$ with $i = r_1, \dots, r_2$ and $j = c_1, \dots, c_2$, is output as a raster file.

3. Raster file of the maximum specific discharge magnitude $DV_{max} \equiv q_{max}$ (ft^2/s).

The magnitude of the specific discharge, which is also denoted DV, is given by the expression:

$$DV \equiv q = \sqrt{{q_x}^2 + {q_y}^2} \tag{7}$$

The computational engine stores the maximum specific discharge magnitude as a separate two-dimensional array $(q_{max})_{i,j}$ with $i = 1, \dots, M$ and $j = 1, \dots, N$.

- At time $t = 0$, i.e. the beginning of simulation, the components of specific discharge are null everywhere $(q_x)_{i,j}^{t=0} = \left(q_y\right)_{i,j}^{t=0} = 0$. Thus, the two dimensional array for the maximum magnitude of specific discharge is initialized with $(q_{max})_{i,j} = 0$.
- The time is advanced to $t = t_{old} + \Delta t$ and the new values of $(q_x)_{i,j}^t$ and $(q_x)_{i,j}^t$ are computed from the known values of the independent variables at the previous time $t = t$. At the end of the time step, the array of maximum specific discharge is updated using the following method:

$$(q_{max})_{i,j} = \begin{cases} (q_{max})_{i,j} & if \quad \sqrt{\left[(q_x)_{i,j}^t\right]^2 + \left[\left(q_y\right)_{i,j}^t\right]^2} \leq (q_{max})_{i,j} \\ \sqrt{\left[(q_x)_{i,j}^t\right]^2 + \left[\left(q_y\right)_{i,j}^t\right]^2} & if \quad \sqrt{\left[(q_x)_{i,j}^t\right]^2 + \left[\left(q_y\right)_{i,j}^t\right]^2} > (q_{max})_{i,j} \end{cases} \tag{8}$$

Application of Eq. (8) at the end of each time step until the end of the simulation produces a two-dimensional array containing the maximum specific discharge magnitudes achieved in each cell during the duration of the simulation.

At the end of the simulation, the array of maximum specific discharge magnitude within the bounding box, i.e. $(q_{max})_{i,j}$ with $i = r_1, \dots, r_2$ and $j = c_1, \dots, c_2$, is output as a raster file.

4. Raster file of the maximum velocity magnitude achieved in each cell V_{max} (ft/s).

The velocity magnitude is given by the expression:

$$V = \sqrt{u^2 + v^2} \tag{9}$$

The computational engine stores the maximum velocity magnitude as a separate two-dimensional array $(V_{max})_{i,j}$ with $i = 1, \dots, M$ and $j = 1, \dots, N$.

- At time $t = 0$, i.e. the beginning of simulation, the components of the velocity are null everywhere $(u)_{i,j}^{t=0} = (u)_{i,j}^{t=0} = 0$. Thus, the two dimensional array for the maximum magnitude of specific discharge is initialized with $(V_{max})_{i,j} = 0$.
- The time is advanced to $t = t_{old} + \Delta t$ and the new values of $(u)_{i,j}^t$ and $(v)_{i,j}^t$ are computed from the known values of the independent variables at the previous time t_{old}. The maximum velocity magnitude is updated using the following method

$$(V_{max})_{i,j} = \begin{cases} (V_{max})_{i,j} & if \quad \sqrt{\left[(u)_{i,j}^t\right]^2 + \left[(v)_{i,j}^t\right]^2} \leq (V_{max})_{i,j} \\ \sqrt{\left[(u)_{i,j}^t\right]^2 + \left[(v)_{i,j}^t\right]^2} & if \quad \sqrt{\left[(u)_{i,j}^t\right]^2 + \left[(v)_{i,j}^t\right]^2} > (V_{max})_{i,j} \end{cases} \tag{10}$$

Application of Eq. (10) at the end of each time step until the end of the simulation produces a two-dimensional array containing the maximum velocity magnitude achieved in each cell during the duration of the simulation.

At the end of the simulation, the array of maximum velocity magnitude within the bounding box, i.e. $(V_{max})_{i,j}$ with $i = r_1, \dots, r_2$ and $j = c_1, \dots, c_2$, is output as a raster file.

5. Raster file of the final flow depths h_{final} (ft).

   Let T_{end} be the time at the end of the simulation. Then the final flow depth is defined as

$$(h_{final})_{i,j} = (h)_{i,j}^{T_{end}} \tag{11}$$

   At the end of the simulation, the array of final flow depths in the bounding box, i.e. $(h)_{i,j}^{T_{end}}$ with $i = r_1, \dots, r_2$ and $j = c_1, \dots, c_2$, is output as a raster file.

6. Raster file of flood arrival time T_{arr} (hrs)

   Flood arrival time is defined as the time at which an initially dry cell received water regardless of its depth. The units is hours. The computational engine stores the flood arrival time as a separate two-dimensional array $(T_{arr})_{i,j}$ and outputs it as a results file at the end of the simulation.

   - At time $t = 0$, i.e. the beginning of simulation, the flood arrival time is assigned a very large number everywhere. The longest simulation time that the user can specify is 60 days, which corresponds to 1,440 hours. Thus any number greater than 1,440 hours could be considered as a sufficiently big number for the flood arrival time. Let the big number for arrival time to be defined as $TBIG \geq 1{,}440$. Then, the two dimensional array for the maximum magnitude of specific discharge is initialized with $(T_{arr})_{i,j} = TBIG$.
   - The time is advanced to $t = t_{old} + \Delta t$ and the new values of $(h)_{i,j}^{t}$ are computed from the known values of the independent variables at the previous time $t = t_{old}$. At the end of each time step, the flood arrival time array is updated using the following method:

$$(T_{arr})_{i,j} = min\big((T_{arr})_{i,j}, t\big) \;\; if \;\; (h)_{i,j}^{t} > 0 \tag{12}$$

     Application of Eq. (12) at the end of each time step until the end of the simulation produces a two-dimensional array containing the flood arrival time for all cells.

   At the end of the simulation, the array of flood arrival time within the bounding box, i.e. $(T_{arr})_{i,j}$ with $i = r_1, \dots, r_2$ and $j = c_1, \dots, c_2$, is output as a raster file after converting any cell with $(T_{arr})_{i,j} = TBIG$ to "NO DATA" value[16].

7. Raster file of the arrival time of maximum specific discharge magnitude Tq_{arr} (hrs)

[16] It should be noted that, all cells that contain water at the beginning of the simulation, i.e. filled reservoir cells in reservoir-type simulations, have a flood arrival time of zero. This is transparent to the user because the arrival time raster and shapefile include only the area downstream of the dam. The initial reservoir area is not included in these files.

- At time $t = 0$, i.e. the beginning of simulation, the arrival time of maximum specific discharge is assigned a very large number everywhere: $(Tq_{arr})_{i,j} = TBIG$.
- The time is advanced to $t = t_{old} + \Delta t$ and the new values of $(h)_{i,j}^{t}$ are computed from the known values of the independent variables at the previous time $t = t_{old}$. The maximum velocity magnitude is updated suing the following method

  At the end of each time step, the arrival time of maximum specific discharge is updated using the following method:

$$(Tq_{arr})_{i,j} = min\big((Tq_{arr})_{i,j}, t\big) \;\; if \;\; (h)_{i,j}^{t} > \; 0 \tag{13}$$

  Application of Eq. (13) at the end of each time step until the end of the simulation produces a two-dimensional array containing the flood arrival time for all cells.

At the end of the simulation, the array of the arrival time of maximum specific discharge within the bounding box, i.e. $(Tq_{arr})_{i,j}$ with $i = r_1, \dots, r_2$ and $j = c_1, \dots, c_2$, is output as a raster file after converting any cell with $(Tq_{arr})_{i,j} = TBIG$ to "NO DATA" value.

The aim of this chapter was to briefly explain how the results raster files provided by DSS-WISE Lite are calculated. It is important to note that the mathematical expressions and explanations given above are oversimplified and does not reflect how they are handled in the computer code for the computational engine or for the backend applications. The computer code is written in a different manner that takes into account the efficiency of the code.

This chapter purposefully avoided going into a lengthy description of the 2D SWE and how they are solved numerically. Additional information on DSS-WISE Lite capability and detailed description of the mathematical basis and various system components can be found in Altinakar et al. (2017 and 2018).

It is also important to underline that the computational engine of DSS-WISE Lite has been rigorously verified using analytical solutions and validated based on laboratory experiments and field data from past experiments (Altinakar et al., 2010). In a blind study undertaken in collaboration with U.S. Army Corps of Engineers, sunny day failure of five selected dams using DSS-WISE Lite were compared with simulations using 1D HEC-RAS and FLO-2D (Altinakar et al., 2012).

Chapter 4 GEOSPATIAL DATA LAYERS USED BY DSS-WISE HCOM

In addition to simulation results provided by DSS-WISE Lite, DSS-WISE HCOM uses two types of geospatial data layers for the PAR analysis:

1. U.S. population data, and
2. U.S. county data

This section briefly presents the most important features of these geospatial data layers.

4.1 U.S. Population Data Used by DSS-WISE HCOM

DSS-WISE HCOM extracts the PAR numbers that will be potentially affected by the flood by interfacing the simulation results, such as the inundation extent, maximum flood depth (h_{max}) and maximum specific discharge magnitude, DV_{max}) provided by DSS-WISE™ Lite, with the geospatial population data.

DSS-WISE HCOM module uses two different sets of population data for this purpose:

1. 2010 Census Block data provided by the U.S. Census Bureau. This data can be considered as the nighttime population data.
2. LandScan USA gridded nighttime and daytime population data, which is developed and maintained by the Oak Ridge National Laboratory (ORNL) located in Oak Ridge, TN.

The information about these two datasets is provided in the following subsections.

4.1.1 2010 Census Block Population Data

4.1.1.1 General Information on U.S. Census Data

The United States Census Bureau (USCB, or officially the Bureau of the Census) is a federal government agency in charge of producing data about the people and economy of the U.S. The USCB is part of the U.S. Department of Commerce.

USCB is in charge of conducting the U.S. Census every 10 years for the purpose allocating the seats of the U.S. House of Representatives based on population data. The last U.S. Census was conducted in 2010.

Information related to population in the U.S. and related facts, statistics and projections can be found at the website of U.S. Census Bureau (https://www.census.gov/). A quick summary of population statistics can be found by accessing the website https://www.census.gov/quickfacts/fact/table/US/PST120217, which is the QuickFacts page maintained by USCB.

USCB makes geospatial census data available to the public and professionals through the Topologically Integrated Geographic Encoding and Referencing (TIGER) database system, which can accessed at the website https://www.census.gov/geo/maps-data/data/tiger.html. USCB disseminates various census related data also through its American FactFinder website (https://www.census.gov/geo/maps-data/data/tiger.html).

The population data is reported at geographic summary levels that follow a hierarchical order. From smaller to larger, some of these levels can be listed as follows:

1. **Census Blocks** (https://www.census.gov/geo/reference/gtc/gtc_block.html):
   A census block is the smallest geographic unit for which USCB collects data from all the houses in the unit (rather than a sample of houses). Census Blocks are bounded by visible features such as streets, roads, streams and nonvisible features such as property lines and limits of city, township, school district, and counties, etc. They are defined as polygons covering the entire territory of the U.S. including Puerto Rico and the island areas (American Samoa, the Commonwealth of the Northern Mariana Islands, Guam, and the United States Virgin Islands).

   Each census block is identified by a unique four-digit ID number from 0000 to 9999 within a census tract. The first digit of the census block ID number identifies the number of the block group. Block numbers beginning with a zero (i.e. blocks in Block Group 0) are associated with water-only areas.

   2010 Census includes 11,166,336 Census Blocks and 545,653 “water-only” Census Blocks covering the Unites States, Puerto Rico and the Island Areas. It should be noted that 4,871,270 blocks have zero population (http://tumblr.mapsbynik.com/post/82791188950/nobody-lives-here-the-nearly-5-million-census). The area covered by these uninhabited census blocks is 4.61 million square kilometers, which corresponds to 47% of the total territory of the U.S.

   DSS-WISE™ Lite calculates nighttime PAR using 2010 census block data.

1. Census Block Groups (https://www.census.gov/geo/reference/gtc/gtc_bg.html):
   A census block is a group of census blocks in the same census tract that share the same first digit in their census block ID. A census block group may contain between 600 to 3,000 people. Census blocks comprising a census block generally define a contiguous area.

   Each census block group has a unique single digit number from 0 to 9 within a census tract. In the 2010 Census a block group 0, i.e. “water-only” census blocks, can be part of any census tract; not just part of a “water only” census tract.

   2010 Census includes 220,742 Census Block Groups and 607 “water-only” Census Block Groups covering the Unites States, Puerto Rico and the Island Areas.

2. Census Tracts (https://www.census.gov/geo/reference/gtc/gtc_ct.html):
   A census tract comprises a number of census block groups. A census tract may contain between 1,200 to 8,000 people. In order to be able to make comparisons between census data taken at different periods, a special effort is made to define census tract boundaries unchanged over a long period. Nevertheless, as the population increases or declines, census tracts may have to be split or merged.

   Each census tract is uniquely identified by a number with up to four digits, which may be followed by an optional suffix of two digits. It is considered that the two-digit suffix is separated from the preceding digits by an implied decimal point. More information about the tract codes can be found on the web page given above.

The 2010 Census includes 74,134 Census Tracts and 366 "water-only" Census Tracts covering the Unites States, Puerto Rico and the Island Areas.

3. Counties (https://www.census.gov/geo/reference/gtc/gtc_cou.html):
   Each county or statistically equivalent entity comprises a number of census tracts.

   Each county or statistically equivalent entity is assigned a three-character numeric Federal Information Processing Series (FIPS) code based on alphabetical sequence that is unique within state and an eight-digit National Standard feature identifier.

   For more information, please consult the web page given above.

4. States (https://www.census.gov/geo/reference/gtc/gtc_state.html)
   Each state or statistically equivalent entity comprises a number of census tracts. USCB provides the data for 50 states, the District of Columbia, Puerto Rico, American Samoa, the Commonwealth of the Northern Mariana Islands, Guam, and the U.S. Virgin Islands. They are identified by a numeric Federal Information Processing Series (FIPS) code.

The tally of Census Blocks, Census Block Groups and Census Tracks by State and Territory can be found at https://www.census.gov/geo/maps-data/data/tallies/tractblock.html. A dictionary for the definitions of various geographic terms and concepts used in 2010 Census is available at https://www.census.gov/geo/reference/terms.html.

The next U.S. census will be conducted in 2020. However, the USCB provides a Planning Database (PDB) (https://www.census.gov/research/data/planning_database/) with projected values of housing, demographic, socioeconomic, and census operational data at the block group and tract levels for years 2012, 2014, 2015, 2016, and 2018. The website also explains the methodology used.

One of the two data sets used by DSS-WISE HCOM for PAR analysis is the 2010 population data at the census block level.

4.1.1.2 2010 Census Block Data

The Tiger/Line® Shapefiles and Tiger/Line® Files for different years (vintages) can be downloaded from https://www.census.gov/geo/maps-data/data/tiger-line.html. The shapefiles are available for the fifty states, the District of Columbia, Puerto Rico, and the island areas (American Samoa, the Commonwealth of the Northern Mariana Islands, Guam, and the United States Virgin Islands). They include polygon boundaries of geographic areas and features, linear features including roads and hydrography, and point features. They do not contain any sensitive data.

- FTP site for 2010 TIGER data
  https://www2.census.gov/geo/tiger/TIGER2010/
- The technical documentation on 2010 Tiger/Line® Shapefiles is available at
  https://www2.census.gov/geo/pdfs/maps-data/data/tiger/tgrshp2010/TGRSHP10SF1.pdf
- The guidance on downloading Tiger/Line® Shapefiles is available at:
  https://www2.census.gov/geo/pdfs/education/tiger/Downloading_TIGERLine_Shp.pdf

USCB has produced a special version of shapefiles that provide the 2010 Census block geography together with population and housing unit counts. These shapefiles were created for a special project. They contain only selected attributes of the TIGER/Line Shapefiles. The record layout for these shapefiles are shown in Table 3. These shapefiles are available directly at the state level for the 50 states and the District of Columbia. They were downloaded from https://www2.census.gov/geo/tiger/TIGER2010/TABBLOCK/2010/

Table 3 Record layout of census block shapefile with housing and population for Census 2010.

Field	Length	Type	Description
STATEFP10	2	String	2010 Census state FIPS code
COUNTYFP10	3	String	2010 Census county FIPS code
TRACTCE10	6	String	2010 Census census tract code
BLOCKCE	4	String	2010 Census tabulation block number
BLOCKID10	15	String	Block identifier; a concatenation of 2010 Census state FIPS code, county FIPS code, census tract code and tabulation block number.
PART	1	String	Part Flag Indicator – Y = partial block, N = whole block; Part Flag should always be N in these files
HOUSING10	100	Number	2010 Census Housing Unit Count
POP10	100	Number	2010 Census Population Count

For American Samoa (4 files), Guam (1 file), Commonwealth of the Mariana Islands (4 files), Puerto Rico (78 files), and Virgin Islands of the United States (91 files), 2010 census data containing population and housing unit counts are available at the county or equivalent entity level. The numbers in parenthesis indicate the number of the individual files that need to be combined to create state or territory level shapefiles similar to those that are available for the 50 states and the District of Columbia. These files can be downloaded from https://www2.census.gov/geo/tiger/TIGER2010/TABBLOCK/2010/. They can also be downloaded from the USCB website using an API (Application Programming Interface)[17].

DSS-WISE Lite Development Team prepared the state level shapefiles with the same record layout as the one listed in Table 3 by downloading the individual files using the API provided by USCB. The county level files has more attributes than those listed in Table 3. Therefore, the files for the U.S. territories were downloaded by querying only selected fields and were appended to form a single file at the state level.

Table 4 lists all 2010 census block files that are stored in the DSS-WISE Lite system and used by DSS-WISE HCOM. The first 51 files are the state level shapefiles that were directly downloaded from the USCB website. The five rows highlight in light yellow are the U.S. Territory-level shapefiles, which were created by the DSS-WISE Lite Development Team. The row for the U.S. Minor Outlying Islands, for which no data is available, is highlighted in pink.

[17] For more information on APIs, consult the USCB webpage for developers (https://www.census.gov/developers/), which provides links to various API related information for developers.

Table 4 List of 2010 census block files with population and housing data.

No	File Name	State FIPS Code	Abbreviation	State Name
1	tabblock2010_01_pophu	01	AL	Alabama
2	tabblock2010_02_pophu	02	AK	Alaska
3	tabblock2010_04_pophu	04	AZ	Arizona
4	tabblock2010_05_pophu	05	AR	Arkansas
5	tabblock2010_06_pophu	06	CA	California
6	tabblock2010_08_pophu	08	CO	Colorado
7	tabblock2010_09_pophu	09	CT	Connecticut
8	tabblock2010_10_pophu	10	DE	Delaware
9	tabblock2010_11_pophu	11	DC	District of Columbia
10	tabblock2010_12_pophu	12	FL	Florida
11	tabblock2010_13_pophu	13	GA	Georgia
12	tabblock2010_15_pophu	15	HI	Hawaii
13	tabblock2010_16_pophu	16	ID	Idaho
14	tabblock2010_17_pophu	17	IL	Illinois
15	tabblock2010_18_pophu	18	IN	Indiana
16	tabblock2010_19_pophu	19	IA	Iowa
17	tabblock2010_20_pophu	20	KS	Kansas
18	tabblock2010_21_pophu	21	KY	Kentucky
19	tabblock2010_22_pophu	22	LA	Louisiana
20	tabblock2010_23_pophu	23	ME	Maine
21	tabblock2010_24_pophu	24	MD	Maryland
22	tabblock2010_25_pophu	25	MA	Massachusetts
23	tabblock2010_26_pophu	26	MI	Michigan
24	tabblock2010_27_pophu	27	MN	Minnesota
25	tabblock2010_28_pophu	28	MS	Mississippi
26	tabblock2010_29_pophu	29	MO	Missouri
27	tabblock2010_30_pophu	30	MT	Montana
28	tabblock2010_31_pophu	31	NE	Nebraska
29	tabblock2010_32_pophu	32	NV	Nevada
30	tabblock2010_33_pophu	33	NH	New Hampshire
31	tabblock2010_34_pophu	34	NJ	New Jersey
32	tabblock2010_35_pophu	35	NM	New Mexico
33	tabblock2010_36_pophu	36	NY	New York
34	tabblock2010_37_pophu	37	NC	North Carolina
35	tabblock2010_38_pophu	38	ND	North Dakota
36	tabblock2010_39_pophu	39	OH	Ohio
37	tabblock2010_40_pophu	40	OK	Oklahoma
38	tabblock2010_41_pophu	41	OR	Oregon
39	tabblock2010_42_pophu	42	PA	Pennsylvania
40	tabblock2010_44_pophu	44	RI	Rhode Island
41	tabblock2010_45_pophu	45	SC	South Carolina

42	tabblock2010_46_pophu	46	SD	South Dakota
43	tabblock2010_47_pophu	47	TN	Tennessee
44	tabblock2010_48_pophu	48	TX	Texas
45	tabblock2010_49_pophu	49	UT	Utah
46	tabblock2010_50_pophu	50	VT	Vermont
47	tabblock2010_51_pophu	51	VA	Virginia
48	tabblock2010_53_pophu	53	WA	Washington
49	tabblock2010_54_pophu	54	WV	West Virginia
50	tabblock2010_55_pophu	55	WI	Wisconsin
51	tabblock2010_56_pophu	56	WY	Wyoming
52	tl_2010_60_tabblock10	60	AS	American Samoa
53	tl_2010_66_tabblock10	66	GU	Guam
54	tl_2010_69_tabblock10	69	MP	Commonwealth of the Mariana Islands
55	tl_2010_72_tabblock10	72	PR	Puerto Rico
	Not Available	74	UM	U.S. Minor Outlying Islands
56	tl_2010_78_tabblock10	78	VI	Virgin Islands of the United States

4.1.2 LandScan USA Gridded Nighttime and Daytime Population Data

LandScan USA[18] is a collection of gridded nighttime and daytime population datasets developed by the Oak Ridge National Laboratory (ORNL), Department of Energy. These gridded population datasets are available as raster files with reference to WGS 84 horizontal datum and have a resolution of 3 arc-second. They were developed by combining satellite remote sensing data, geospatial infrastructure datasets, and demographic data provided by USCB.

Nighttime population is the number of resident population, who resides in a given area during the nighttime hours. During daytime the same area may have a different population because:

- some of the population, ainly the area go to work in another area

In contrast, the daytime population refers to the number of people who are present in an area during typical business hours, including workers, children in school, people in hospitals or other short-term medical facilities, people temporarily staying in lodging facilities, and customers present at retail locations (McKenzie et al. 2013).

The census block population data should be considered as nighttime population data because it accounts for the resident population.

$$CAAP = TAP + TWWA - TWLA \tag{14}$$

The variables in the above expression are defined as follows:
$CAAP$: commuter adjusted area population
TAP: total area population

[18] https://landscan.ornl.gov/

$TWWA$: total number of workers working in the area
$TWLA$: total number of workers living in the area

and is equal to the nighttime population given by the census block data

The spatial distribution of the population in census blocks is not available for distributing the population into 3 arc-second grid cells. Rather than assuming a uniform distribution of the population over the census block area, researchers at ORNL used the "Intelligent" dasymetric modeling method to assign the population counts to the grid cells (Dobson et al. 2000 and Bhaduri et al. 2007). In this method, for each grid cell first a statistical value for "likelihood of being populated" is determined based on proximity to landmarks and geographic features such as roads and water bodies, and by considering terrain features such as slope. ORNL has even incorporated the structure location data into their methodology. In order to maintain the integrity of the census data, it was imposed that the sum of the population numbers for all the cells in a census block remains equal to the total population of that census block. The LandScan USA datasets used in this report are projections for 2016 (McKee et al. 2014). Daytime data is generated using specially developed techniques for population dynamics[19].

The available LandScan USA datasets are listed in Table 5. Daytime gridded population data for Puerto Rico is not available. The histograms of number of cells with different population counts are plotted in Figure 22 for all available LandScan USA datasets.

Table 5 Available LandScan USA datasets.

Dataset Name (all datasets have a resolution of 90 m)	Number of Grid Cells in the Dataset	Total Population for the Dataset	Number of Cells without Population	Max. Population in a Grid Cell
CONUS nighttime population (CONUS_NIGHT)	1,223,614,768	320,957,062	1,189,592,346	3,287
CONUS daytime population (CONUS_DAY)	1,223,614,772	320,957,062	1,191,123,851	34,661
Alaska nighttime population (AK_NIGHT)	450,553,781	741,716	450,342,823	609
Alaska daytime population (AK_DAY)	450,553,781	741,716	450,427,445	13,911
Hawaii nighttime population (HI_NIGHT)	3,556,221	1,423,033	3,449,721	12,043
Hawaii daytime population (HI_DAY)	3,556,221	1,423,033	3,499,370	12,348
Puerto Rico nighttime population (PR_NIGHT)	1,097,714	3,411,307	820,350	773

[19] https://www.csm.ornl.gov/workshops/RAMSworkshop07/presentations/bhaduri.ppt

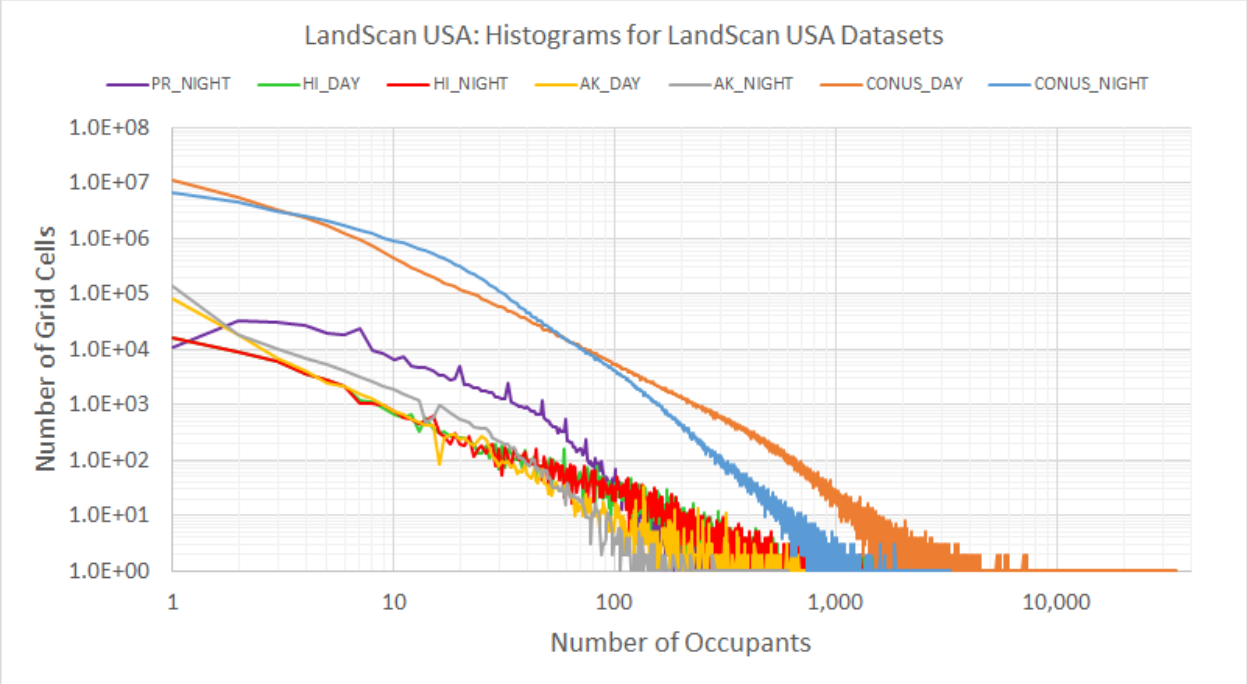

Figure 22 Histograms of cell counts with different populations.

4.1.3 Converting Gridded Population Data to Gridded Population Density Data

Consider the superposition of the LandScan USA population data grid and the computational grid shown based on UTM projection in Figure 23. The computational grid has a uniform projected cell size, which is specified by the user in the range 20 ft. (6.1 m) to 200 ft (61 m). LandScan population data refers to WGS 84 datum and has a uniform grid size of 3 arc-second. When projected using the UTM system, the edge length of a 3 arc-second cell size varies from 52.68 m at the northernmost tip of Alaska (71.295556°) to 90.25 m at the southernmost tip of Puerto Rico (17.883174°). Thus, the results produced by DSS-WISE Lite, have always a higher resolution than that of the population data.

Figure 23 also shows the computed maximum inundation polygon and the computational cells that are under or touching the polygon. In order to have an estimate of the number of people affected, it is necessary to use the inundation polygon as a mask and count the population in each cell. This is a challenging task not only due to the difference in cell sizes of the population grid and computational grid but also due to the difference in the origin and positioning of the two grids as can be seen in Figure 23.

The solution is to create a gridded population density data layer that can be readily interfaced with the computational grid. Consider the inundated computational cell identified by row and column indices (i, j) having a surface area of $(A_c)_{i,j}$. Let the center of the cell (i, j) be located in the population density cell (k, ℓ). Let also the population density of the cell (k, ℓ) be $(\rho_P)_{k,\ell}$. Then the number of people affected by the flood in the cell (i, j) becomes a simple multiplication

$$(N_C)_{i,j} = (A_c)_{i,j} \times (\rho_P)_{k,\ell} \tag{15}$$

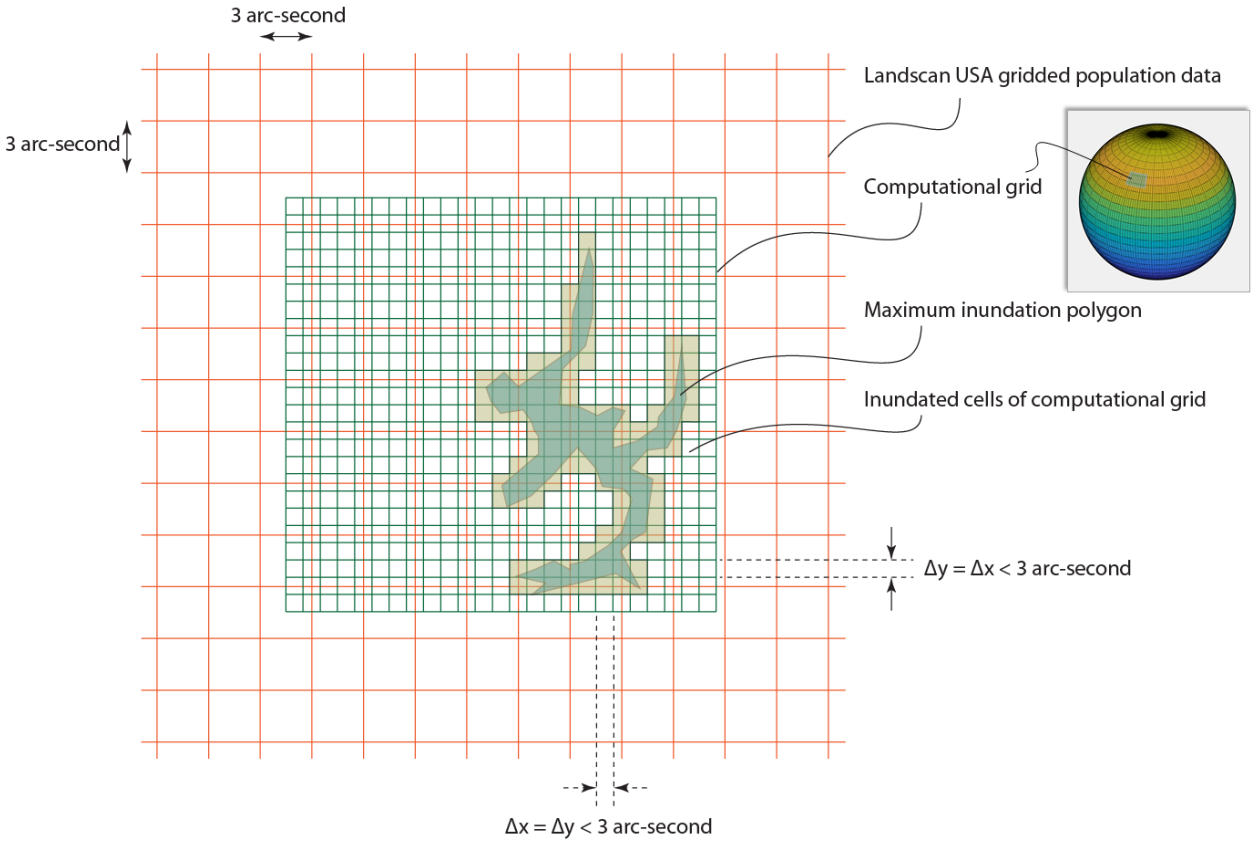

Figure 23 Gridded population data and the computational grid.

In order to apply this methodology, the LandScan USA gridded nighttime and daytime population data must be converted into gridded nighttime and daytime population density data. The population density can be calculated by dividing the population count in the cell by the cell area. Consider the population grid cell (k, ℓ) with a population count of $(N_P)_{k,\ell}$ and the surface area $A_{k,\ell}$. The population density can be calculated from

$$(\rho_P)_{k,\ell} = \frac{(N_P)_{k,\ell}}{A_{k,\ell}} \tag{16}$$

Eq. (16) looks simple but its application is more complicated than it looks due to the fact that the area of a 3 arc-second quadrangle on the reference ellipsoid is not constant but varies with latitude. Consider the reference ellipsoid shown in Figure 24. Meridians, which are also called longitudes, and parallels, which are also called latitudes, are shown at 12° intervals for legibility (3 arc-second intervals would be impossible to see at this scale).

ϕ denotes geographic latitude, which is also called geodetic latitude. It is defined as the angle a line perpendicular to the surface of the reference ellipsoid at a given point makes with the plane of the Equator. The equator serves as the reference latitude of $\phi = 0°$. To the north, the latitude varies from $\phi = 0°$ at the Equator to $\phi = +90°$ at the North Pole. To the south, the latitude varies from $\phi = 0°$ at the equator to $\phi = -90°$ at the South Pole.

In Figure 24, four quadrangles at different latitudes are highlighted in magenta and numbered from 1 to 4. All four quadrants have edges defined by 12° arcs of longitude and latitude but the shapes and corresponding areas and edge lengths are different. The quadrangle 1 is near the equator. It has a shape close to a square and has the largest area among the four selected quadrants. Since the meridians converge towards north and south poles, away from the Equator, the quadrants become elongated and their areas become smaller. Quadrangle 4 has an elongated shape and its areas is the smallest among the four selected quadrants. In fact, near the poles, quadrangles become triangles. Thus the variation of the surface area of 3 arc-second quadrangles of the gridded population data must be taken into account for converting population counts in 3 arc-second cells into population densities.

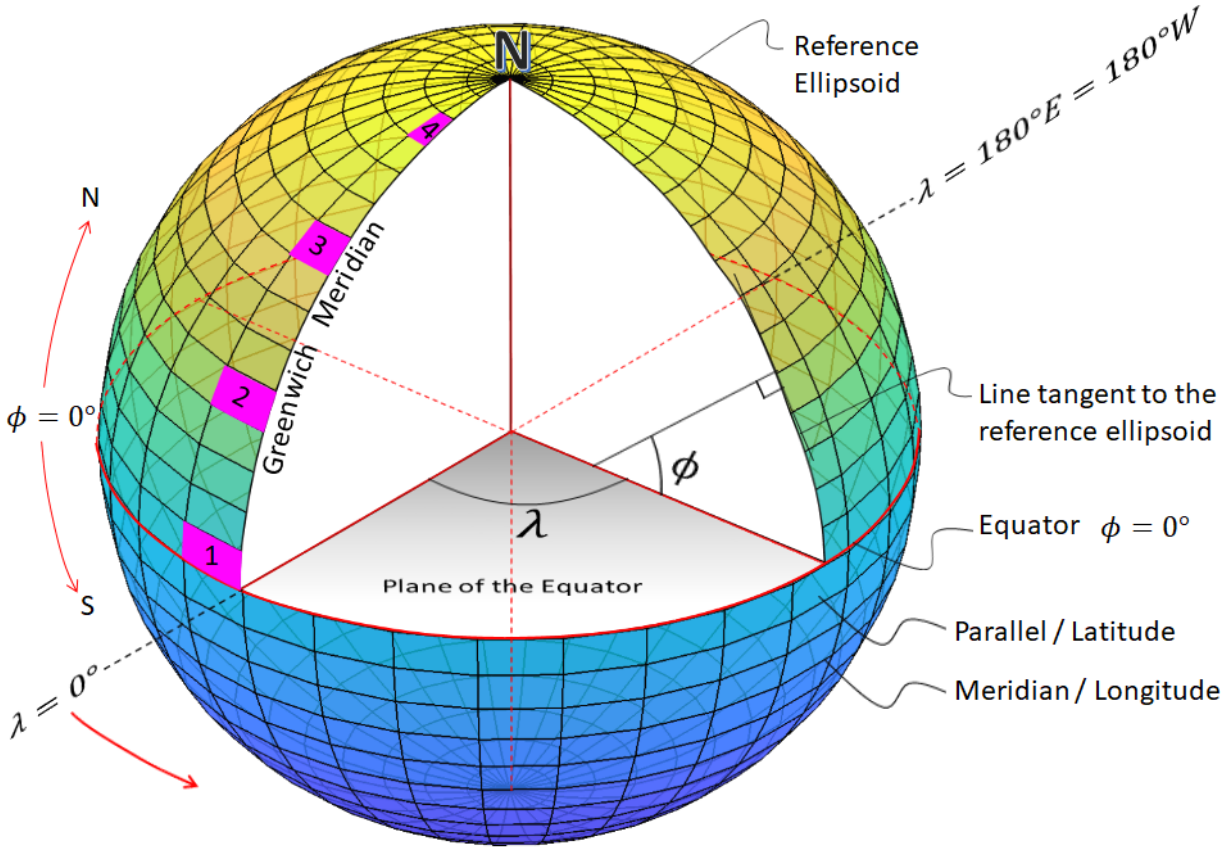

Figure 24 Definition of latitude and longitude and the areas of quadrangles on the reference ellipsoid.

Consider the lines of latitudes and longitudes at regularly placed intervals form a grid as shown in Figure 25. The cells of the grid are quadrangles, except around north and south poles, where they become triangles. Consider the quadrangle on the reference ellipsoid defined by two geodetic latitudes, ϕ_1 and ϕ_2, and two longitudes, λ_1 and λ_2. The surface area of this quadrangle can be computed by projecting the quadrangle onto the associated authalic sphere, which is defined as the cylinder having the same radius as the reference ellipsoid. When the quadrangle is projected onto the authalic sphere, the geodetic latitudes ϕ_1 and ϕ_2 on the reference ellipsoid are transformed into authalic latitudes β_1 and β_2, respectively. The longitudes λ_1 and λ_2 are unaffected by the projection and remain the same.

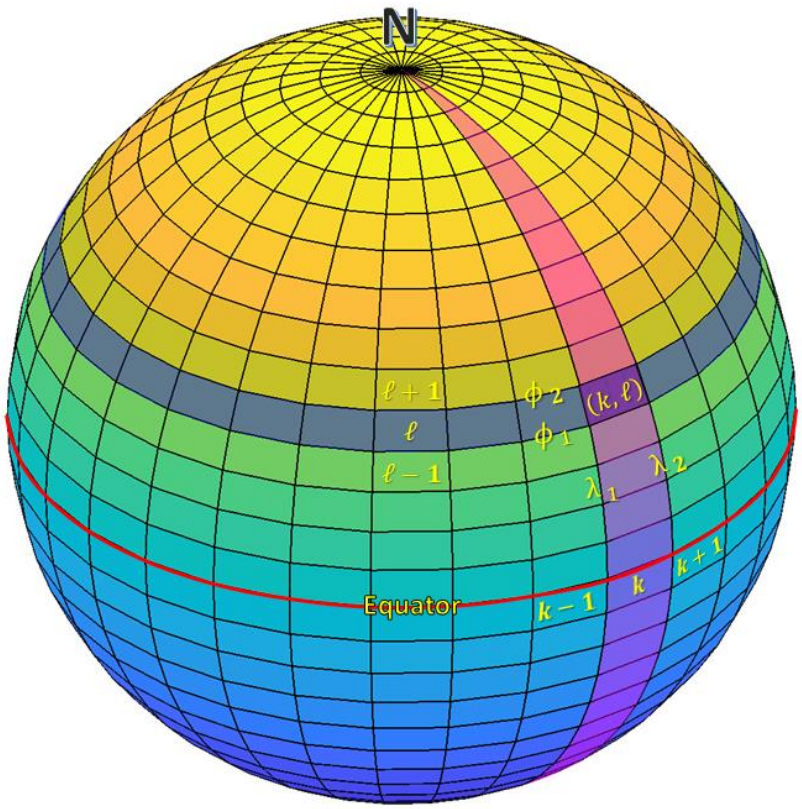

Figure 25 Definition of the quadrangle on the reference ellipsoid.

The area of the quadrangle projected onto the authalic sphere is given by the surface integral (Tobler and Chen, 1986)

$$A = \int_{\beta_1}^{\beta_2} R \left[\int_{\lambda_1}^{\lambda_2} R \cos\varphi \, d\lambda \right] d\varphi = \int_{\beta_1}^{\beta_2} R^2 \cos\varphi \, d\varphi \int_{\lambda_1}^{\lambda_2} d\lambda = R^2 (\lambda_2 - \lambda_1) \int_{\beta_1}^{\beta_2} \cos\varphi \, d\varphi \qquad (17)$$

Simplification of Eq. (17) leads to the expression

$$A = R^2 (\lambda_2 - \lambda_1) (\sin\beta_2 - \sin\beta_1) \qquad (18)$$

The quadrangle projected onto the authalic sphere has the same surface area as the quadrangle on the reference ellipsoid. Moreover, any closed shape on the ellipsoid and its projection on the authalic sphere have the same surface area. Thus, Eq. (18) is also the equation of the quadrangle on the reference ellipsoid defined by the geodetic latitudes ϕ_1 and ϕ_1 and longitudes λ_1 and λ_2.

In order to use Eq. (18) to calculate the area of a quadrangle between geodetic latitudes ϕ_1 and ϕ_1 and longitudes λ_1 and λ_2 on the ellipsoid, the geodetic latitudes ϕ_1 and ϕ_2 must first be converted to the authalic latitudes β_1 and β_2, respectively.

Consider a latitude ϕ on a reference ellipsoid with an (first) eccentricity of e. Referring to Snyder (1986), the corresponding authalic latitude, β, is given by the expression

$$\beta = \sin^{-1}\left(\frac{q}{q_p}\right) \tag{19}$$

where

$$q = (1 - e^2)\left\{\frac{\sin\phi}{(1 - e^2\sin^2\phi)} - \frac{1}{2e}\ln\left(\frac{1 - e\sin\phi}{1 + e\sin\phi}\right)\right\} \tag{20}$$

and q_p is the value of q at the polar latitude of $\phi = \pi/2$. The eccentricity of the reference ellipsoid is defined as

$$e = \sqrt{1 - \frac{b^2}{a^2}} \tag{21}$$

Referring to Figure 1, a is the semimajor axis (also called equatorial radius) of the spheroid, and b is the semi-minor axis (also called polar radius) of the ellipsoid of reference. Note that the semi-minor axis can be related to semi-major axis a using the flattening of the reference ellipsoid, f, or the eccentricity e of the reference ellipsoid as follows:

$$b = a(1 - f) = a\sqrt{1 - e^2} \tag{22}$$

The radius of the authalic sphere having the same surface area as a specific reference ellipsoid is calculated from

$$R_2 = a\sqrt{\frac{q_p}{2}} \tag{23}$$

where a is the semi-major axis of the reference ellipsoid. Note that authalic radius is also defined as

$$R_2 = c\left(\int_0^{\pi/2} \frac{\cos\Phi}{(1 + e'^2\cos^2\Phi)^2}\, d\Phi\right) \tag{24}$$

and it can be calculated using the following series approximation

$$R_2 = c\left(1 - \frac{2}{3}e'^2 + \frac{26}{45}e'^2 - \frac{100}{189}e'^6 + \frac{7034}{14175}e'^8\right) \tag{25}$$

It should be noted that, in Eqs (17) through (20) and (24), the longitude λ and the latitudes Φ and β are all expressed in radians. The longitude is assumed to vary in the range:

$$0 \le \lambda_1 \le \lambda \le \lambda_2 \le 2\pi \tag{26}$$

whereas the geodetic and authalic latitudes vary in the range

$$-\pi/2 \le \Phi_1 \le \Phi \le \Phi_2 \le +\pi/2 \qquad \text{and} \qquad -\pi/2 \le \beta_1 \le \beta \le \beta_2 \le +\pi/2 \tag{27}$$

In Eq. (16), the gridded population data is considered as a matrix $(N_P)_{k,\ell}$ with $k = 1, \dots, M$ and $\ell = 1, \dots, N$. Figure 26 shows a schematic illustration of the LandScan USA population data grid for CONUS on the background image of the globe taken from Google Earth, which uses WGS 84 datum. The population data grid cells are defined with an interval of 3 arc second in both geodetic latitude and longitude, thus

$$\Delta\phi = \Delta\lambda = 3 \text{ arc-second} \tag{28}$$

In order to be able to apply Eq. (16), one should generate an exactly matching grid for the surface area of the grid cells, $(A)_{k,\ell}$ with $k = 1, \dots, M$ and $\ell = 1, \dots, N$. On the other hand, it can easily be seen that the surface area $(A)_{k,\ell}$ is only a function of the latitude (see Figure 25). In other words, on a given latitude, the surface area $(A)_{k=const,\ell}$ remains constant for any longitude (see for example the latitude band between ϕ_1 and ϕ_2, which is highlighted in blue). This means that the generated $M \times N$ matrix of surface area will have the same value along a row $k = 1, \dots, N$. Based on this observation, it is sufficient to create only one column of surface-area matrix as a one-dimensional vector $(A)_\ell$. Then, Eq. (16) can be used in the following simplified form

$$(\rho_P)_{k,\ell} = \frac{(N_P)_{k,\ell}}{A_\ell} \tag{29}$$

One dimensional array of surface-area vector A_ℓ was computed on the WGS 84 ellipsoid.

The nighttime and daytime gridded population data are provided in WGS 84 geographic coordinates with a uniform resolution of 3 arc-seconds. WGS 84 stands for World Geodetic System of 1984. It is an earth-centered and earth-fixed reference system and geodetic datum. The reference ellipsoid, although very similar, is slightly different than the GRS 80, which is the reference ellipsoid for the NAD 83 datum used by the USGS 1/3 arc-second DEM tiles.

The column vector is between any two meridional ellipses ϕ_1 and ϕ_2 satisfying the relationship $\Delta\lambda = \lambda_2 - \lambda_1 = 3$ arc-second. The latitude was varied from north pole $\phi = +90°$ to south pole $\phi = -90°$ using the interval ($\Delta\phi = \phi_2 - \phi_1 = 3$ arc-second $= 0.0008333333330° = 0.000014544410$ rad). This leads to a column vector of 216,000 elements.

For each element, the surface area was calculated using Eq. (18). The authalic latitudes β_1 and β_2 appearing in Eq. (18) were computed from the bounding geodetic latitudes ϕ_1 and ϕ_2 using Eq. (19). This computation requires the knowledge of the eccentricity of the ellipsoid e. The eccentricity of the WGS 84 ellipsoid is given in Table 1 as $e = 0.081819191$. By inserting $\phi = \pi/2$ in Eq. (19), one calculates the constant value of:

$$q_p = 1.995531088 \tag{30}$$

Using this q_p-value, the authalic latitudes β_1 and β_2 corresponding to the pairs of geodetic latitudes ϕ_1 and ϕ_2 (with $\Delta\phi = \phi_2 - \phi_1 = 3$ arc-second) are obtained using Eq. (19)

$$\beta_1 = \sin^{-1}\left(\frac{q_1}{q_p}\right) \qquad \text{and} \qquad \beta_2 = \sin^{-1}\left(\frac{q_2}{q_p}\right) \tag{31}$$

in which, values of latitudes q_1 and q_2 are given by Eq. (20)

$$q_1 = (1-e^2)\left\{\frac{\sin\phi_1}{(1-e^2\sin^2\phi_1)} - \frac{1}{2e}\ln\left(\frac{1-e\sin\phi_1}{1+e\sin\phi_1}\right)\right\} \tag{32}$$

$$q_2 = (1-e^2)\left\{\frac{\sin\phi_2}{(1-e^2\sin^2\phi_2)} - \frac{1}{2e}\ln\left(\frac{1-e\sin\phi_2}{1+e\sin\phi_2}\right)\right\} \tag{33}$$

Finally, the area of the quadrangle between latitudes ϕ_1 and ϕ_2 are computed using Eq. (18).

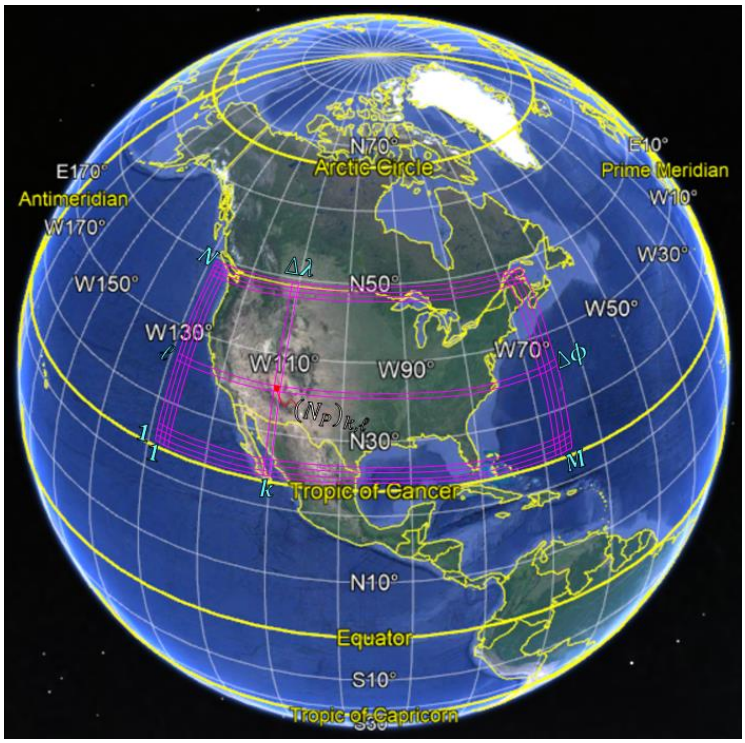

Figure 26 Schematic illustration of LandScan USA population data grid (in magenta color) for CONUS (background image is taken from Google Earth).

Using this procedure, NCCHE development team created two gridded population density data layers: one for nighttime and the other for the daytime population densities. Each layers combines all available data as a seamless raster. The nighttime layer shown in Figure 29 includes data layers for CONUS, Alaska, Hawaii, and Puerto Rico. Daytime layer shown in Figure 30 includes data layers for CONUS, Alaska, and Hawaii. Stored in the DSS-WISE Lite system, these two files are used for PAR analysis computations using gridded LandScan USA data. The methodology for using these files is presented later in Chapter 18.2.

Before closing this chapter, it would be interesting to look at the quantitative difference between authalic latitude and geodetic latitude. Figure 27 shows the difference (in degrees) between geodetic

and authalic latitudes, $(\phi - \beta)$, as a function of geodetic latitude, ϕ. The difference between geodetic and authalic latitudes is zero at the poles and at the equator. The difference $(\phi - \beta)$ has the maximum value of $|(\phi - \beta)_{max}| = 0.128\ 297\ 358\ 920°$ at the geodetic latitudes $\phi = \mp 45.055°$.

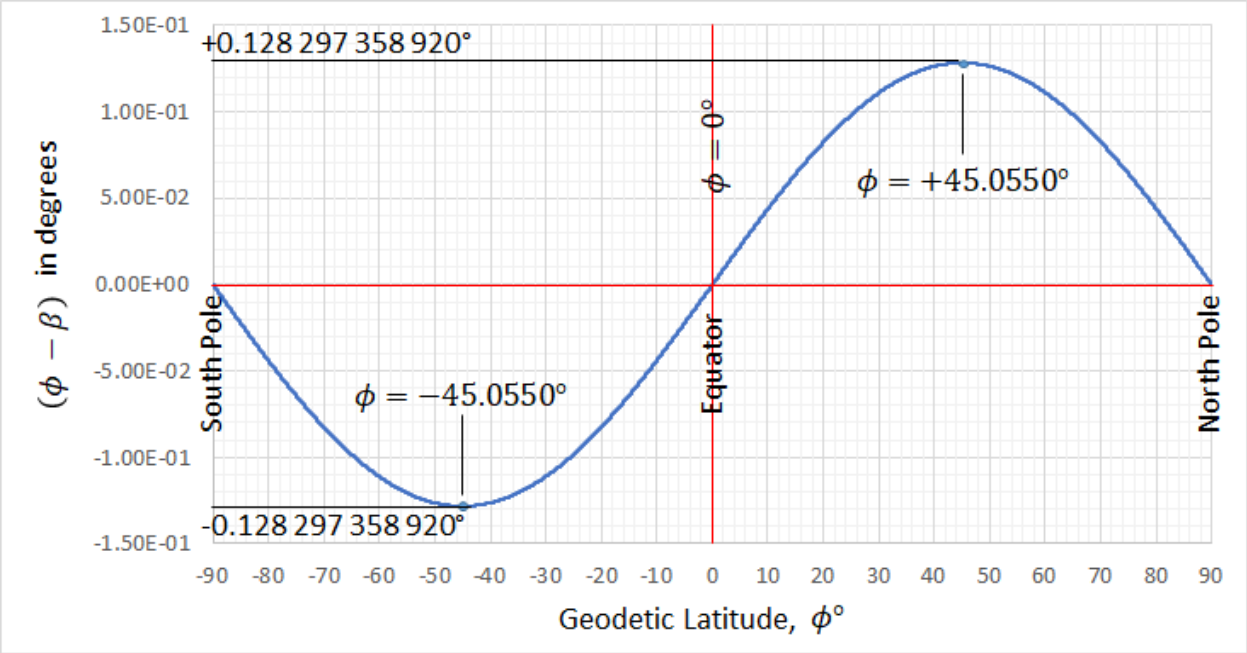

Figure 27 Difference between geodetic and authalic latitudes $(\phi - \beta)$ as a function of geodetic latitude, ϕ (computed for GRS 80 ellipsoid).

Finally, Figure 28 shows the variation of the area of a 3 arc-second quadrangle as a function of latitude. As it can be seen the maximum value of the quadrangle area is at the equator $A = 8547.967\ m^2$. This roughly corresponds to a square area having an edge length of 92.46 m. The quadrangle area decreases away from the equator and becomes zero at the poles.

The importance of using the correct grid area when calculating population density can be better understood by considering the quadrangle areas at the northernmost and southernmost latitudes of the CONUS, for example

- The northernmost incorporated place in all U.S. territory is Utqiaġvik, Alaska, which has the geodetic coordinates 71°17'44"N 156°45'59"W. At this latitude ($\phi = 71.29556°$), the surface area of the quadrangle is 2774.94 m^2 and corresponds roughly to a square area having an edge length of 52.68 m.
- The northernmost incorporated place in CONUS is Sumas, Washington, which has the geodetic coordinates 49°00'08.6"N 122°15'40"W. At this latitude ($\phi = 49.00238889°$), the surface area of the quadrangle is 5650.84 m^2 and corresponds roughly to a square area having an edge length of 75.17 m.
- The southernmost incorporated place in CONUS is Key West, Florida, which has the geodetic coordinates 24°32'38.724"N 81°48'17.658"W. At this latitude ($\phi = 24.54409°$), the surface area of the quadrangle is 7731.69 m^2 and corresponds roughly to a square area having an edge length of 87.93 m.

- The southernmost incorporated place in all U.S. territory is Southern tip of Isla Caja de Muertos in Puerto Rico, which has the geodetic coordinates 17° 52' 59.4264"N 66° 31' 43.5252"W. At this latitude ($\phi = 17.883174°$), the surface area of the quadrangle is 8145.26 m^2 and corresponds roughly to a square area having an edge length of 90.25 m.

As it can be seen, between the southernmost and northernmost latitudes of CONUS, the change in quadrangle area is about 27% whereas the change in the edge of the cell is about 14%.

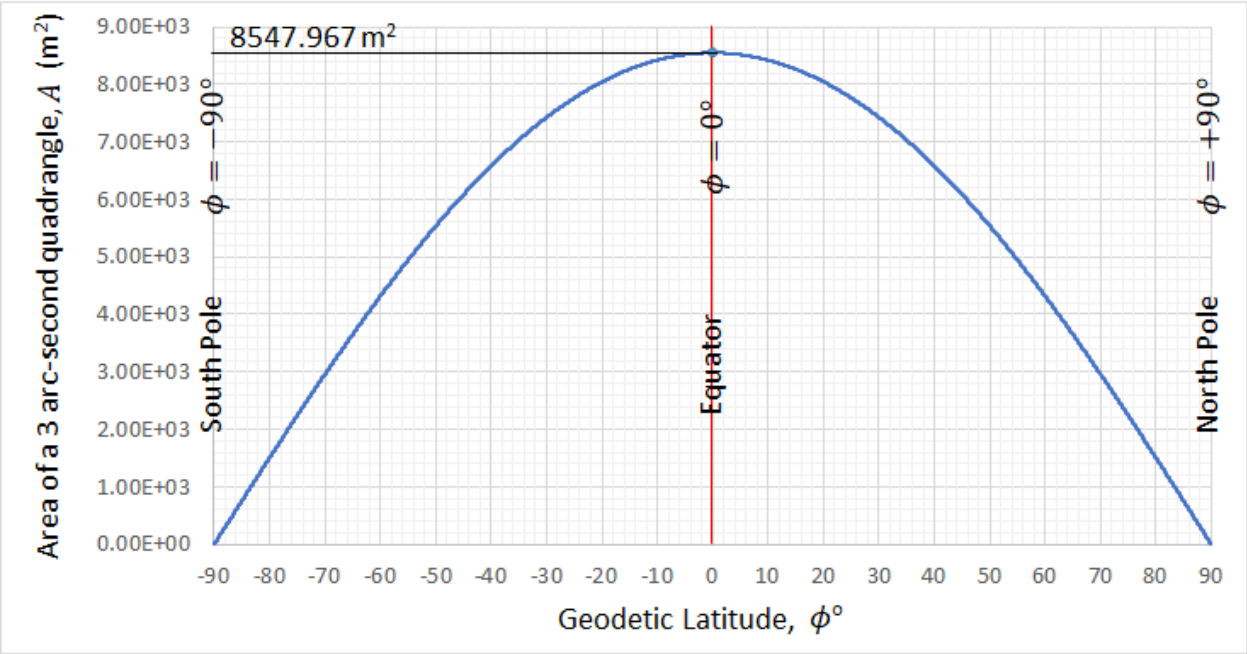

Figure 28 Area of a 3 arc-second quadrangle on the GRS 80 reference ellipsoid as a function of geodetic latitude, ϕ (computed for GRS 80 ellipsoid).

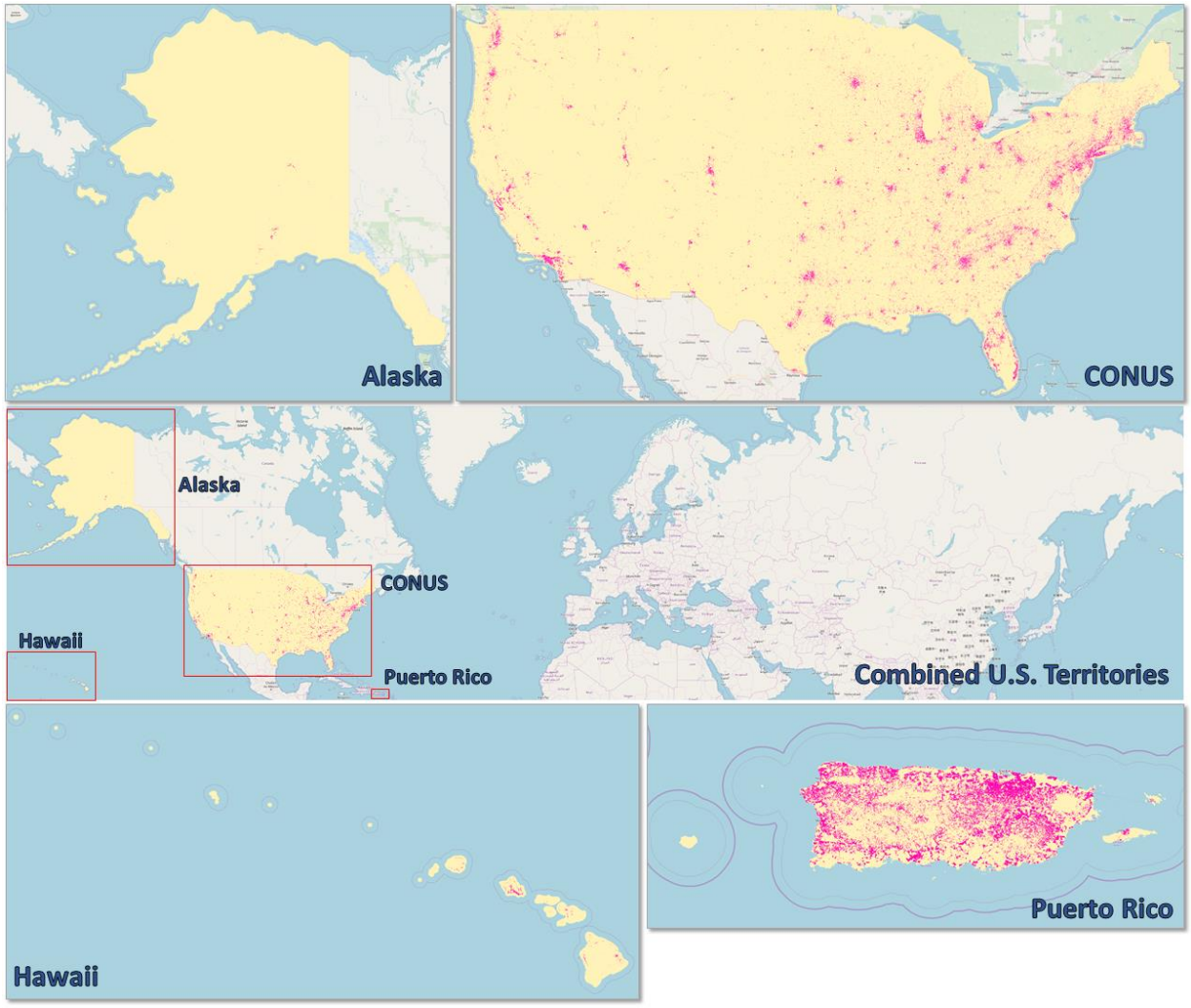

Figure 29 Combined nighttime population density raster at 1/3 arc-second resolution. The scale for the population density in the inserts is locally varied for visibility purposes.

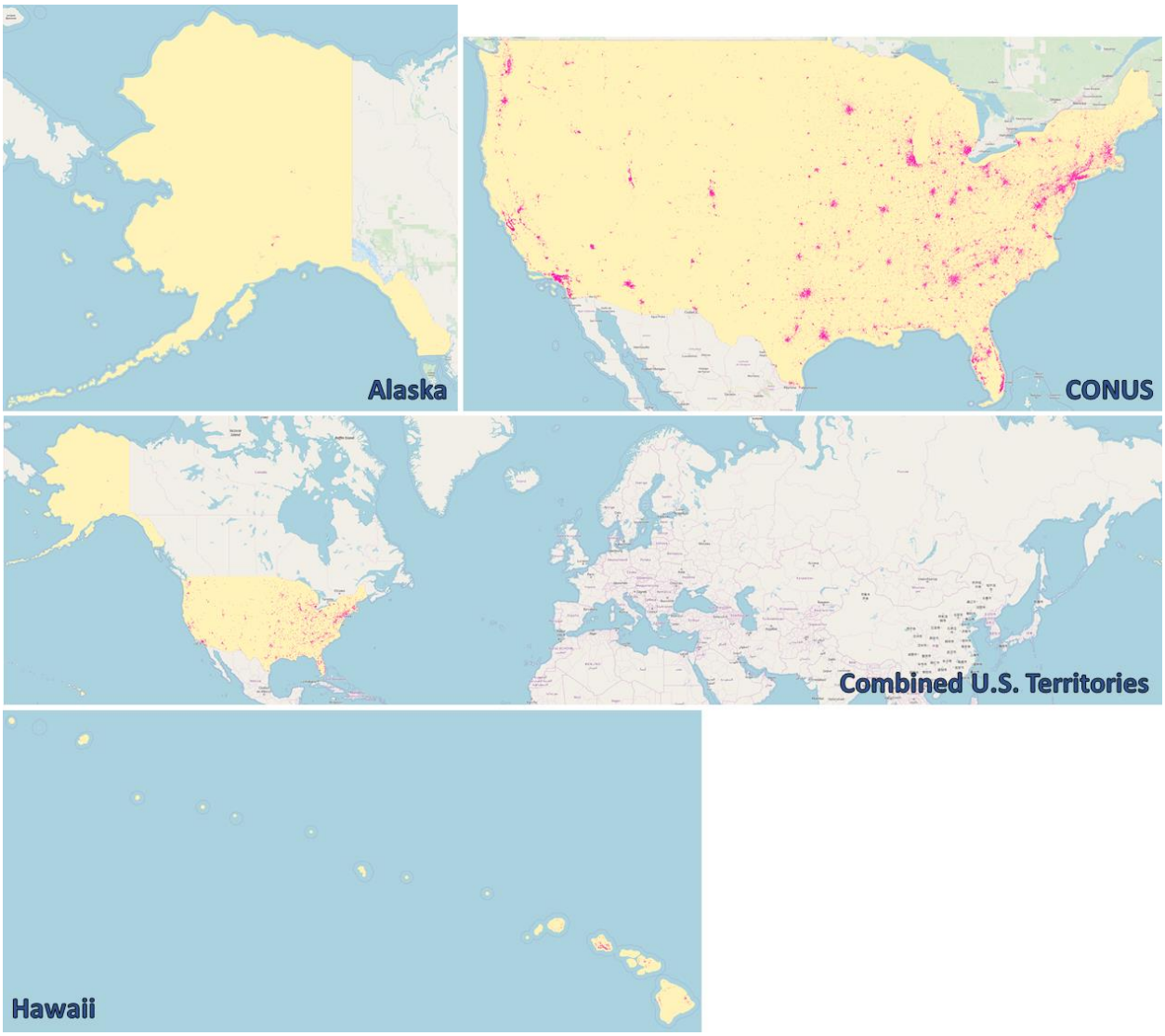

Figure 30 Combined daytime population density raster at 1/3 arc-second resolution. The scale for the population density in the inserts is locally varied for visibility purposes.

4.2 U.S. County Shapefiles Used by DSS-WISE HCOM

2010 county data shapefiles by state and U.S. Territory was downloaded from the USCB website ftp://ftp2.census.gov/geo/tiger/TIGER2010/COUNTY/2010/. Table 6 shows the record layout of these shapefiles.

Table 6 2010 U.S. County and equivalent entity shapefile from TIGER/line Shapefiles

Field	Length	Type	Description[20]
STATEFP10	2	string	2010 Census state FIPS code
COUNTYFP10	3	string	2010 Census county FIPS code
COUNTYNS10	8	string	2010 county GNIS code
GEOID10	5	string	County identifier; a concatenation of 2010 state FIPS code and county FIPS code
NAME10	100	string	2010 county name
NAMELSAD10	100	string	2010 name and the translated legal/statistical area description for county
LSAD10	2	string	2010 legal/statistical area description code for county
CLASSFP10	2	string	2010 FIPS class code
MTFCC10	5	string	2010 MAF/TIGER feature class code (G4020)
CSAFP10	3	string	2010 combined statistical area code
CBSAFP10	5	string	2010 metropolitan statistical area/micropolitan statistical area code
METDIVFP10	5	string	2010 metropolitan division code
FUNCSTAT10	1	string	2010 functional status
ALAND10	14	number	2010 land area
AWATER10	14	number	2010 water area
INTPTLAT10	11	string	2010 latitude of the internal point
INTPTLON10	12	string	2010 longitude of the internal point

DSS-WISE HCOM uses county shapefiles only for the purposes of improving the efficiency of search for census blocks. Many of the fields listed in Table 6 are not needed. The county shapefiles of the 50 states and U.S. Territories were combined into a single shapefile by removing unnecessary attributes. The combined TIGER/Line shapefile of U.S. counties and equivalent entities contains 3,221 records. The geographic location of the polygons are shown in Figure 31. The attributes of the features in the shapefile are listed in Table 7.

[20] For the descriptions of the fields, see https://www2.census.gov/geo/pdfs/maps-data/data/tiger/tgrshp2017/TGRSHP2017_TechDoc.pdf

Figure 31 USA county polygons from the TIGER/Line shapefile.

Table 7 Attributes for the features in the combined TIGER/Line shapefile of U.S. counties and equivalent entities.

Field	Length	Type	Description
NO			
GEO_ID	14	string	County identifier; a concatenation of 2010 state FIPS code and county FIPS code
STATE	2	string	Census state FIPS code
COUNTY	2	string	Census county FIPS code
NAME	100	string	County name
LSAD	2	string	Legal/statistical area description code for county
CENSUSAREA		number	Surface area of the polygon feature.

Chapter 5 BRIEF DESCRIPTION OF DSS-WISE HCOM

DSS-WISE HCOM is essentially a post-processing module. It provides an assessment of human consequences of a dam-break (or a levee-break) floods simulated by DSS-WISE Lite. The analysis is based on the post processing the computational results and two types of population data: 1) 2010 Census Block data provided by the U.S. Census Bureau; and 2) LandScan USA gridded nighttime and daytime population data developed and maintained by the Oak Ridge National Laboratory (ORNL).

DSS-WISE HCOM generates four types of analysis:

1. Flood Hazard Mapping for humans
    a. Flood hazard mapping for population caught outdoors
    b. Flood hazard mapping for population caught indoors
2. Mapping of Potentially Lethal Flood Zones (PLFZ) for humans
    a. PLFZ for children
    b. PLFZ for adults
3. Analysis of the evolution of inundation areas by hazard classes
4. Analysis of Population at Risk (PAR) numbers by interfacing results from DSS-WISE Lite with population data
    a. Nighttime PAR using LandScan USA nighttime population
    b. Daytime PAR using LandScan USA daytime population
    c. PAR analysis using 2010 census block data

DSS-WISE HCOM generates a results package containing three types of files:

1. A PDF report with text, tables and maps presenting a summary of the results produced by DSS-WISE HCOM
2. A Microsoft Excel file with the following worksheets containing analysis results
    a. Project Summary
    b. Hazard Categories
    c. Tabular data and stacked bar chart showing evolution of inundation area as a function of both time and flood hazard category
    d. Tabular data and stacked bar chart showing evolution of nighttime PAR as a function of both time and flood hazard category
    e. Tabular data and stacked bar chart showing evolution of daytime PAR as a function of both time and flood hazard category
    f. Tabular data for all 2010 census blocks completely or partially affected by the inundation
3. A series of shape files as listed below
    a. Shapefile of flood hazard categories
        i. ESRI shapefile of polygon type containing the polygons of flood hazard categories for people caught outdoors.
        ii. ESRI shapefile of polygon type containing the polygons of flood hazard categories for people caught indoors.
    b. ESRI shapefile of polygon type containing the polygons of potentially lethal flood zones (PLFZs) for adults and children.
    c. Shapefiles of population densities
        i. ESRI shapefile of polygon type containing the polygons of nighttime population density computed from LandScan USA
        ii. ESRI shapefile of polygon type containing the polygons of daytime population density computed from LandScan USA

d. ESRI shapefile of polygon type containing the 2010 census block polygons completely or partially filled by the inundation along with computed statistics of selected flood parameters within each area.

5.1 Launching DSS-WISE HCOM Analysis and Monitoring its Progress

DSS-WISE HCOM does not require any additional data from the user. The population data used in the PAR analysis is stored in DSS-WISE Web Cluster. The simulation results are directly taken from the DSS-WISE Lite simulation.

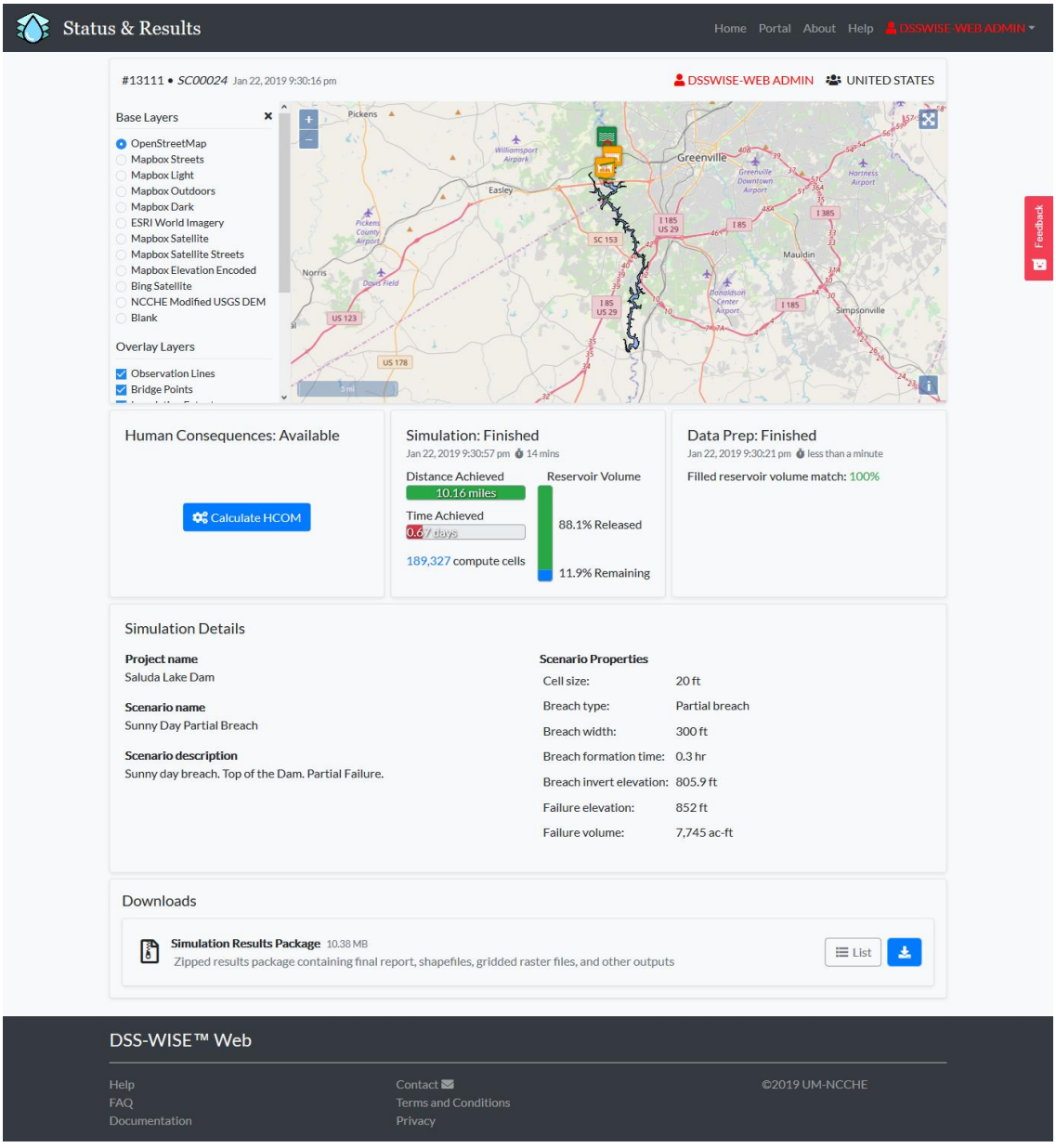

Figure 32 Status and Results page after a successful DSS-WISE Lite simulation.

Figure 32 shows the Status and Results page after successful completion of a DSS-WISE Lite simulation. Note that the "Downloads" panel at the bottom of the page displays the "Simulation Results Package, which is available for download as a single zipped file by clicking on the blue download icon far right. Clicking on the "List" button displays the list of DSS-WISE Lite results files included in the package.

Since the simulation has been launched on or before January 21, 2019[21], the Status and Results page displays a panel called "Human Consequences" on the left immediately below the map. The panel shows the status as "Available" and includes a blue button with the label "Calculate HCOM". DSS-WISE HCOM analysis is launched simply by clicking on the blue button.

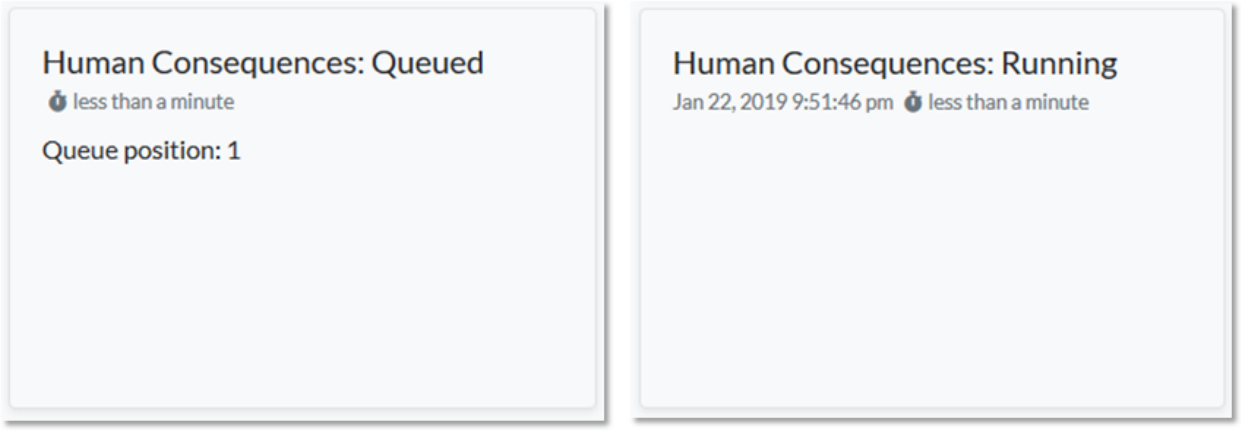

Figure 33 "Human Consequences" panel when the analysis queued (left) and running (right).

Immediately after DSS-WISE HCOM is launched, the panel displays the status as "Queued" and the position in the queue (left side in Figure 33). Current duration of the wait in the queue is shown as "less than a minute". As the analysis request remains in the queue, the duration of the wait is updated at regular intervals.

When the DSS-WISE HCOM analysis is launched, the panel displays the status as "Running" (right side in Figure 33). The panel displays the date and time when the analysis started to run. Duration since the beginning of the simulation is shown as "less than a minute". As the computations continue, the duration of the computation is updated at regular intervals.

Figure 34 shows the Status and Results page after the completion of the DSS-WISE HCOM analysis. The contents of "Human Consequences" panel have been updated. The status is changed to "Finished". The duration of the computation is shown as 12 minutes. The panel summarizes some key findings:

- Nighttime PAR is found to be 229
- Daytime PAR is found to be 93
- Inundated area (maximum inundated area) covers 1,264 acres, and
- The number of South Carolina counties affected by the flood is 3.

Human Consequences Results Package has now been added into the "Downloads" panel at the bottom of the Status and Results page. The package can be downloaded as a single zipped file by clicking on the

[21] DSS-WISE HCOM analysis is not available for DSS-WISE Lite simulations launched before January 21, 2019. For these simulations, the Status and Results page will not display the "Human Consequences" panel.

blue download icon far right. Clicking on the “List” button displays the list of DSS-WISE HCOM results files included in the package. Figure 35 shows the final results packages for DSS-WISE Lite and DSS-WISE HCOM and the individual files that they contain.

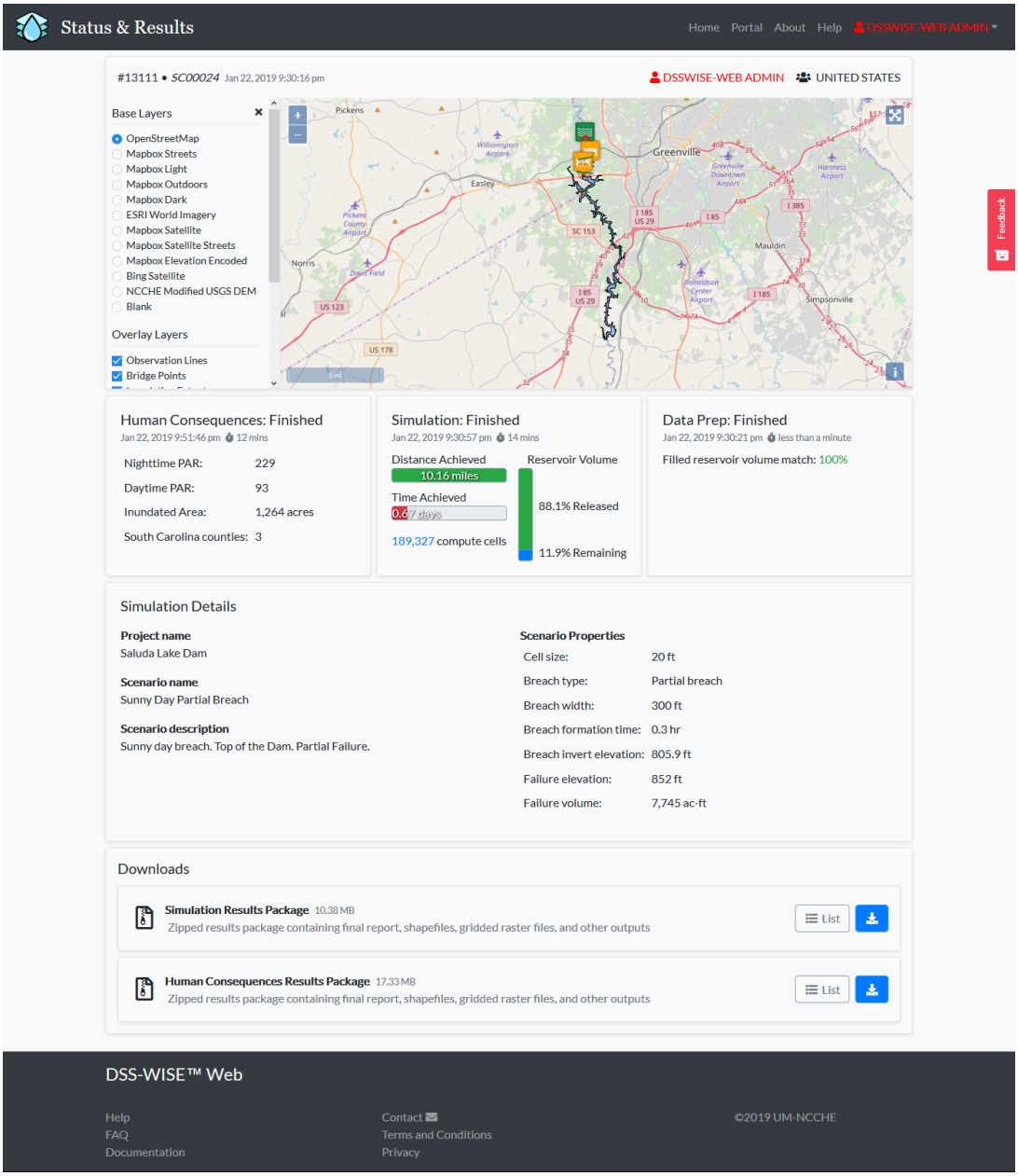

Figure 34 Status and Results page after successful completion of DSS-WISE HCOM analysis.

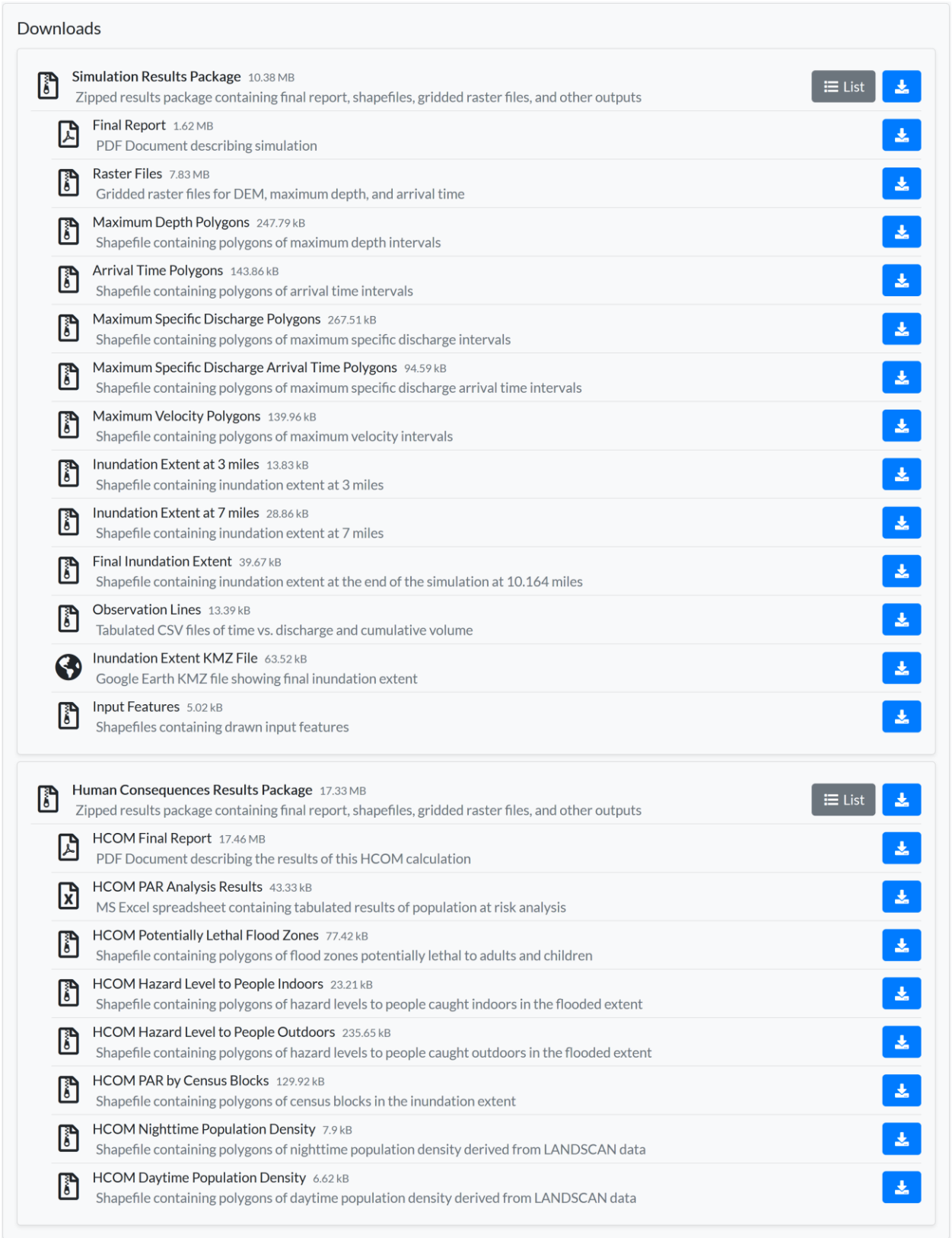

Figure 35 List of files in the final results packages of DSS-WISE Lite and DSS-WISE HCOM.

5.2 Naming Convention for Results Files of DSS-WISE Lite and DSS-WISE HCOM

The names of the output files
<JOB ID>_<Results Name>_<Units>_<Type>_<Qualifier>.<File Extension>

<JOB ID> JOB ID is an integer number corresponding to the serial number of DSS-WISE Lite simulation request. DSS-WISE HCOM analysis results for a DSS-WISE Lite simulation have the same JOB ID number. For the explanations and examples given in this chapter, the JOB ID will be denoted by "X".

<Results Name> This field describes the type of results output in the file. The possible results types are listed below:

1. DVmax_Arrival_Time
2. DVmax
3. Flood_Arrival_Time
4. Hmax
5. Input_Shapes (Folder)
6. breachpoint
7. bridges
8. observationlines
9. reservoirs
10. structures
11. Inundation_Extent_3_mi
12. Inundation_Extent_7_mi
13. Inundation_Extent_15_mi
14. Inundation_Extent_60_mi
15. Inundation_Extent_Final_<Y>_mi
    <Y> stand for the farthest distance in miles between the breach point and the farthest tip of the flood extent at the end of the simulation
16. Arrival_Time
17. DEM
18. H
19. Vmax
20. DSS-WISE_Lite_Final_Report

<Units> This field specifies the units in which the results are provided. The possible units are:

1.	hr	hour
2.	ft2ps	ft^2/s
3.	ft	ft
4.	ftps	ft/s
5.	persqmi	number of people per square miles

<Qualifier> Qualifier is optional in the file name. When it is included as part of the file name, it provides additional information on the types of results being provided

1. polygons_upto_final
2. polygons
3. upto_final

<File Extension> The filename extension is an identifier indicating the characteristics of the files and/or using which software it can be opened and used. Under the Windows operating to system, it is also used by different software packages to identify the files they can open and use. Filename extension is specified as a suffix, which is separated by a period from the name of the computer file. The file extensions in the results packages of DSS-WISE Lite and DSS-WISE HCOM are listed below:

1. zip compressed file containing one or more folders and files
2. dbf shapefile feature geometry
3. prj shapefile projection metadata
4. shp shapefile future geometries
5. shx shapefile index format
6. kmz Keyhole Markup language Zipped file
7. csv comma separated value file
8. tif GeoTiff file, which is a TIFF (Tagged Image File Format) with embedded georeferencing information
9. pdf Adobe Acrobat file (PDF stands for Portable Document Format)
10. xlsx Microsoft Excel file

The ESRI shapefile of polygon type or point type is in fact a collection of files containing different type of information. In the case of results provided by DSS-WISE Lite and DSS-WISE HCOM, each shapefile of polygon or point type is collection of four files residing in the same directory. All files have the same file name (*filename*) but different file extensions as listed below:

filename.shp shape format: this file contains the feature geometry itself

filename.shx shape index format: positional index of the feature geometry to facilitate forward or backward searches

filename.dbf attributes format: this file contains columnar attributes for each feature in dBase IV[22] format

filename.prj projection format: this file contains the information on the coordinate system and projection information as a text file using WKT (Well Known Text) format.

When working with a GIS software, such as QGIS, it is sufficient to load only the file *filename*.shp. The other files with the same file name but different files extension are automatically loaded into the software. Since the collection of the files include the projection format file (*filename*.prj), the shapes are displayed at their correct geospatial location.

[22] dBase is a data base software (http://www.dbase.com/)

Table 8 List of results files provided by DSS-WISE Lite.

No	Folder or File Name	Type	Explanation	Remarks
1	X_All_Files.zip	Zipped Root folder	This is the zipped root folder which contains all DSS-WISE Lite simulation results for the simulation with ID number "X", which is an integer number.	This file is used for downloading all DSS-WISE Lite results together.
1.2	X_Report	Subfolder		
1.2.a	X_DSS-WISE_Lite_Final_Report.pdf	PDF	Automatically generated final report	
1.3	X_Raster_Files	Subfolder		
1.3.a	X_Arrival_Time_hr_upto_final.tif	Raster	Flood arrival time, T_{arr}. This raster file is generated at the end of the simulation.	Can be used for estimating the time available for d/s population to escape.
1.3.b	X_DEM_ft.tif	Raster	DEM used as computational grid. It provides the digital map of ground elevation Z_b. Note that in reservoir type simulations, the elevation of computational cells under the foot print of the breached section of the dam are modified based on the specified failure scanerio.	USGS 1/3 arc-second DEM tiles are used as base layer, which is then modified by removing large water bodies, bridges specified by the user, and by burning in NLD levees and estimated reservoir bottom topography
1.3.c	X_DVmax_Arrival_Time_hr_upto_final.tif	Raster	Flood arrival time of the maximum specific discharge, Tq_{arr}. This raster file is generated at the end of the simulation. Although provided for the sake of completeness, this result is difficult to interpret given the fact that each cell has a different value of DV_{max}. It can be helpful when it is used together with the DV_{max} raster (X_DVmax_ft2ps_upto_final.tif).	Provides information on when the DV_{max} value was achieved over the inundation area. Note that DV_{max} values for different cells are different.

No	Folder or File Name	Type	Explanation	Remarks
1.3.d	X_DVmax_ft2ps_upto_final.tif	Raster	Maximum specific discharge, i.e. maximum value of the depth times velocity, DV_{max}, achieved during the simulation. This raster is generated at the end of the simulation.	Used for estimating hazard levels for humans, buildings and infrastructures. Since in different cells DV_{max} is achieved at different times, this raster does not correspond to any specific time.
1.3.e	X_Hmax_ft_upto_final.tif	Raster	Maximum flood depth, H_{max}, achieved during the simulation. This raster is generated at the end of the simulation.	Since in different cells H_{max} is achieved at different times, this raster does not correspond to any specific time.
1.3.f	X_H_ft_at_final.tif	Raster	This is raster file of final flow depths at the end of the simulation, h_{final}. This raster is generated at the end of the simulation.	Provided that the simulation duration is sufficient, it can be used to evaluate how soon the flood recedes and which areas will have ponding water.
1.3.g	X_Vmax_ftps_upto_final.tif	Raster	Maximum flow velocity magnitude, V_{max}, achieved during the simulation. This raster is generated at the end of the simulation.	Since in different cells V_{max} is achieved at different times, this raster does not correspond to any specific time.
1.4	X_Hmax_ft_polygons_upto_final	Subfolder		
1.4.1.a	X_Hmax_ft_polygons_upto_final.dbf	Shapefile	Up to 9 stacked polygons of H_{max} delineating areas of flood depth greater than predefined depths values.	Based on H_{max} raster See
1.4.1.b	X_Hmax_ft_polygons_upto_final.prj			
1.4.1.c	X_Hmax_ft_polygons_upto_final.shp			
1.4.1.d	X_Hmax_ft_polygons_upto_final.shx			
1.5	X_Flood_Arrival_Time_hr_polygons_upto_final	Subfolder		

1.5.a	X_Flood_Arrival_Time_hr_polygons_upto_final.dbf	Shapefile	Up to 8 stacked polygons of T_{arr}, which delineate areas of flood arrival from the time of the breach to a predefined time.	Based on T_{arr}raster
1.5.b	X_Flood_Arrival_Time_hr_polygons_upto_final.prj			
1.5.c	X_Flood_Arrival_Time_hr_polygons_upto_final.shp			
1.5.d	X_Flood_Arrival_Time_hr_polygons_upto_final.shx			
1.6	X_DVmax_ft2ps_polygons_upto_final	Subfolder		
1.6.a	X_DVmax_ft2ps_polygons_upto_final.dbf	Shapefile	Up to 9 polygons of DV_{max} delineating areas of flood velocity corresponding to predefined velocity intervals.	Based on DV_{max} raster.
1.6.b	X_DVmax_ft2ps_polygons_upto_final.prj			
1.6.c	X_DVmax_ft2ps_polygons_upto_final.shp			
1.6.d	X_DVmax_ft2ps_polygons_upto_final.shx			
1.7	X_DVmax_Arrival_Time_hr_polygons_upto_final	Subfolder	Subfolder containing the ESRI shapefile of polygon type containing the polygons of the arrival time of DVmax.	
1.7.a	X_DVmax_Arrival_Time_hr_polygons_upto_final.dbf	ESRI Shapefile of polygon type	Up to 8 polygons of Tq_{arr}, which delineate areas of arrival time of DV_{max} corresponding to predefined time intervals.	Based on Tq_{arr}raster
1.7.b	X_DVmax_Arrival_Time_hr_polygons_upto_final.prj			
1.7.c	X_DVmax_Arrival_Time_hr_polygons_upto_final.shp			
1.7.d	X_DVmax_Arrival_Time_hr_polygons_upto_final.shx			
1.8	X_Vmax_ftps_polygons_upto_final	Subfolder		
1.8.a	X_Vmax_ftps_polygons_upto_final.dbf	ESRI Shapefile of polygon type	Up to 8 polygons of V_{max}, which delineate areas of flood velocity corresponding to predefined velocity intervals.	Based on V_{max} raster
1.8.b	X_Vmax_ftps_polygons_upto_final.prj			
1.8c	X_Vmax_ftps_polygons_upto_final.shp			
1.8.d	X_Vmax_ftps_polygons_upto_final.shx			
1.9	X_Inundation_Extent_3_mi	Subfolder		
1.9.a	X_Inundation_Extent_3_mi.dbf	ESRI Shapefile of polygon type	Intermediate inundation extent polygon generated when the flood front has reached 3 miles from the breach point.	Generated only if the flood propagates 3 miles from the breach point
1.9.b	X_Inundation_Extent_3_mi.prj			
1.9.c	X_Inundation_Extent_3_mi.shp			
1.9.d	X_Inundation_Extent_3_mi.shx			
1.10	X_Inundation_Extent_7_mi	Subfolder		
1.10.a	X_Inundation_Extent_7_mi.dbf	ESRI Shapefile of polygon type	Intermediate inundation extent polygon generated when the flood front has reached 7 miles from the breach point.	Generated only if the flood propagates 7 miles from the breach point
1.10.b	X_Inundation_Extent_7_mi.prj			
1.10.c	X_Inundation_Extent_7_mi.shp			
1.10.d	X_Inundation_Extent_7_mi.shx			
1.11	X_Inundation_Extent_15_mi	Subfolder		
1.11.a	X_Inundation_Extent_15_mi.dbf	ESRI Shapefile of polygon type	Intermediate inundation extent polygon generated when the flood front has reached 15 miles from the breach point.	Generated only if the flood propagates 15 miles from the breach point
1.11.b	X_Inundation_Extent_15_mi.prj			
1.11.c	X_Inundation_Extent_15_mi.shp			
1.11.d	X_Inundation_Extent_15_mi.shx			

1.12	X_Inundation_Extent_60_mi	Subfolder		
1.12.1.a	X_Inundation_Extent_60_mi.dbf	ESRI Shapefile of polygon type	Intermediate inundation extent polygon generated when the flood front has reached 60 miles from the breach point.	Generated only if the flood propagates 60 miles from the breach point
1.12.1.b	X_Inundation_Extent_60_mi.prj			
1.12.1.c	X_Inundation_Extent_60_mi.shp			
1.12.1.d	X_Inundation_Extent_60_mi.shx			
1.13	X_Inundation_Extent_Final_Y_mi	Subfolder		
1.13.a	X_Inundation_Extent_Final_Y_mi.dbf	ESRI Shapefile of polygon type	This is the maximum inundation polygon generated at the end of the simulation. It covers all computational cells affected by the flood even if it were temporarily.	Always generated.
1.13.b	X_Inundation_Extent_Final_Y_mi.prj			
1.13.c	X_Inundation_Extent_Final_Y_mi.shp			
1.13.d	X_Inundation_Extent_Final_Y_mi.shx			
1.14	X_Observation_Lines	Subfolder		
1.14.a	OLIN_0000001.csv	Comma Separated Value (csv) file	For reservoir-type simulation the last csv file is the one automatically defined by DSS-WISE Lite by using the crest line of the breached structure.	Provides discharge hydrographs and total volume passing over the obs. line
1.14.b	OLIN_0000002.csv			
…	…..			
1.14.NN	OLIN_00000NN.csv			
1.15	X_KMZ			
1.15.a	X_Inundation_Extent_Final_10.215_mi.kmz	KMZ file	This is the maximum inundation polygon to be viewed using Google Earth.	Can be used for easy dissemination of the inundation extent.
1.16	X_Input_Shapes	Subfolder		
1.16.a.1	X_breachpoint.dbf	ESRI Shapefile of point type	Shapefile contains the breach point located at the center of the breach.	Always generated.
1.16.a.2	X_breachpoint.prj			
1.16.a.3	X_breachpoint.shp			
1.16.a.4	X_breachpoint.shx			
1.16.b.1	X_bridges.dbf	ESRI Shapefile of point type	Shapefile contains the center of the user specified bridges that are taken out from the DEM.	It is generated only if the user has defined bridges to be removed from DEM.
1.16.b.2	X_bridges.prj			
1.16.b.3	X_bridges.shp			
1.16.b.4	X_bridges.shx			
1.16.c.1	X_observationlines.dbf	ESRI Shapefile of polygon type	Shapefile contains the polylines captured by the user as observation lines. In reservoir-type simulation, there is at least one observation line corresponding to the crest line of breached structure.	It is generated only if the system extends the crest line of the breached structure.
1.16.c.2	X_observationlines.prj			
1.16.c.3	X_observationlines.shp			
1.16.c.4	X_observationlines.shx			
1.16.d.1	X_reservoirs.dbf	ESRI Shapefile of point type	Shapefile, contains the reservoir point, which is the location clicked by the user on the map when user was asked to provide the “upstream point”.	Always generated.
1.16.d.2	X_reservoirs.prj			
1.16.d.3	X_reservoirs.shp			
1.16.d.4	X_reservoirs.shx			

1.16.e.1	X_structures.dbf	ESRI Shapefile of polygon type	Shapefile contains the polylines by the user as crest lines for the impounding structures.	Always generated.
1.16.e.2	X_structures.prj			
1.16.e.3	X_structures.shp			
1.16.e.4	X_structures.shx			
1.16.f.1	X_extendedstructures.dbf	ESRI Shapefile of polygon type	Shapefile contains the polyline corresponding to the crested line of the breach structure corrected by extending it to contain the reservoir.	It is generated only if the system extends the crest line of the breached structure.
1.16.f.2	X_extendedstructures.prj			
1.16.f.3	X_extendedstructures.shp			
1.16.f.4	X_extendedstructures.shx			

Table 9 List of results files provided by DSS-WISE HCOM.

No	Folder or File Name	Type	Explanation	Remarks
1	X_All_Files.zip	Zipped Root folder	This is the zipped root folder which contains all DSS-WISE HCOM results for the DSS-WISE Lite simulation with ID number "X", which is an integer number.	This file is used for downloading all DSS-WISE Lite results together.
1.1	X_HCOM_Report		Subfolder containing the PDF file of the report automatically generated by DSS-WISE HCOM.	
1.1.a	X_HCOM_Final_Report.pdf	PDF	This is the automatically produced report at the end of the DSS-WISE HCOM analysis.	The file contains text, tables and maps summarizing the results of DSS-WISE HCOM analysis.
1.2	X_HCOM_Analysis	Subfolder	Subfolder containing the Microsoft Excel file of the results of PAR and inundation area extent analysis	
1.2.a	X_HCOM_Analysis.xlsx	Excel file with 6 worksheets	This excel file contains the results of the PAR analysis using both 2010 census block data and gridded nighttime and daytime populations.	Results are available as tables and stacked bar charts
1.3	X_HCOM_PLFZ_polygons		Subfolder containing the ESRI shapefile of polygon type containing the polygons of potentially lethal flood zones (PLFZs) for adults and children.	
1.3.a	X_HCOM_PLFZ_polygons.dbf	ESRI Shapefile of polygon type	It contains up to two stacked polygons: 1) PLFZ for children; and 2) PLFZ for adults.	Polygons are generated only if predefined thresholds are exceeded
1.3.b	X_HCOM_PLFZ_polygons.prj			
1.3.c	X_HCOM_PLFZ_polygons.shp			
1.3.d	X_HCOM_PLFZ_polygons.shx			
1.4	X_HCOM_Indoor_Hazard_Categories_polygons	Subfolder	Subfolder containing the ESRI shapefile of polygon type containing the polygons of flood hazard categories for people caught outdoors.	
1.4.a	X_HCOM_Indoor_Hazard_Categories_polygons.dbf	ESRI Shapefile	It contains up to five polygons corresponding	Polygons are generated only if
1.4.b	X_HCOM_Indoor_Hazard_Categories_polygons.prj			

1.4.c	X_HCOM_Indoor_Hazard_Categories_polygons.shp	of polygon type	to the five potential flood hazard levels for humans caught indoors by the flood as listed in Table 15	predefined thresholds are exceeded
1.4.d	X_HCOM_Indoor_Hazard_Categories_polygons.shx			
1.5	X_HCOM_Outdoor_Hazard_Categories_polygons		Subfolder containing the ESRI shapefile of polygon type containing the polygons of flood hazard categories for people caught outdoors.	
1.5.a	X_HCOM_Outdoor_Hazard_Categories_polygons.dbf	ESRI Shapefile of polygon type	It contains up to five polygons corresponding to the five potential flood hazard levels for humans caught outdoors by the flood as listed in Table 13	Polygons are generated only if predefined thresholds are exceeded
1.5.b	X_HCOM_Outdoor_Hazard_Categories_polygons.prj			
1.5.c	X_HCOM_Outdoor_Hazard_Categories_polygons.shp			
1.5.d	X_HCOM_Outdoor_Hazard_Categories_polygons.shx			
1.6	X_HCOM_Census_Block_polygons			
1.6.a	X_HCOM_Census_Block_polygons.dbf	ESRI Shapefile of polygon type	It contains the outline polygons of 2010 census blocks that are inside or touched by the maximum inundation polygon.	Attributes of the polygons are also listed in the Excel file of PAR analysis
1.6.b	X_HCOM_Census_Block_polygons.prj			
1.6.c	X_HCOM_Census_Block_polygons.shp			
1.6.4	X_HCOM_Census_Block_polygons.shx			
1.7	X_HCOM_NT_PopDensity_persqmi_polygons		Subfolder containing the ESRI shapefile of polygon type containing the polygons of nighttime population density computed from LandScan USA.	
1.7.a	X_HCOM_NT_PopDensity_persqmi_polygons.dbf	ESRI Shapefile of polygon type	The bounding box of maximum inundation extent polygon is converted to WGS 84 coordinate system. It is then used as a mask to extract a portion of the nighttime population density raster at 3 arc-second resolution. The extracted portion of the nighttime population density is then projected in UTM. The cells that are touching or inside the maximum inundation polygon are selected and polygonized to create this shapefile.	This shapefile shows where the nighttime population is located. The polygonized cells can be colored based on the nighttime population density. See Table 57 for attributes, and Table 58 for explanation of attributes.
1.7.b	X_HCOM_NT_PopDensity_persqmi_polygons.prj			
1.7.c	X_HCOM_NT_PopDensity_persqmi_polygons.shp			
1.7.d	X_HCOM_NT_PopDensity_persqmi_polygons.shx			
1.8	X_HCOM_DT_PopDensity_persqmi_polygons	Subfolder	Subfolder containing the ESRI shapefile of polygon type containing the polygons of daytime population density computed from LandScan USA.	

1.8.a	X_HCOM_DT_PopDensity_persqmi_polygons.dbf	ESRI Shapefile of polygon type	The bounding box of maximum inundation extent polygon is converted to WGS 84 coordinate system. It is then used as a mask to extract a portion of the daytime population density raster at 3 arc-second resolution. The extracted portion of the daytime population density is then projected in UTM. The cells that are touching or inside the maximum inundation polygon are selected and polygonized to create this shapefile.	This shapefile shows where the daytime population is located. The polygonized cells can be colored based on the daytime population density. See Table 60 for attributes, and Table 61 for explanation of attributes.
1.8.b	X_HCOM_DT_PopDensity_persqmi_polygons.prj			
1.8.c	X_HCOM_DT_PopDensity_persqmi_polygons.shp			
1.8.d	X_HCOM_DT_PopDensity_persqmi_polygons.shx			

5.3 Test Case Used for Demonstrating Methodologies Used by DSS-WISE HCOM

The methodologies used in DSS-WISE HCOM will be demonstrated using the test case of the hypothetical breach of the Saluda Lake Dam (SC00024), in South Carolina. The permission to use this test case was given courtesy of the Dam Safety and Stormwater Permitting Division, S.C. Dept. of Health & Environmental Control (DHEC) and CDM Smith in Columbia, SC.

The DSS-WISE Lite simulation concerns a sunny day breach using a cell size of 20 ft. The downstream distance is 10 miles. The embankment has a hydraulic height of 46.1 ft. The crest elevation is at 852 ft NAVD 88. The length of the crest line captured on the map is 766 ft. The maximum pool volume at elevation 852 ft NAVD 88 is 7,745 acre-ft whereas the normal pool volume at elevation 849.7 ft. is 5,641 acre-ft. The failure type is total dam breach (i.e. sudden and complete failure). The failure pool volume is 7,745 acre-ft at elevation 852 ft NAVD 88. The unknown bed topography of the reservoir was estimated by account for 100% of the failure volume.

When the DSS-WISE Lite simulation request was received, DSS-WISE Web assigned it the Job ID of "5464". This Job ID appears in the names of all files generated by DSS-WISE Lite and DSS-WISE HCOM. DSS-WISE Lite simulation began one minute after the simulation request was received by the system. Thus the automated input data preparation took less than one minute. The DSS-WISE Lite simulation was completed in 28 minutes. At the end of the simulation, 88.643% of the initial failure pool volume had been released and 11.357% was still in the reservoir. The simulation was terminated because the flood front has reach the downstream distance specified by the user. The user had specified a downstream distance of 10 miles. DSS-WISE Lite continues for a while after the flood front reaches the user specified distance. In this specific case, the simulation was terminated when the flood front reached a downstream distance of 10.215 miles. The computed breach discharge hydrograph ("OLIN_0000003.xlsx") is plotted in Figure 36.

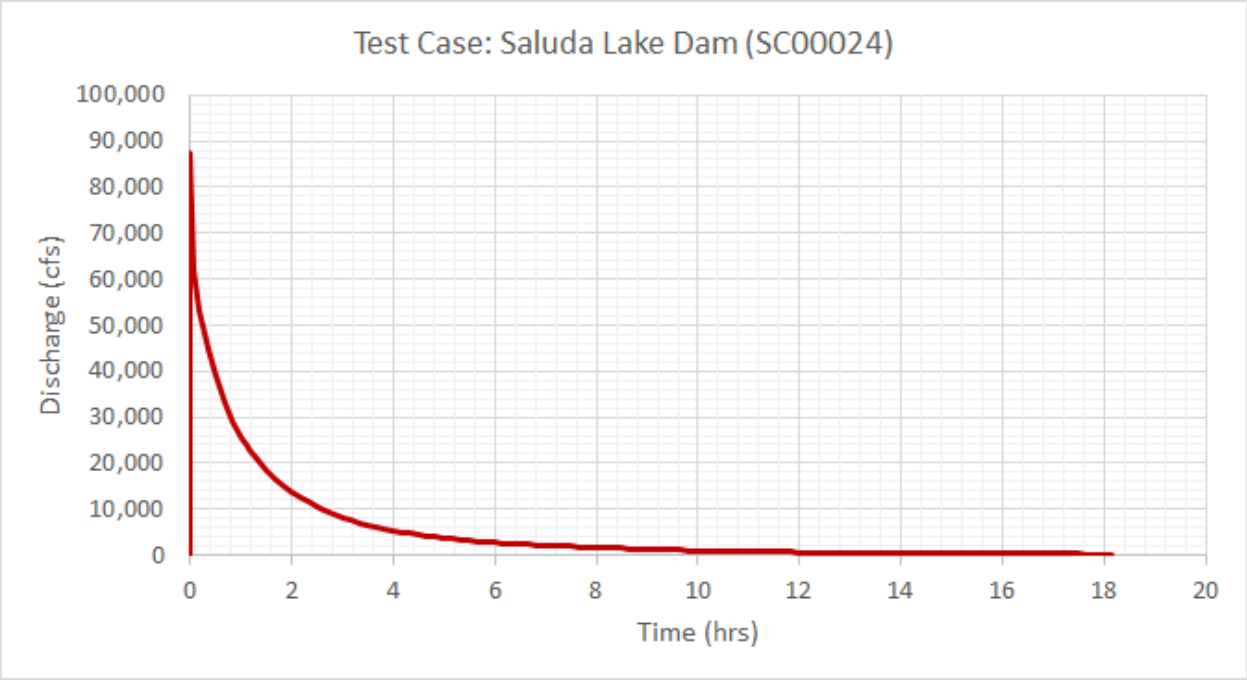

Figure 36 Breach discharge hydrograph for the test case.

DSS-WISE HCOM analysis was completed in 30 minutes. The results of the DSS-WISE HCOM analysis are summarized in Table 10. The results show that the inundation area concerns only one state, three counties and 104 census blocks. The PAR analysis based on census block data gives a total population count of 7,057, whereas the PAR analysis based on gridded LandScan USA data gives a nighttime population of 235 people.

Table 10 Summary of the DSS-WISE HCOM Results for the test case of Saluda Lake Dam.

INUNDATION EXTENT	
Total inundated area (acres):	1329.02
ANALYSIS BASED ON CENSUS BLOCK DATA	
Population in completely or partially inundated census blocks:	7057
Housings in completely or partially inundated census blocks:	2924
Number of states in inundated area:	1
Number of counties in inundated area:	3
Number of census blocks in inundated area:	104
ANALYSIS BASED ON GRIDDED LANDSCAN USA DATA	
Total Nighttime PAR in inundated area (see figure 2):	235
Total Daytime PAR in inundated area (see figure 3):	95

The complete list of files generated by DSS-WISE Lite and DSS-WISE HCOM is provided in Table 11and Table 12, respectively.

Table 11 DSS-WISE Lite Simulation Results Package after downloading and unzipping all folders. Folders are highlighted in yellow together with the corresponding title in the Status and Results page.

Folder of File Name		Name in Status and Results page (Figure 35)
5464_Report		Final Report
	5464_DSS-WISE_Lite_Final_Report.pdf	
5464_Raster Files		Raster Files
	5464_DEM_ft.tif	
	5464_Arrival_Time_hr_upto_final.tif	
	5464_DVmax_Arrival_Time_hr_upto_final.tif	
	5464_DVmax_ft2ps_upto_final.tif	
	5464_H_ft_at_final.tif	
	5464_Hmax_ft_upto_final.tif	
	5464_Vmax_ftps_upto_final.tif	
5464_Hmax_ft_polygons_upto_final		Maximum Depth Polygons
	5464_Hmax_ft_polygons_upto_final.dbf	
	5464_Hmax_ft_polygons_upto_final.prj	
	5464_Hmax_ft_polygons_upto_final.shp	
	5464_Hmax_ft_polygons_upto_final.shx	
5464_Flood_Arrival_Time_hr_polygons_upto_final		Arrival Time Polygons
	5464_Flood_Arrival_Time_hr_polygons_upto_final.dbf	

	5464_Flood_Arrival_Time_hr_polygons_upto_final.prj	
	5464_Flood_Arrival_Time_hr_polygons_upto_final.shp	
	5464_Flood_Arrival_Time_hr_polygons_upto_final.shx	
5464_DVmax_ft2ps_polygons_upto_final		Maximum Specific Discharge Polygons
	5464_DVmax_ft2ps_polygons_upto_final.dbf	
	5464_DVmax_ft2ps_polygons_upto_final.prj	
	5464_DVmax_ft2ps_polygons_upto_final.shp	
	5464_DVmax_ft2ps_polygons_upto_final.shx	
5464_DVmax_Arrival_Time_hr_polygons_upto_final		Maximum Specific Discharge Arrival Time Polygons
	5464_DVmax_Arrival_Time_hr_polygons_upto_final.dbf	
	5464_DVmax_Arrival_Time_hr_polygons_upto_final.prj	
	5464_DVmax_Arrival_Time_hr_polygons_upto_final.shp	
	5464_DVmax_Arrival_Time_hr_polygons_upto_final.shx	
5464_Vmax_ftps_polygons_upto_final		Maximum Velocity Polygons
	5464_Vmax_ftps_polygons_upto_final.dbf	
	5464_Vmax_ftps_polygons_upto_final.prj	
	5464_Vmax_ftps_polygons_upto_final.shp	
	5464_Vmax_ftps_polygons_upto_final.shx	
5464_Inundation_Extent_3_mi		Inundation Extent at 3 miles
	5464_Inundation_Extent_3_mi.dbf	
	5464_Inundation_Extent_3_mi.prj	
	5464_Inundation_Extent_3_mi.shp	
	5464_Inundation_Extent_3_mi.shx	
5464_Inundation_Extent_7_mi		Inundation Extent at 7 miles
	5464_Inundation_Extent_7_mi.dbf	
	5464_Inundation_Extent_7_mi.prj	
	5464_Inundation_Extent_7_mi.shp	
	5464_Inundation_Extent_7_mi.shx	
5464_Inundation_Extent_Final_10.215_mi		Final Inundation Extent
	5464_Inundation_Extent_Final_10.215_mi.dbf	
	5464_Inundation_Extent_Final_10.215_mi.prj	
	5464_Inundation_Extent_Final_10.215_mi.shp	
	5464_Inundation_Extent_Final_10.215_mi.shx	
5464_Observation_Lines		Observation lines
	OLIN_0000001.csv	
	OLIN_0000002.csv	
	OLIN_0000003.csv	
	OLIN_0000004.csv	
5464_KMZ		Inundation Extent KMZ File
	5464_Inundation_Extent_Final_10.215_mi.kmz	
5464_Input_Shapes		Input Features
	5464_breachpoint.dbf	
	5464_breachpoint.prj	
	5464_breachpoint.shp	
	5464_breachpoint.shx	

	5464_observationlines.dbf
	5464_observationlines.prj
	5464_observationlines.shp
	5464_observationlines.shx
	5464_reservoirs.dbf
	5464_reservoirs.prj
	5464_reservoirs.shp
	5464_reservoirs.shx
	5464_structures.dbf
	5464_structures.prj
	5464_structures.shp
	5464_structures.shx

Table 12 Human Consequences Results Package after downloading and unzipping all folders. Folders are highlighted in yellow together with the corresponding title in the Status and Results page.

Folder of File Name	Name in Status and Results page (Figure 35)
5464_HCOM_Report	HCOM Final Report
5464_HCOM_Final_Report.pdf	
5464_HCOM_Analysis	HCOM PAR Analysis Results
5464_HCOM_Analysis.xlsx	
5464_HCOM_PLFZ_polygons	HCOM Potentially Lethal Flood Zones
5464_HCOM_PLFZ_polygons.dbf	
5464_HCOM_PLFZ_polygons.prj	
5464_HCOM_PLFZ_polygons.shp	
5464_HCOM_PLFZ_polygons.shx	
5464_HCOM_Indoor_Hazard_Categories_polygons	HCOM Hazard Level to People Indoors
5464_HCOM_Indoor_Hazard_Categories_polygons.dbf	
5464_HCOM_Indoor_Hazard_Categories_polygons.prj	
5464_HCOM_Indoor_Hazard_Categories_polygons.shp	
5464_HCOM_Indoor_Hazard_Categories_polygons.shx	
5464_HCOM_Outdoor_Hazard_Categories_polygons	HCOM Hazard Level to People Outdoors
5464_HCOM_Outdoor_Hazard_Categories_polygons.dbf	
5464_HCOM_Outdoor_Hazard_Categories_polygons.prj	
5464_HCOM_Outdoor_Hazard_Categories_polygons.shp	
5464_HCOM_Outdoor_Hazard_Categories_polygons.shx	
5464_HCOM_Census_Block_polygons	HCOM PAR by Census Blocks
5464_HCOM_Census_Block_polygons.dbf	
5464_HCOM_Census_Block_polygons.prj	
5464_HCOM_Census_Block_polygons.shp	
5464_HCOM_Census_Block_polygons.shx	
5464_HCOM_NT_PopDensity_persqmi_polygons	HCOM Nighttime Population density
5464_HCOM_NT_PopDensity_persqmi_polygons.dbf	
5464_HCOM_NT_PopDensity_persqmi_polygons.prj	
5464_HCOM_NT_PopDensity_persqmi_polygons.shp	

5464_HCOM_NT_PopDensity_persqmi_polygons.shx	
5464_HCOM_DT_PopDensity_persqmi_polygons	HCOM Daytime Population density
5464_HCOM_DT_PopDensity_persqmi_polygons.dbf	
5464_HCOM_DT_PopDensity_persqmi_polygons.prj	
5464_HCOM_DT_PopDensity_persqmi_polygons.shp	
5464_HCOM_DT_PopDensity_persqmi_polygons.shx	

Chapter 6 FLOOD HAZARD RISK MAPPING

Flood-hazard risk mapping consists of partitioning the inundation area into zones of pre-defined potential danger classes for humans. The resulting map is an ESRI shapefile of polygon type. The polygons correspond to different levels of potential danger for humans caught outdoors and indoors.

The potential danger classes are identified based on the ranges of the value of the maximum specific discharge, q_{max}, which is equivalent to the maximum value of the product of depth and velocity, DV_{max}. The ranges of $q_{max} \equiv DV_{max}$ values are different for persons outdoors or indoors.

6.1 Flood Hazard Mapping for People Caught Outdoors

Flood hazard mapping for people caught outdoors attempts to define zones of different hazard levels for human subjects in relation with their stability in flowing water. Defining stability of a human subjected to flood waters is not an easy task as it depends on numerous factors. In addition to the characteristics of the flow represented by its depth and the hydrodynamic forces exerted on the human due to its velocity, numerous factors related to the environment itself,

- Bottom conditions: uneven surface, slippery surface, visible or invisible obstacles;
- Flow conditions: floating debris, low temperature, poor visibility, unsteady flow and flow aeration;
- Human subject: standing or moving, experience and training, clothing and footwear, physical attributes additional to height and mass including muscular development and/or other disability, psychological factors;
- Others: strong wind, poor lighting, p (i.e. feeling unsafe or complete loss of footing).

Numerous studies have been undertaken to study the stability of humans in flood waters experimentally, theoretically and numerically. Cox et al. (2010) provides an excellent summary of the research behind these safety criteria for people and discusses methods proposed by different researchers.

One could use various methods to map danger for humans. One possibility would be to use the plot of Figure 3 taken from AR&R.

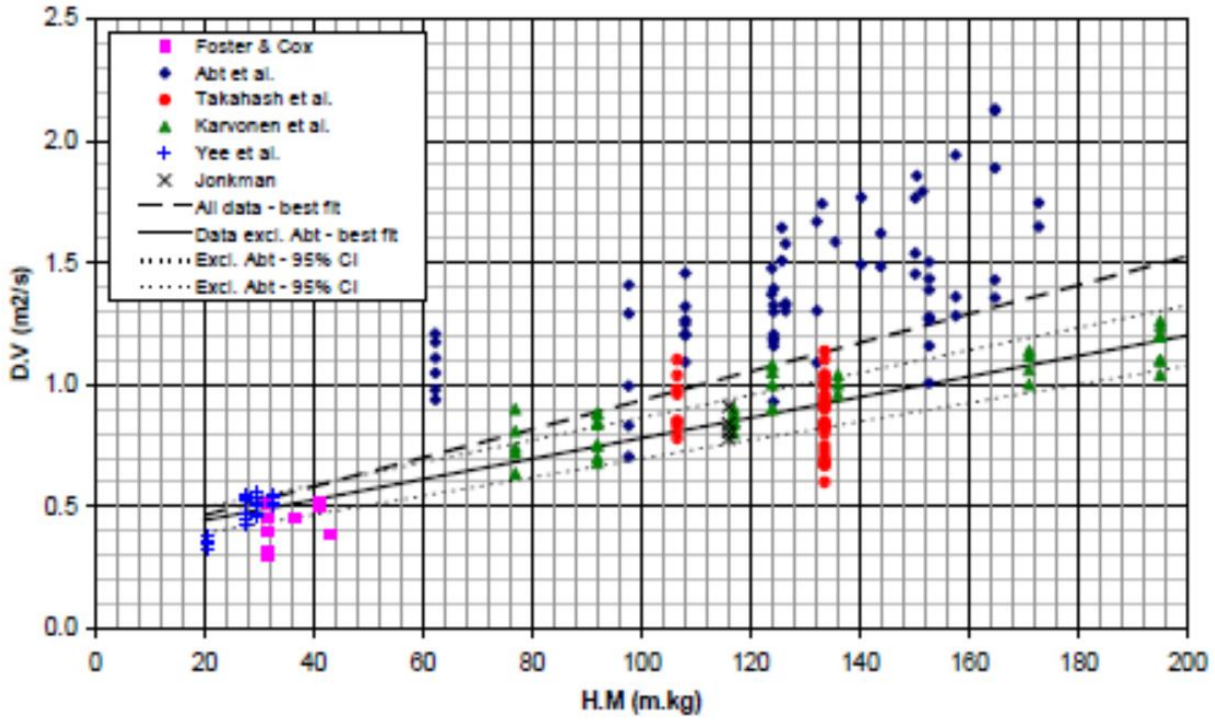

Figure 3 Combined limiting flow rates (D.V) found as function of subject Height*Mass (H.M) including the linear regression line for all data (- - -), for all data excluding that of Abt et al. (1989) (—) and the 95% confidence intervals for all data excluding that of Abt et al. (····).

For humans caught outdoors, the ranges of $q_{max} \equiv DV_{max}$ values taken from Cox et al. (2010) are summarized in Table 13 in both the SI units (m^2/s) and US customary units (ft^2/s). It is important to note that the original values are provided in SI units and have been converted to US customary units for the purposes of this document. As it can be seen, three levels of danger are recognized:

1. Safe,
2. Low Hazard,
3. Moderate Hazard; Dangerous to some,
4. Significant Hazard; Dangerous to most, and
5. Extreme Hazard; Dangerous to all.

Table 13 Potential danger classes for humans caught outdoors by the flood (based on Cox et al. 2010).

				Flood Hazard Regimes for Infants, Children and Adults[1]		
$q_{max} \equiv DV_{max}$ (m^2/s)		$q_{max} \equiv DV_{max}$ (ft^2/s)		Infants, Small Children and Frail/Older Persons	Children	Adults
from	to	from	to			
0.0	0.0	0.0	0.0	Safe	Safe	Safe
0.0	0.4	0.0	4.3	Extreme Hazard; Dangerous to all	Low Hazard	Low Hazard

0.4	0.6	4.3	6.5		Significant Hazard; Dangerous to most	Low Hazard
0.6	0.8[2]	6.5	8.7[2]		Extreme Hazard; Dangerous to all	Moderate Hazard; Dangerous to some
0.8	1.2[3]	8.7	13.0[3]			Significant Hazard; Dangerous to most
1.2[3]		13.0[3]				Extreme Hazard; Dangerous to all
1) Small children, children and adult categories are defined based on height (H) time mass (M) Small children: H×M ≤ 25 (m.kg) H×M ≤ 181 (ft.Lb) Children: 25 < H×M (m.kg) ≤ 50 181 < H×M (m.kg) ≤ 362 Adult: 50 < H×M (m.kg) 362 < H×M (ft.Lb)						
2) Recommended upper limit of tolerable working flow regime for trained safety workers or experienced and well-equipped persons						
3) Above this value, the hazard is extreme according to majority of the past studies.						

As it can be seen in Table 13, different limits of these danger levels are defined for the three categories of populations caught outdoors:

1. Infants, Small Children and Frail/Older Persons.
   Note that this category is special because "Frail/Older Persons" of a different age group are put into the same category with "Infants, Small Children" considering their independent mobility level and stability in case of flood.
2. Children.
3. Adults.

Referring to Table 14, the distinction between the categories "Infants and Small Children", "Children" and "Adult" is based on the product of the height (H) times the mass (M).

Table 14 Age categories for humans based on the product of the height (H) times the mass (M).

Category	$H \times M$ (where H is height and M is mass)	
	(m.kg)	(ft.Lb)[1]
Infant and Small children	$H \times M \leq 25$	$H \times M \leq 181$
Children	$25 < H \times M \leq 50$	$181 < H \times M \leq 362$
Adult	$50 < H \times M$	$362 < H \times M$
1) The product $H \times M$ is originally given in SI units. For the purposes of this document, they are converted into US customary units.		

It is important to note that the potential danger levels given in Table 13 loosely correspond to loss of stability for different population categories. Cox et al. (2010) provides an excellent summary of the research behind these safety criteria for people and discusses methods proposed by different researchers. Cox et al. (2004) underlines the lack of test data for very young children and frail/older persons. They emphasize that these populations are unlikely to be safe under any flow conditions and recommend locating care centers for old age people, retirement villages, childcare centers and kindergartens within flood zones as part of preparedness efforts.

Cox et al. (2010) notes that the limits of $q_{max} \equiv DV_{max}$ for loss of stability of different population categories are loosely defined and they should not be considered as strict limits. Sometimes, individual values of flow depth (h or D) and flow velocity (V) may also be considered as additional criteria.

For example, the laboratory tests showed that children, $25 < H \times M\ (m.kg) \leq 50$ or $181 < H \times M\ (ft.Lb) \leq 362$, retained their footing and felt safe for $q_{max}(DV_{max})$ values less than 4.3 ft^2/s (0.4 m^2/s) provided that the flow depth is less than 1.64 ft. (0.5 m) regardless of velocity. At shallow flood depths of less than 0.66 ft. (0.2 m), the children will not be safe if the flow velocity is equal to greater than 9.8 ft/s (3 m/s). Similarly, for adults, $50\ (m.kg) < H \times M$ or $362\ (ft.kg) < H \times M$, the hazard is low for $q_{max}(DV_{max})$ values less than 6.5 ft^2/s (0.6 m^2/s) provided that the flow depth is less than 3.9 ft. (1.2 m). The recommended upper limit of tolerable $q_{max}(DV_{max})$ range for trained safety workers or experienced and well-equipped persons is 8.7 ft^2/s (0.8 m^2/s). Majority of the past studies show that (Cox at al. 2010), the limiting value of $q_{max}(DV_{max})$ for stability of adults is 13 ft^2/s (1.2 m^2/s). For $q_{max}(DV_{max})$-values greater than 13 ft^2/s (1.2 m^2/s), the hazard is extreme for all adults.

It is important to note that various additional factors may cause loss of stability at lower values of $q_{max}(DV_{max})$ than those listed in Table 13. Following Cox et al. (2010), these additional factors can be listed as

- Bottom conditions: uneven surface, slippery surface, visible or invisible obstacles;
- Flow conditions: floating debris, low temperature, poor visibility, unsteady flow and flow aeration;
- Human subject: standing or moving, experience and training, clothing and footwear, physical attributes additional to height and mass including muscular development and/or other disability, psychological factors;
- Others: strong wind, poor lighting, p (i.e. feeling unsafe or complete loss of footing).

6.2 Flood Hazard Mapping for People Caught Indoors

For people caught indoors during the flood, it will be assumed that the potential danger is associated with the collapse of the building (see FEMA 2011, p. 43). Table 15 lists the $q_{max}(DV_{max})$-values for the potential collapse of different types of buildings, which are taken from the technical report of the Life Safety Model (LSM) developed by British Columbia Hydro (BCH 2006).

Table 15 BC Hydro LSM Building Stability Criteria.

Building Type	$q_{max} \equiv DV_{max}$	
	(m^2/s)	(ft^2/s)
Poorly Constructed Building	5	54
Well Built Timber Building	10	108
Well Built Masonry Building	15	162
Concrete Building	20	215
Large Concrete Building	35	377

Chapter 7 MAPPING POTENTIALLY LETHAL FLOOD ZONES (PLFZs) FOR CHILDREN AND ADULTS CAUGHT OUTDOORS

The mapping of potentially lethal flood zones (PLFZs) for humans consists of partitioning the inundation area into zones of pre-defined potential lethality classes for humans. The resulting map is an ESRI polygon shapefile. The polygons correspond to different levels of potential lethality that are defined based on the maximum depth, $h_{max} \equiv D_{max}$, and maximum specific discharge, $q_{max} \equiv DV_{max}$. The PLFZs for different categories of people caught outdoors, cars, mobile homes and typical residential structures are listed in Table 16.

Table 16 Definition of potentially lethal flood zones (PLFZs) for different categories (Feinberg, 2017).

Category	$h_{max} \equiv D_{max}$ (ft.)	$q_{max} \equiv DV_{max}$ (ft^2/s)
Children caught outdoors (tent camping, fishing, hiking, etc.)	> 2	> 5.4
Adults caught outdoors (tent camping, fishing, hiking, etc.)	> 4	> 6.5
Motor vehicle (compact car) floating	> 1	> 4.3
Motor vehicle (compact car) sliding/toppling		> 5.4
Mobile homes	> 2	> 30
Typical residential structures	> 4	> 75

Chapter 8 POPULATION AT RISK (PAR) ANALYSIS

PAR analysis consists of tallying population count that would be directly affected by the inundation. In general, the population directly affected by the inundation is considered to be the population living/working within the inundation area. In this report, the inundation area is the inundation extent computed by DSS-WISE Lite for a given breach or release scenario.

Traditionally, the tallying of PAR is accomplished based on the maximum inundation extent (see Figure 21). This traditional approach based on maximum inundation extent presents weaknesses:

1. The approach ignores the population living outside the maximum inundated extent who may
    - have their livelihoods and/or businesses in the maximum inundation area, or
    - depend on the services that are delivered from the maximum inundation area.
2. The approach ignores the spatial distribution of the severity of the flood in the maximum inundation extent. In some places, the population may be subjected to deep and/or fast flowing flows in some other inundated areas the flow depths and velocities may be negligible.
3. Since the tallying of the population is carried out based on maximum inundation extent, the approach ignores the spatial variation of the arrival time of the flood. Thus, the approach does not take into account the time available to escape from flood waters.

DSS-WISE HCOM addresses the second and third issues are to some extent by tallying the population counts in up to 10 hazard classes for up to 17 predefined times by using LandScan USA gridded nighttime and daytime population data.

Referring to Section 4.1, the population data is available in census blocks or in gridded format. Taking into account these data types, in practice the extraction of the PAR tally can be accomplished in several ways:

1. Tally the entire population inside the census blocks, or the grid cells, that are completely or partially (regardless how small the inundated portion can be) included in the maximum inundation area.
2. Tally the entire population inside the census blocks, or the grid cells, whose centroid is within the maximum inundation extent polygon.
3. Use method 1 or 2 but, instead of tallying entire population, tally the population count in proportion with the percent inundated area, which is computed by dividing the inundated portion of the census block, or the grid cell, area by the total area of the census block, or the grid cell. It should be noted that, this approach implicitly assumes that the population is uniformly distributed over the entire area of the census block, or the grid cell.

DSS-WISE HCOM uses the first method and tallies the population of any census block or computational cell that completely or partially included in the inundation area. There are, however, differences in methodology and the quality of results depending on the type of population data used.

8.1 PAR Analysis Based on Census Block Data

The 2010 census blocks provide housing and population counts in their attribute field (HOUSING10 and POP10 fields, respectively, in Table 3). The operation of tallying population and the housings and the census blocks is carried out at the end of the simulation based on the maximum inundation extent polygon. The census blocks have varying sizes and some of them can be extremely large. Moreover, the

distribution of the population inside the census bock is not known. When a census block is partially inundated, it is not known if any population lives or works in the inundated area. Thus, tallying the population in census blocks partially covered by the maximum inundation extent generally leads to an overestimation of the PAR count.

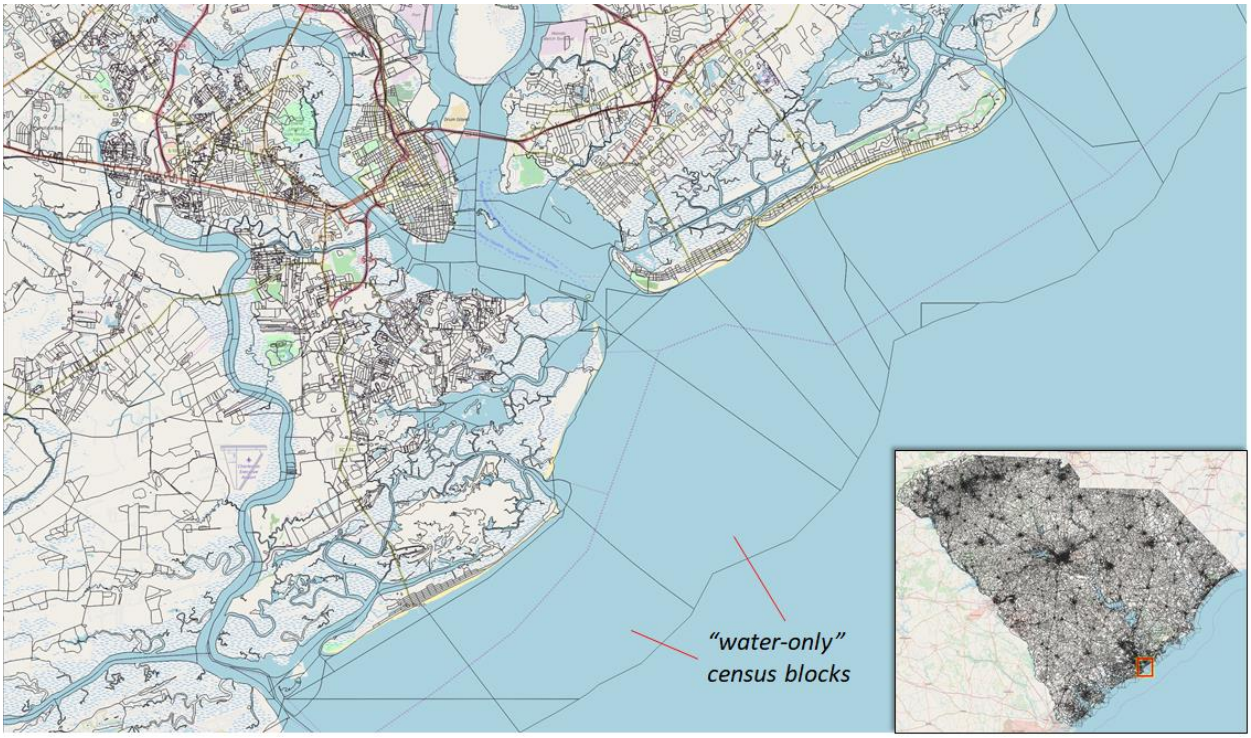

Figure 37 Detailed view of 2010 census block polygons around the city of Charleston, South Carolina. The river, the estuary and the coastal areas are defined as "water-only" blocks.

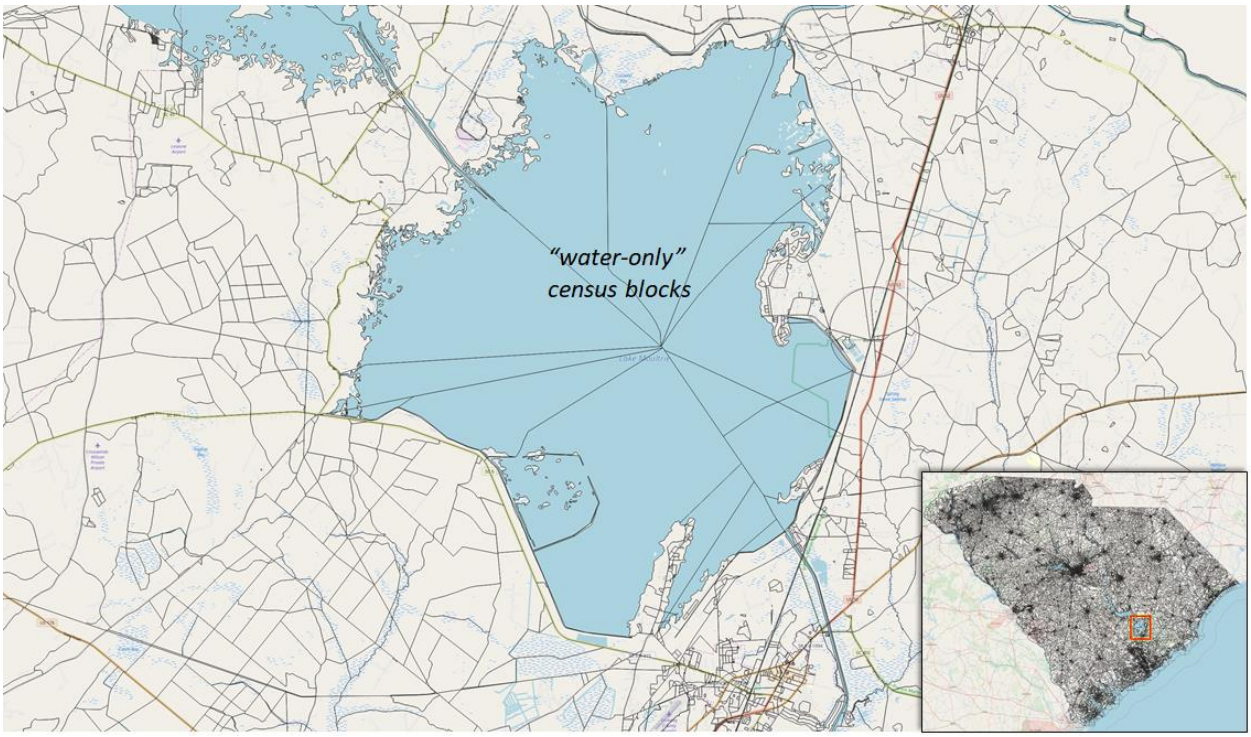

Figure 38 Detailed view of 2010 census blocks in the area of Lake Moultrie, South Carolina. The lake surface has some "water-only" blocks.

To illustrate the observations mentioned above, consider the census blocks around the city of Charleston (Figure 37), and Lake Moultrie (Figure 38), South Carolina. As it can be seen, the sizes of the census blocks can vary greatly and there is no information on where the population is located. Note that some of the census bock are "water-only" blocks covering the ocean or lake areas.

Since the only criteria of selection for the census block is to be partially or completely included in the maximum inundation polygon, there is no information as to when the flood reached the PAR or what the severity of the flood was. In order to mitigate these weaknesses of the methodology to some extent, in addition the population count, DSS-WISE HCOM extracts numerous additional derived and computed information for each census block inundated completely or partially:

- Total area (AREATOT) and inundate area (AREAINUND) of the census block are provided together with the percent area inundated (AINUND_PCT) are extracted. These values are given as attributes in the shapefile and also listed in the MS Excel file given as part of the final results package. If one makes the assumption of homogenous distribution of housings and population in the census block, multiplication of HOUSING10 and POP10 with AINUND_PCT provides an estimation of inundated houses and inundated PAR numbers, respectively.
- After the list of census blocks completely or partially inundated The computational cell blocks in each cell are post treated to provide statistical information on four variables:
    - The arrival time of the flood (FLDAT) into each census block is provided to give at least some level of information on how long after the breach the flood reaches the census block.
    - The arrival time of DV_{max} (DVMAXAT) into each census block is provided to give at least some level of information on how long after the breach maximum flood hazard, measured by DV_{max}, reaches the census block.

- The maximum flood depth H_{max} (HMAX) in each census block is provided to give a level of the severity of the flood in relation with the flow depth.
- The maximum value of DV_{max} (DVMAX) in each census block is provided to give a level of the hazard level of the flood in relation with the maximum specific discharge.

In general, a census block polygon covers more than one computational cell. Thus, the value of FLDAT, DVMAXAT, HMAX, and DVMAX varies from cell to cell within a given census block polygon. Therefore, DSS-WISE HCOM performs statistical analysis over all the cells in a census block to extract the minimum value, maximum value and average value for all four variables listed above.

Let the number of inundated computational cells whose center is within a given census block be denoted as nc. This list is readily generated using tools available in Geospatial Data Abstraction Library (GDAL). Operations performed on this list to extract the following statistical information:

1. Let $FLDAT(1, \dots, nc)$ represent one-dimensional array of the arrival time of the flood for the inundated cells in the census block. The following statistical are extracted:
   a. The minimum value of $FLDAT(1, \dots, nc)$ in the census block is calculated as

$$FLDAT\_MIN = \min_{i=1,\dots nc} [FLDAT(i)] \tag{34}$$

   This represents the time when the floodwaters reached the census block for the first time.

   b. The maximum value of $FLDAT(1, \dots, nc)$ in the census block is calculated as

$$FLDAT\_MAX = \max_{i=1,\dots nc} [FLDAT(i)] \tag{35}$$

   This represents the last time a new cell was added to the list of inundated cells within the census block.

   c. The average value of $FLDAT(1, \dots, nc)$ within the census block is calculated as

$$FLDAT\_AVG = \frac{\sum_{i=1}^{nc} FLDAT(i)}{nc} \tag{36}$$

   This value represents the average value of the arrival time for the inundated computational cells within the census block.

2. Let $DVMAXAT(1, \dots, nc)$ represent one-dimensional array of the arrival time of the DV_{max} for the inundated cells in the census block. Note that each cell may have a different DV_{max} value. The following statistical values are extracted:
   a. The minimum value of $DVMAXAT(1, \dots, nc)$ in the census block is calculated as

$$DVMAXAT\_MIN = \min_{i=1,\dots nc} [DVMAXAT(i)] \tag{37}$$

   This represents the earliest time a computational cell in the census block achieved its DV_{max} value.

b. The maximum value of $FLDAT(1, \dots, nc)$ in the census block is calculated as

$$DVMAXAT\_MAX = \max_{i=1,\dots nc} [DVMAXAT(i)] \quad (38)$$

This represents the latest time a computational cell in the census block achieved its DV_{max} value.

c. The average value of $DVMAXAT(1, \dots, nc)$ within the census block is calculated as

$$DVMAXAT\_AVG = \frac{\sum_{i=1}^{nc} DVMAXAT(i)}{nc} \quad (39)$$

This value represents the average value of the arrival time of DV_{max} for the inundated computational cells within the census block.

Since DV_{max} values for the cells in a census block are achieved at different times, the above values for DV_{max} have little statistical value and are difficult to interpret. Nevertheless, when they are considered together with the statistical data for the DV_{max} values in the census block (see bullet item 4), they can provide some useful idea on how long after the breach DV_{max} values are achieved in the census block.

3. Let $HMAX(1, \dots, nc)$ represent one-dimensional array of the maximum flood depth H_{max} for the inundated cells in the census block. The following statistical values can be calculated:
   a. The minimum value of $HMAX(1, \dots, nc)$ in the census block is calculated as

$$HMAX\_MIN = \min_{i=1,\dots nc} [HMAX(i)] \quad (40)$$

This represents the minimum value of maximum flood depth $HMAX$ among all inundated computational cells within the census block. It is important to note there may be dry computational cells in the census block. These are not considered in the analysis.

   b. The maximum value of $HMAX(1, \dots, nc)$ in the census block is calculated as

$$HMAX\_MIN = \max_{i=1,\dots nc} [HMAX(i)] \quad (41)$$

This represents the maximum value of maximum flood depth $HMAX$ among all inundated computational cells within the census block.

   c. The average value of $HMAX(1, \dots, nc)$ within the census block is calculated as

$$HMAX\_AVG = \frac{\sum_{i=1}^{nc} HMAX(i)}{nc} \quad (42)$$

This represents the average value maximum flood depth $HMAX$ for the inundated part of the census block. Dry cells are not included in the computation of the average value.

4. Let $DVMAX(1, \dots, nc)$ represent one-dimensional array of the maximum specific discharge DV_{max} for the inundated cells in the census block. The following statistical values can be calculated:
    a. The minimum value of $DVMAX(1, \dots, nc)$ in the census block is calculated as

$$DVMAX\_MIN = \min_{i=1,\dots nc}[DVMAX(i)] \tag{43}$$

This represents the minimum value of DV_{max} among all inundated computational cells within the census block. It is important to note there may be dry computational cells in the census block. These are not considered in the analysis. Thus $DVMAX_{MIN} > 0$.

    b. The maximum value of $FLDAT(1, \dots, nc)$ in the census block is calculated as

$$DVMAX\_MIN = \max_{i=1,\dots nc}[DVMAX(i)] \tag{44}$$

This represents the maximum value of DV_{max} among all inundated computational cells within the census block.

    c. The average value of $DVMAX(1, \dots, nc)$ within the census block is calculated as

$$DVMAX\_AVG = \frac{\sum_{i=1}^{nc} DVMAX(i)}{nc} \tag{45}$$

This represents the average value of DV_{max} for the inundated part of the census block. Dry cells are not included in the computation of the average value.

In order to be able to use the methodology described above it is necessary to extract the list of the census blocks that are completely or partially inundated by the maximum inundation polygon. This operation requires searching for census block polygons that are intersected by the maximum inundation polygon. The challenge for this search operation is the large number of census blocks. There are 11,166,336 census block polygons (see Section 4.1.1.1) that are stored in 56 shapefiles listed in Table 4. Intersecting the maximum inundation polygon with all 11,166,336 census-block polygons would take an unreasonable amount of time; thus it is impractical

One way to reduce the computational burden is to reduce the number of census-lock polygons to be searched using a preselection criteria. One could, for example first determine the states that are concerned by the flood by intersecting the maximum inundation extent polygon with the polygon boundaries of 56 state and U.S. territories listed in Table 4.

Searching through only 56 polygons would be very quick; but we would still be left with too many census-block polygons to search through. To illustrate this consider the test case of Saluda Lake Dam in South Carolina (Section 5.3). The inundation extent is entirely within the state boundary of South

Carolina. Thus, intersection of the maximum inundation polygon with 56 state boundary polygons (see Table 4) indicate that only the census-block polygons in the shapefile "tabblock2010_45_pophu" need to be searched by intersecting with the maximum inundation extent polygon.

Figure 39 shows all the census blocks in the state of South Carolina. The maximum inundation area for the test case of Saluda Lake Dam (in the area highlighted by the red rectangle) is superposed on the census block polygons. At the scale of Figure 39, the maximum inundation polygon is too small to be seen. Figure 40 shows an enlarged view of the census blocks around the maximum inundation area colored in magenta.

The attribute table of "tabblock2010_45_pophu" is shown in Table 17. It can be seen that it contains the records of 181,908 census-block polygons in the state of South Carolina. Searching only through the census blocks of the state of South Carolina reduces the number of census block to be intersected with the maximum inundation polygon from 11,166,336 to 181,908. This is a significant reduction. However, the search operation would still involve a large number of census-block polygons. Moreover, the number of polygons to be searched could two times or higher if the intersection of the maximum inundation extent polygon with the state boundaries returns two or more states.

A better solution, which is the one adopted by DSS-WISE HCOM, is to filter the number of census-block polygons to be searched intersecting the maximum inundation polygon with the county boundary polygons shapefile shown in Figure 31 (see Section 4.2). The attribute table of this shapefile, which is shown in Table 18, contains the records of 3,221 counties. A preliminary search by intersecting maximum inundation polygon with 3,221 county polygons, is computationally acceptable.

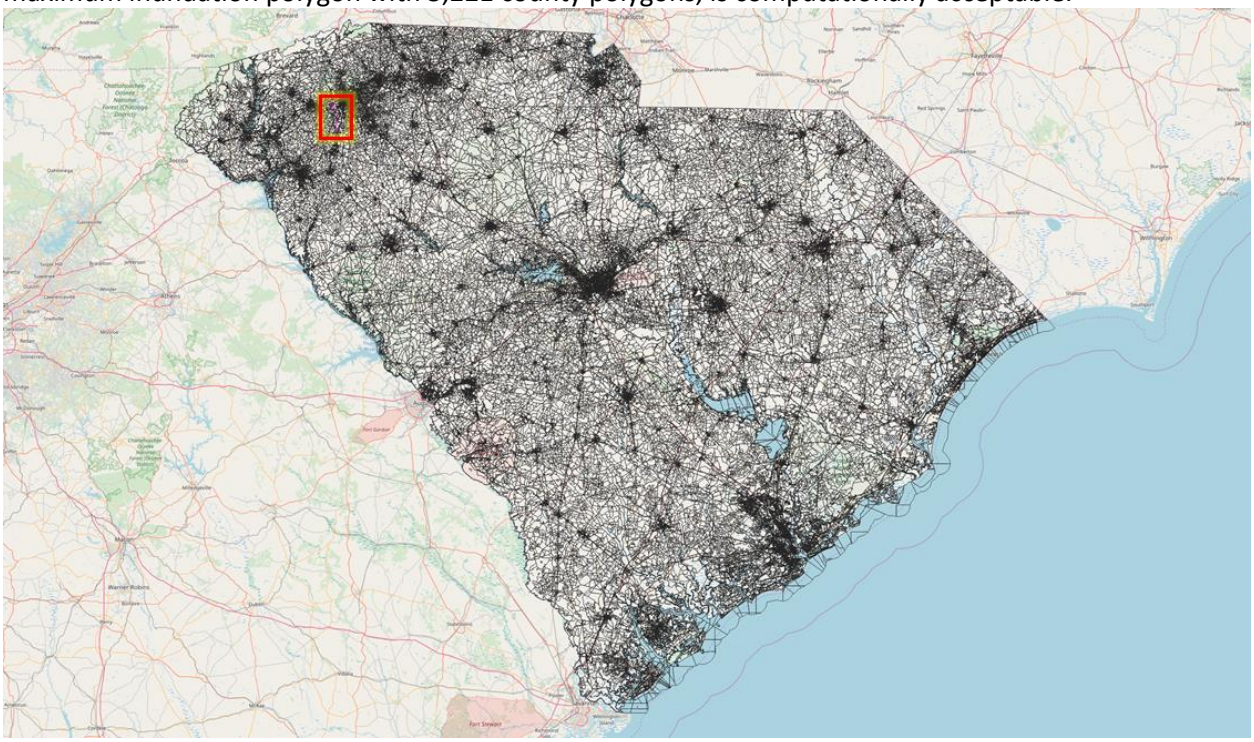

Figure 39 Maximum inundation extent polygon (in the area highlighted by the red rectangle) superposed on the 2010 census block polygons.

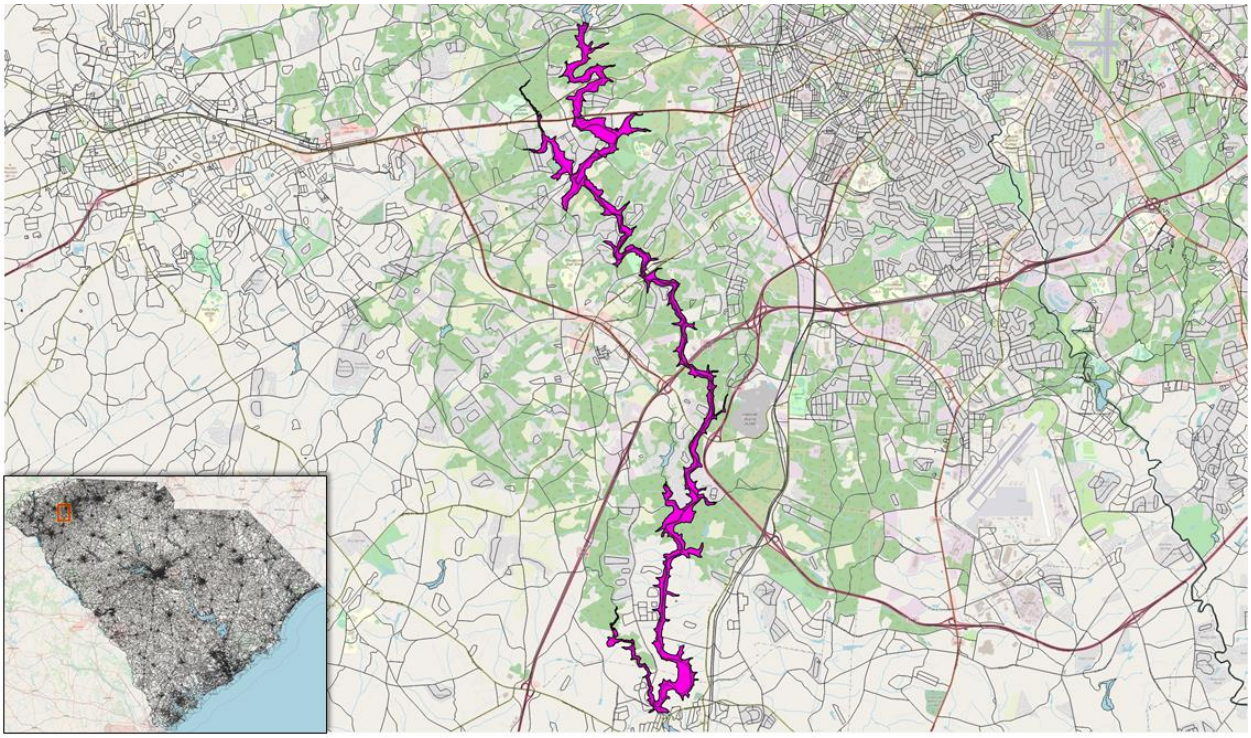

Figure 40 Detailed view of maximum flood extent polygon superposed on 2010 census block polygons.

Table 17 Attribute table for "tabblock2010_45_pophu.shp" includes 181,908 census-block records.

No	STATEFP10	COUNTYFP10	TRACTCE10	BLOCKCE10	GEOID10	NAME10	MTFCC10	UR10	UACE10	UATYPE	FUNCSTAT10	ALAND10	AWATER10	INTPTLAT10	INTPTLON10
1	45	1	950300	2000	450019503002000	Block 2000	G5040	R			S	1402	41707	34.3130581	-82.5741542
2	45	77	10100	2117	450770101002117	Block 2117	G5040	R			S	2363423	71365	35.0077188	-82.6902535
3	45	19	2400	1286	450190024001286	Block 1286	G5040	R			S	0	538	32.7647064	-80.4457162
4	45	65	920300	2136	450659203002136	Block 2136	G5040	R			S	0	6287807	33.6784319	-82.2032106
.....	....	....	.....	.....	.....	.....	.....	....	.....	....	....	.....	.....	.....	.....
181905	45	33	970400	2016	450339704002016	Block 2016	G5040	U	24202	C	S	12498	0	34.4165279	-79.3767755
181906	45	43	920201	1053	450439202011053	Block 1053	G5040	R			S	119402	0	33.4014188	-79.4806477
181907	45	53	950100	2040	450539501002040	Block 2040	G5040	R			S	3793726	0	32.6096772	-81.1424842
181908	45	25	950800	2253	450259508002253	Block 2253	G5040	R			S	207552	0	34.5553344	-80.318453

Table 18 Attributes for the features in the TIGER/Line shapefile of U.S. counties.

NO	GEO_ID	STATE	COUNTY	NAME	LSAD	CENSUSAREA
1	0500000US20011	20	11	Bourbon	County	635.471
2	0500000US20009	20	9	Barton	County	895.4
3	0500000US20015	20	15	Butler	County	1429.863
4	0500000US20013	20	13	Brown	County	570.872
….	….	….	….	….	….	….
3217	0500000US20187	20	187	Stanton	County	680.345
3218	0500000US20149	20	149	Pottawatomie	County	841.022
3219	0500000US20143	20	143	Ottawa	County	720.733
3220	0500000US20165	20	165	Rush	County	717.763
3221	0500000US20161	20	161	Riley	County	609.771

Figure 41 shows an enlarged view of the South Carolina counties around the maximum inundation polygon. The search operation of intersecting maximum inundation polygon with 3,221 county polygons of the U.S. states and territories identifies three counties, which are highlighted in yellow; i.e. Anderson, Pickens, and Greenville. Table 19 shows the records of these three counties in the county shapefile.

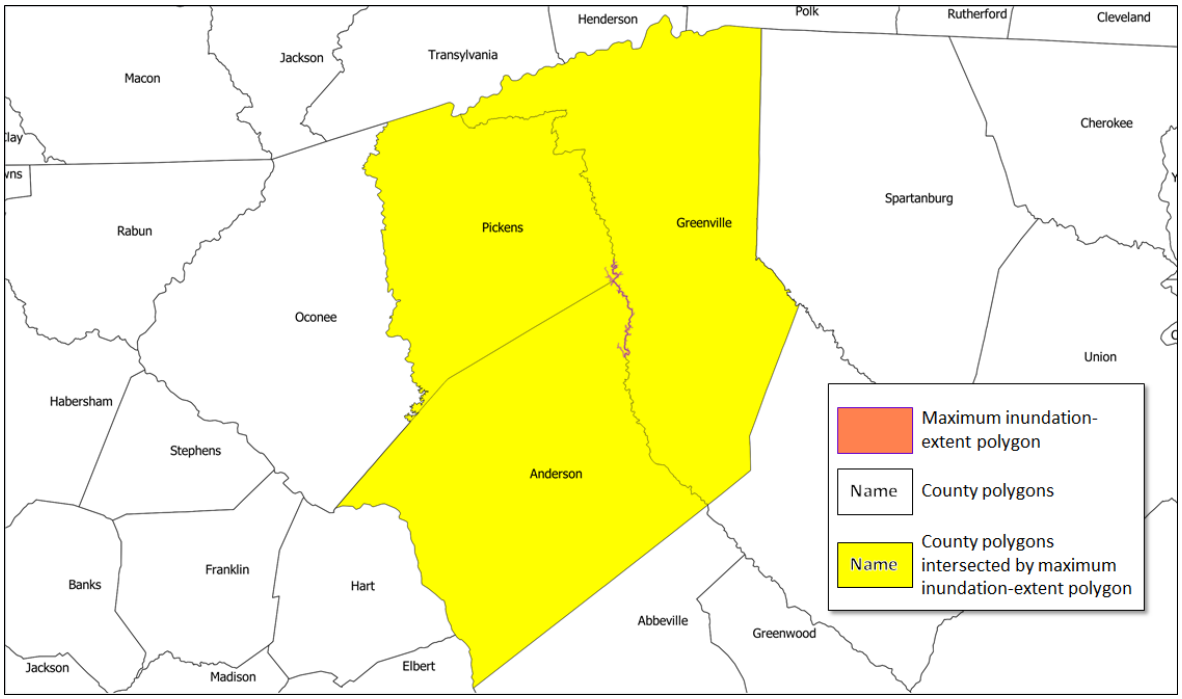

Figure 41 Maximum inundation-extent polygon intersects three counties highlighted in yellow.

Table 19 Counties whose outline polygons are intersected by the maximum flood-extent polygon.

GEO_ID	STATE	COUNTY	NAME	LSAD	CENSUSAREA
0500000US45007	45	7	Anderson	County	715.426
0500000US45077	45	77	Pickens	County	496.407
0500000US45045	45	45	Greenville	County	785.12

The next search operation involves only the list of the census-block polygons in these three counties. Since Table 19 already provides the state and county FIPS, the list of census blocks to be intersected by the maximum inundation polygon is easily extracted from the census-block shapefile. This operation extracts a list of 21,383 census block polygons (Anderson has 7,104 census blocks, Pickens has 4,394 census blocks, and Greenville has 9,885 census blocks) to be searched by intersection with the maximum inundation polygon. The extracted census-block polygons are shown in Figure 42. As it can be seen this number is significantly smaller and allows the computations for searching by intersecting polygons to be completed in a reasonable time.

The search operation by intersecting maximum inundation polygon with 21,383 census-block polygons located in three counties (Anderson, Pickens, and Greenville) produces the list of 104 counties affected by the flood. Figure 43 shows these 104 census blocks.

DSS-WISE HCOM generates two products for PAR analysis based on census blocks as part of the final results package:

- An ESRI shapefile of polygon type containing the selected counties, thus 104 counties in the case of the Saluda Lake Dam simulation used as test case for this document. The generic name for the shapefile is

a shapefile containing these selected 104 census blocks. Some of the attributes of these census blocks are directly taken from the attributes of the seamless census block shapefile (see Table 3) of the U.S. states and territories. Others are computed. The complete list of the fields in the attribute table of the shapefile generated by DSS-WISE HCOM is shown in Table 20 together with detailed explanations.

For each census block, the population and housing counts are already given in the

For each census block, GDAL library is used to extract the list of nc computational cells whose centroid is within the census block. Referring to the test case described in Section 5.3, data required for the statistical analysis described earlier is taken from the raster files generated by DSS-WISE Lite simulation (Table 11):

1. One dimensional array for flood arrival time values, $FLDAT(1, \dots, nc)$, is populated from the raster file “5464_Arrival_Time_hr_upto_final.tif”
2. One dimensional array for the arrival time of DV_{max}, $DVMAXAT(1, \dots, nc)$, is populated from the raster file “5464_DVmax_Arrival_Time_hr_upto_final.tif”
3. One dimensional array for the maximum flood depth H_{max}, $HMAX(1, \dots, nc)$, is populated from the raster file “5464_Hmax_ft_upto_final.tif”
4. One dimensional array for the maximum value of DV_{max}, $DVMAX(1, \dots, nc)$, is populated from the raster file “5464_DVmax_ft2ps_upto_final.tif”

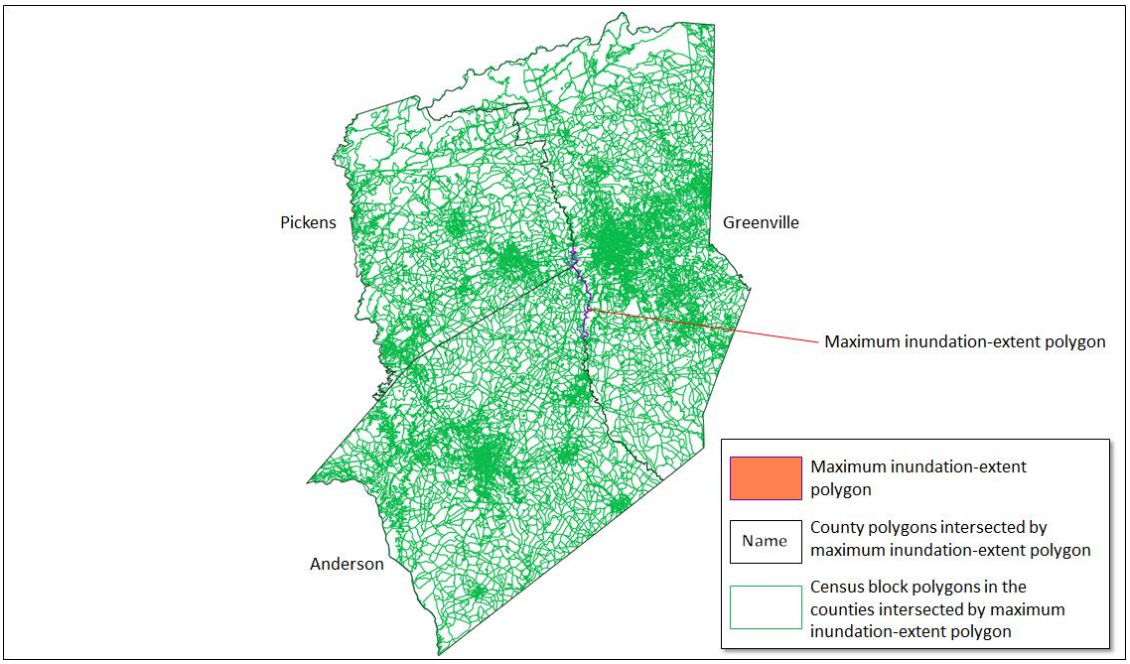

Figure 42 The 2010 census block polygons in three counties intersected by the maximum inundation polygon.

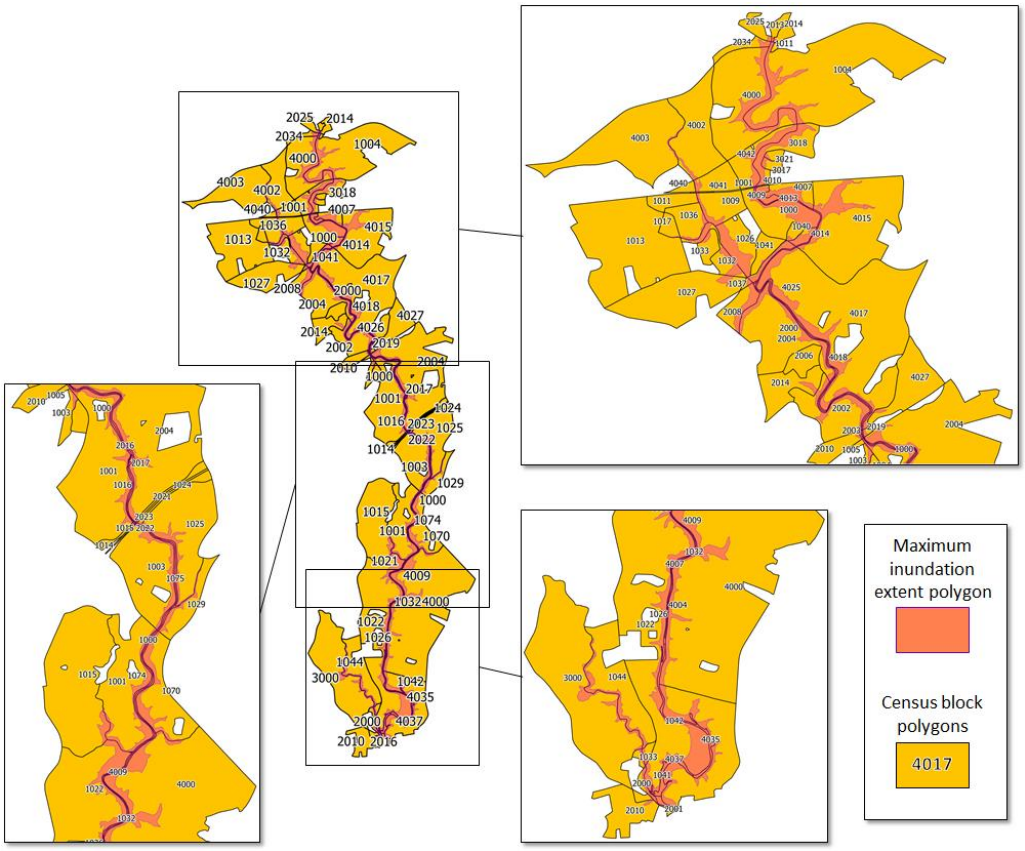

Figure 43 Census block polygons intersected by the maximum flood extent polygon.

Table 20 Attribute table for the shapefile "X_HCOM_Census_Block_polygons" generated by DSS-WISE HCOM.

1	2	3	4	5	6	7	8	9	10	11	12	13	14	15	16	17	18	19	20	21	22	23	24	25
STATE_NAME	CNTY_NAME	STATEFP10	COUNTYFP10	TRACTCE10	BLOCKCE	BLOCKID10	PARTFLG	HOUSING10	POP10	AREATOT	AREAINUND	AINUND_PCT	FLDAT_AVG	FLDAT_MIN	FLDAT_MAX	HMAX_AVG	HMAX_MIN	HMAX_MAX	DVMAXATAVG	DVMAXATMIN	DVMAXATMAX	DVMAX_AVG	DVMAX_MIN	DVMAX_MAX
								Count	Count	Acres	Acres	%	hrs	hrs	hrs	ft	ft	ft	hrs	hrs	hrs	ft2/s	ft2/s	ft2/s

Table 21 Description of the attributes for the shapefile "X_HCOM_Census_Block_polygons" generated by DSS-WISE HCOM.

Col. No	Field Content	Origin of Data	Col. No	Field Content	Origin of Data
1	State Name	Long form of the state name corresponding to STATEFP10	14	Flood Arrival Time (Avg)	Computed using Eq. (36)
2	County Name	County name in full	15	Flood Arrival Time (Min)	Computed using Eq. (34)
3	State FIPS CODE	Populated directly with data from attribute table of census block shapefile (see Table 3)	16	Flood Arrival Time (Max)	Computed using Eq. (35)
4	County FIPS Code		17	Flood Maximum Depth (Avg)	Computed using Eq. (39)
5	Tract Code		18	Flood Maximum Depth (Min)	Computed using Eq. (37)
6	Tabulation Block Number		19	Flood Maximum Depth (Max)	Computed using Eq. (38)
7	Block ID Number		20	Flood Maximum DV Arrival Time (Avg)	Computed using Eq. (42)
8	Partial Block Indicator		21	Flood Maximum DV Arrival Time (Min)	Computed using Eq. (40)
9	Total Number of Housings		22	Flood Maximum DV Arrival Time (Max)	Computed using Eq. (41)
10	Total Number of Population		23	Flood Maximum DV Arrival Time (Avg)	Computed using Eq.(45)
11	Total Area	Total Area of the census block computed from the polygon	24	Flood Maximum DV (Min)	Computed using Eq. (43)
12	Inundated Area	Area of the inundated part of the census block polygon. This is the area of the census block inside the maximum inundation polygon.	25	Flood Maximum DV (Max)	Computed using Eq. (44)
13	Percent Area Inundated	Calculated as $\text{AINUND\_PCT} = \frac{AREAINUND}{AREATOT}$			

8.2 PAR Analysis Based on LandScan USA Gridded Population Data

The LandScan nighttime or daytime gridded population data present numerous advantages over the census block population data. The gridded population data provides a more accurate mapping of the population during the night and the day. The cell size of 3 arc-second is sufficiently small to allow the assumption uniform distribution of the population within each cell. In fact, this assumption was used for the creation of nighttime and daytime population density rasters as described in Section 4.1.3.

These advantages of the LandScan nighttime or daytime gridded population data are exploited in DSS-WISE HCOM to provide a detailed PAR analysis that goes beyond a simple total count of population in the inundation area. PAR analysis using nighttime and daytime gridded population density rasters provides detailed information on the time evolution of the PAR count in different hazard categories.

To understand the richness of the PAR analysis provided by DSS-WISE HCOM, consider Table 22 and Table 23, which show the nighttime and daytime PAR analysis results, respectively, for the test case of Saluda Lake Dam, SC. To facilitate the discussion, the columns in Table 22 and Table 23 are numbered from 1 to 12 and the rows are numbered from 1 to 11. Each row of the table corresponds to a specific time after the beginning of the simulation, which is written in the first column of each row.

As it can be seen, the predefined times in the first column are not equally spaced. The PAR counts are provided at every 0.25 hrs for the first hour then at every hour up to 4 hours, and with further decreasing frequency from then on. This is due to the fact that the early hours after the initiation of a dam-break are the most critical hours for making announcements and for evacuating PAR to save lives. It is assumed that longer it takes for the flood to reach a population, the less critical it will be because there will be enough to time warn the population and evacuate them if necessary.

Table 22 and Table 23 are for the special case of Saluda Lake Dam, SC. In the general case, the tables of nighttime and daytime PAR count may contain up to 17 rows corresponding to the following predefined flood times: 1) 0.25 hrs; 2) 0.50 hrs; 3) 0.75 hrs; 4) 1.00 hrs; 5) 2.00 hrs; 6) 3.00 hrs; 7) 4.00 hrs; 8) 6.00 hrs; 9) 12.00 hrs; 10) 18.00 hrs; 11) 24.00 hrs; 12) 36.00 hrs; 13) 48.00 hrs; 14) 72.00 hrs; 15) 96.00 hrs; 16) 120.00 hrs; and 17) Simulation end time in hrs. The actual number of rows in these tables depends on the simulated duration of the flood. For example, in case of the Saluda Lake Dam, SC, DSS-WISE Lite simulated 18.19 hrs of flood. The end of the simulation at 18.19 hrs flood time falls between 10^{th} (18 hrs) and 11^{th} (24 hrs) predefined flood times. Thus, Table 22 and Table 23 have both 11 rows. The first 10 rows correspond to the first 10 predefined times and the final row correspond to the end time (18.19 hrs) of the simulation.

In each row, i.e. at each PAR analysis time, the PAR numbers are summed up separately in 10 bins of DV_{max}. These 10 bins of DV_{max}, which are represented in columns 2 to 11 of Table 22 and Table 23, correspond to the 10 categories that were defined for mapping flood hazard to people caught outdoors (HZ01 to HZ05) (see Section 6.1) and indoors (HZ06 to HZ10) (see Section 6.2). They are recalled below for convenience accompanied by their interpretation:

Table 22 Results of nighttime PAR analysis presented in tabular format.

	1	2	3	4	5	6	7	8	9	10	11	12
	Flood Time	Nighttime PAR by Highest Flood Hazard Category Achieved										Total
	(hrs	HZ01	HZ02	HZ03	HZ04	HZ05	HZ06	HZ07	HZ08	HZ09	HZ10	NT PAR
1	0.25	2	1	1	1	2	2	1	1	1	0	12
2	0.50	4	1	1	1	3	2	2	1	1	0	16
3	0.75	10	5	5	9	21	3	2	1	1	0	57
4	1.00	13	4	4	9	47	3	2	1	1	0	84
5	2.00	30	8	6	10	65	4	2	1	1	0	127
6	3.00	52	10	8	12	71	5	2	1	1	0	162
7	4.00	71	10	8	14	75	5	2	1	1	0	187
8	6.00	77	13	10	17	79	5	2	1	1	0	205
9	12.00	91	14	11	19	87	5	2	1	1	0	231
10	18.00	95	14	11	19	87	5	2	1	1	0	235
11	18.19	95	14	11	19	87	5	2	1	1	0	235

Table 23 Results of daytime PAR analysis presented in tabular format.

	1	2	3	4	5	6	7	8	9	10	11	12
	Flood Time	Daytime PAR by Highest Flood Hazard Category Achieved										Total
	(hrs	HZ01	HZ02	HZ03	HZ04	HZ05	HZ06	HZ07	HZ08	HZ09	HZ10	DT PAR
1	0.25	2	1	1	1	3	1	1	1	0	0	11
2	0.50	2	1	1	1	3	2	1	1	1	0	13
3	0.75	4	2	2	4	8	2	1	1	1	0	25
4	1.00	5	2	2	4	15	2	1	1	1	0	33
5	2.00	10	3	3	4	20	2	1	1	1	0	45
6	3.00	20	4	3	5	22	2	1	1	1	0	59
7	4.00	31	5	4	6	24	2	1	1	1	0	75
8	6.00	37	5	4	7	26	2	1	1	1	0	84
9	12.00	41	6	5	8	28	2	1	1	1	0	93
10	18.00	43	6	5	8	28	2	1	1	1	0	95
11	18.19	43	6	5	8	28	2	1	1	1	0	95

Table 24 Results of inundated area analysis presented in tabular format.

	1	2	3	4	5	6	7	8	9	10	11	12
	Flood Time	Inundated Area by Highest Flood Hazard Category Achieved										Total Area
	(hrs	HZ01	HZ02	HZ03	HZ04	HZ05	HZ06	HZ07	HZ08	HZ09	HZ10	Acres
1	0.25	12.2	3.0	2.0	3.5	22.1	13.9	10.1	8.0	5.6	0.6	80.9
2	0.50	24.7	5.3	4.1	6.1	38.3	23.4	19.1	12.9	6.1	0.6	140.6
3	0.75	35.3	9.4	7.2	13.0	60.3	32.8	21.9	14.0	6.1	0.6	200.7
4	1.00	37.7	10.4	10.8	25.7	99.4	36.2	23.3	14.5	6.1	0.6	264.7
5	2.00	121.7	25.9	15.8	28.0	170.5	48.8	23.8	14.6	6.1	0.6	455.9
6	3.00	180.2	39.6	24.4	42.9	209.3	57.1	23.8	14.6	6.1	0.6	598.7
7	4.00	216.1	43.4	30.3	53.7	245.4	64.1	23.8	14.6	6.1	0.6	698.1
8	6.00	254.8	55.5	45.9	81.4	303.5	66.6	23.8	14.6	6.1	0.6	852.8
9	12.00	418.8	99.8	78.5	142.8	409.1	66.6	23.8	14.6	6.1	0.6	1260.8
10	18.00	473.7	109.0	80.5	143.6	409.6	66.6	23.8	14.6	6.1	0.6	1328.2
11	18.19	474.5	109.0	80.5	143.6	409.6	66.6	23.8	14.6	6.1	0.6	1329.0

1. HZ01: $0 \leq DV_{max}^{t_i} \leq 4.3$ Very Low Hazard: Shallow flow or deep standing water
2. HZ02: $4.3 \leq DV_{max}^{t_i} \leq 6.5$ Low Hazard: Dangerous to Children
3. HZ03: $6.5 \leq DV_{max}^{t_i} \leq 8.6$ Moderate Hazard: Dangerous to some adults
4. HZ04: $8.6 \leq DV_{max}^{t_i} \leq 13$ Significant Hazard: Dangerous to most adults
5. HZ05: $13 \leq DV_{max}^{t_i} \leq 54$ Extreme Hazard: Dangerous to all
6. HZ06: $54 \leq DV_{max}^{t_i} \leq 108$ Poorly constructed building
7. HZ07: $108 \leq DV_{max}^{t_i} \leq 161$ Well-built timber building
8. HZ08: $161 \leq DV_{max}^{t_i} \leq 215$ Well-built masonry building
9. HZ09: $215 \leq DV_{max}^{t_i} \leq 377$ Concrete building
10. HZ10: $DV_{max}^{t_i} \geq 377$ Large concrete building

In the above list, the 10 bins are specified in terms of the ranges of $DV_{max}^{t_i}$ [23], which stands for the DV_{max} at one of the 17 predefined flood times t_i. Thus, the subscript can have the values $1 \leq i \leq 17$. In Table 22 and Table 23, these 10 flood hazard categories correspond to columns 2 to 11. The last column (column 12) of Table 22 and Table 23 correspond to the total PAR at the flood time shown in column 1. Thus, the value in column 12 in a given row contains the sum of the values in columns 2 to 11 of the same row.

Table 24 is another useful side product generated by DSS-WISE HCOM while performing the PAR analysis with gridded population data. It provides the time evolution of the surface area of the inundation extent in 10 hazard categories. The structure of Table 24 is similar to those of Table 22 and Table 23. The rows 1 to eleven correspond to the predefined flood times at which the surface area of flood is calculated in 10 flood hazard categories and written into the columns 2 to 11. The value in column 12 is the sum of the values in columns 2 through 11 and corresponds to the total inundation area at the time in the first column.

The PAR analyses in Table 22 and Table 23 and the flood inundation area analysis in Table 24 require generation of $DV_{max}^{t_i}$ rasters at up to 16 predefined intermediate flood times. These rasters are generated by the DSS-WISE Lite solver during the dam-break flood simulation solely for use by the DSS-WISE HCOM. They are not included in the final results package; thus they are not available to the user.

As an example, let us look at the temporary files generated for HCOM analysis for the test case of Saluda Lake Dam. Table 22, Table 23 and Table 24 all contain eleven rows corresponding to 11 times at which the nighttime PAR, daytime PAR, and inundation area are extracted in 10 bins corresponding to 10 hazard categories. As it was mentioned before, provided that a flood time greater than 120 hrs is simulated, these table can have up to 17 rows at most. The first 16 of these rows would correspond to the 16 predefined times listed earlier and the last row would correspond to the time at the end of the simulation.

The test case simulation, however, is terminated at 18.19 hrs. Thus, the table includes 11 rows: at the following times: 1) $t_1 = 0.25\ hrs$; 2) $t_2 = 0.50\ hrs$; 3) $t_3 = 0.75\ hrs$; 4) $t_4 = 1.00\ hrs$; 5) $t_5 = 2.00\ hrs$; 6) $t_6 = 3.00\ hrs$; 7) $t_7 = 4.00\ hrs$; 8) $t_8 = 6.00\ hrs$; 9) $t_9 = 12.00\ hrs$; 10) $t_{10} = 18.00\ hrs$;

[23] DV_{max} without the specification of a time value stands for the final values calculated at the end of the simulation DV_{max}^{17}.

and 11) $t_{17} = 18.19\ hrs$. Note that the last row correspond always to t_{17}, which is the time at the end of the simulation.

The procedure for generating PAR analysis results shown in Table 22 will be explained with reference to Figure 44. During the simulation DSS-WISE Lite solver generates $DV_{max}(t_i)$ rasters at predefined intervals. These rasters are stored for the purposes of PAR analysis by DSS-WISE HCOM. They are not included in the final results package; thus, they are unavailable to the user.

Before we proceed with the description of the methodology, let us define some new variables:

- The two dimensional array of nighttime population in Table 22 will be denoted as $NTP_{it,jHZ}$. The ranges of row and column numbers are $1 \leq it \leq 17$ and $1 \leq jHZ \leq 12$, respectively.
- The two dimensional array of daytime population in Table 23 will be denoted as $DTP_{it,jHZ}$. The ranges of row and column numbers are $1 \leq it \leq 17$ and $1 \leq jHZ \leq 12$, respectively.
- The two dimensional array of inundation extent area in Table 24 will be denoted as $IEA_{it,jHZ}$. The ranges of row and column numbers are $1 \leq it \leq 17$ and $1 \leq jHZ \leq 12$, respectively.

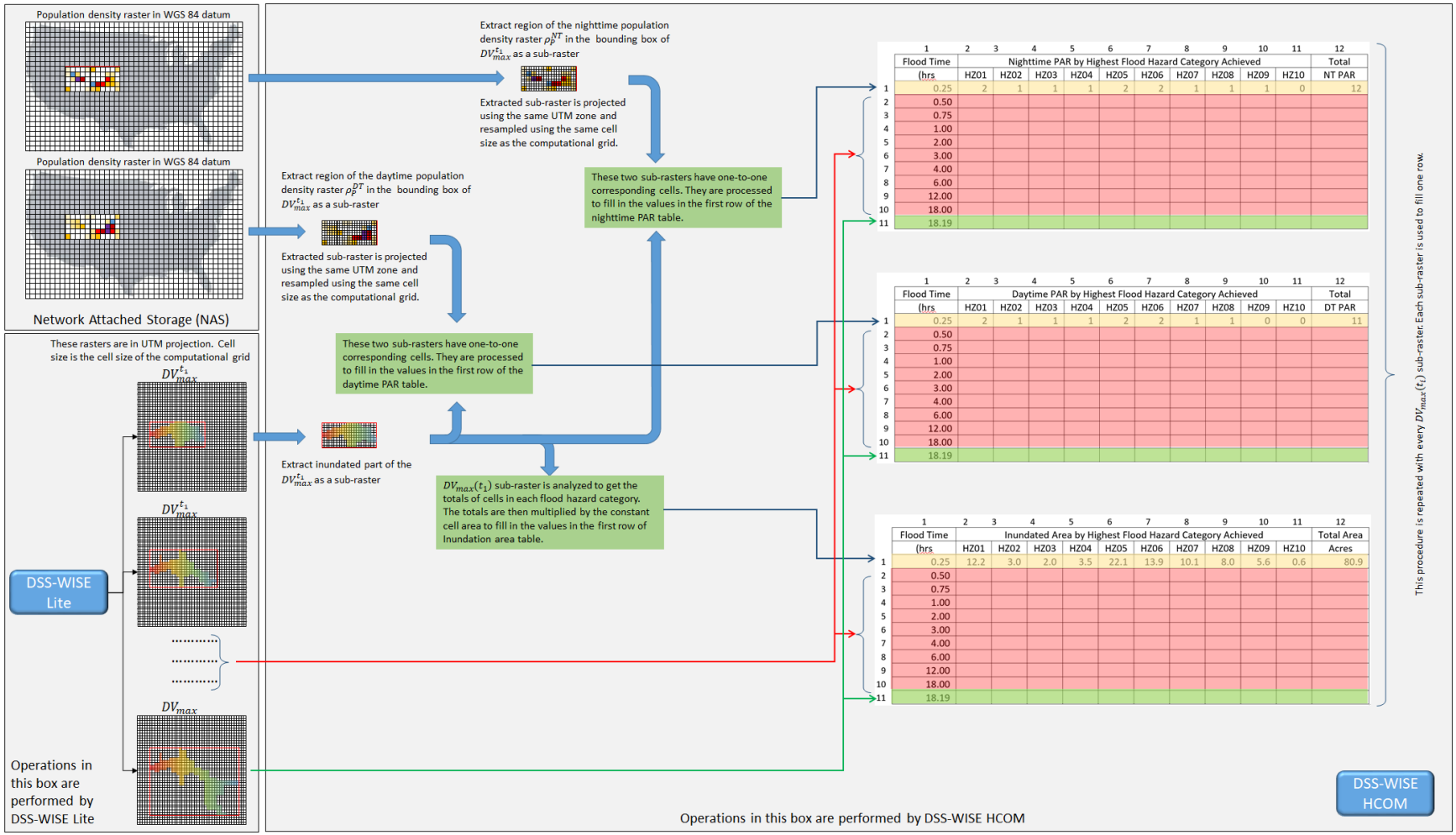

Figure 44 Illustration of the procedure used for filling the table of PAR analysis using nighttime or daytime population density.

- The two dimensional array of $DV_{max}^{t_i}$ generated at time t_i will be denoted as $DVM_{i1,j1}^{it}$. Since the computational domain has M columns and N rows, the ranges of row and column numbers are $1 \leq i1 \leq N$ and $1 \leq j1 \leq M$, respectively. Depending on the number of simulation, DSS-WISE Lite may generate up to 17 $DVM_{i1,j1}^{it}$ arrays. Thus, the range of the superscript is $1 \leq it \leq 17$. $DVM_{i1,j1}^{it}$ rasters are in UTM projection and have the same cell size as the computational grid.
- The nighttime population density raster shown in Figure 29 (see Section 4.1.3) is denoted as $(\rho_{NTP})_{k,\ell}$. The raster is in WGS 84 horizontal datum and has a resolution of 3 arc-second.
- The daytime population density raster shown in Figure 30 (see Section 4.1.3) is denoted as $(\rho_{DTP})_{k,\ell}$. The raster is in WGS 84 horizontal datum and has a resolution of 3 arc-second.

To fill the values in Table 22, Table 23, and Table 24 DSS-WISE HCOM loops through it flood times and calculates according to the following steps.

1. Initialize all elements of the row number it of the arrays NTP, DTP and IEA as zero

$$NTP_{it,jHZ=1\ to\ 10} = 0 \quad ; \quad DTP_{it,jHZ=1\ to\ 10} = 0 \quad ; \quad IEA_{it,jHZ=1\ to\ 10} = 0 \tag{46}$$

2. Let $it = 1$

3. Select the raster $DVM_{i1,j1}^{it}$. The bounding box of the inundated area is extracted as a sub-raster denoted by $SDVM_{i2,j2}^{it}$. Assume that the extracted raster has MS columns and NS rows, the ranges of row and column numbers are $1 \leq i2 \leq NS$ and $1 \leq j2 \leq MS$, respectively.

4. Convert the bounding box of $SDVM_{i2,j2}^{it}$ to WGS 84 datum and use the converted bounding box
   - to extract nighttime population density sub-raster $(S\rho_{NTP})_{i2,j2}$ from the nighttime population raster $(\rho_{NTP})_{k,\ell}$ and
   - to extract daytime population density sub-raster $(S\rho_{DTP})_{i2,j2}$ from the daytime population raster $(\rho_{DTP})_{k,\ell}$

   The extracted sub-rasters are resampled with the same cell size as the computational grid and projected using the appropriate UTM zone. Thus, both sub-rasters have also MS columns and NS rows, and the ranges of row and column numbers are $1 \leq i2 \leq NS$ and $1 \leq j2 \leq MS$, respectively.

   At this stage, it is important to note that the three sub-rasters $SDVM_{i2,j2}^{it}$, as $(S\rho_{NTP})_{i2,j2}$ and $(S\rho_{DTP})_{i2,j2}$ have all one-to-one corresponding cells. The surface area of all cells is the same and equal to A_{cc}, which is the area of the computational cells.

5. Process three sub-rasters cell by cell as follows:
   - If $SDVM_{i2,j2}^{it} = NoData$ then the cell is dry. Skip the cell
   - If $SDVM_{i2,j2}^{it} \neq NoData$ then the cell is inundated. Determine the hazard category of the cell by checking in which interval the $SDVM_{i2,j2}^{it}$ value is located. Assume that the hazard category for the cell is determined to be HZN
     - If $(S\rho_{NTP})_{i2,j2}$ ≠NoData, then increment the population

$$NTP_{it,HZN} = NTP_{it,HZN} + A_{cc}\,(S\rho_{NTP})_{i2,j2} \tag{47}$$

6. First, the totals for 10 hazard categories are initialized to zero. Then the sub-rasters of $DV_{max}(t_1)$ and population density are processed cell by cell as follows:
   - If the cell of the $DV_{max}(t_1)$ sub-raster has a NoData value, the cell has not yet been inundated. Skip the cell.
   - If the cell of the $DV_{max}(t_1)$ sub-raster has a valid DV_{max} value, check the value of the corresponding cell in the population density sub-raster:
     - If the corresponding cell in the population density sub-raster has a valid value of ρ_P then the population count in the cell, N_P, is found by multiplying the surface area of the computational cell, A, with the population density ρ_P

$$N_P = A\,\rho_P \tag{48}$$

       The hazard category of the cell is determined based on the DV_{max} value and the N_P value is added to the corresponding total.
     - If the corresponding cell in the population density sub-raster has a NoData value, the hazard category of the cell is determined based on the DV_{max} value and the background color of the column corresponding to the hazard class is changed to yellow to inform the user that the population count given in that row and column involves at least one NoData value in the population density sub-raster.

7. Proceed to the following time interval and repeat the calculations above.

Since the inundation grid differs from the rasterized population source datasets, there will be some discrepancies between the overlapping cells. Cells in the population datasets may be partially covered by the inundated area, so their counts must be counted proportionally by assuming equal population distribution throughout the cell.

Figure 45 shows the maximum inundation polygon superposed on the 3 arc-second population density grid. In this particular figure, the nighttime population density is used but the following discussion applies also to the daytime population density raster. The population density raster is rendered using shades of green. Lighter shades correspond to low population density whereas darker shades correspond to higher population density. The right side of the figure shows the area in the black rectangle. It is important to note that the raster and maximum inundation polygon are not projected although for the sake of illustration they are shown on a flat surface. Both data layers are in fact on the WGS 84 ellipsoid. The enlarged area on the right shows the 3 arc-second grid of the population density data. Since the data layer is on the ellipsoid, the cell size is not constant but varies with latitude (north-south direction). Due to the short distances shown in the figure, however, the differences are too small to be noticed at the scale of the figure.

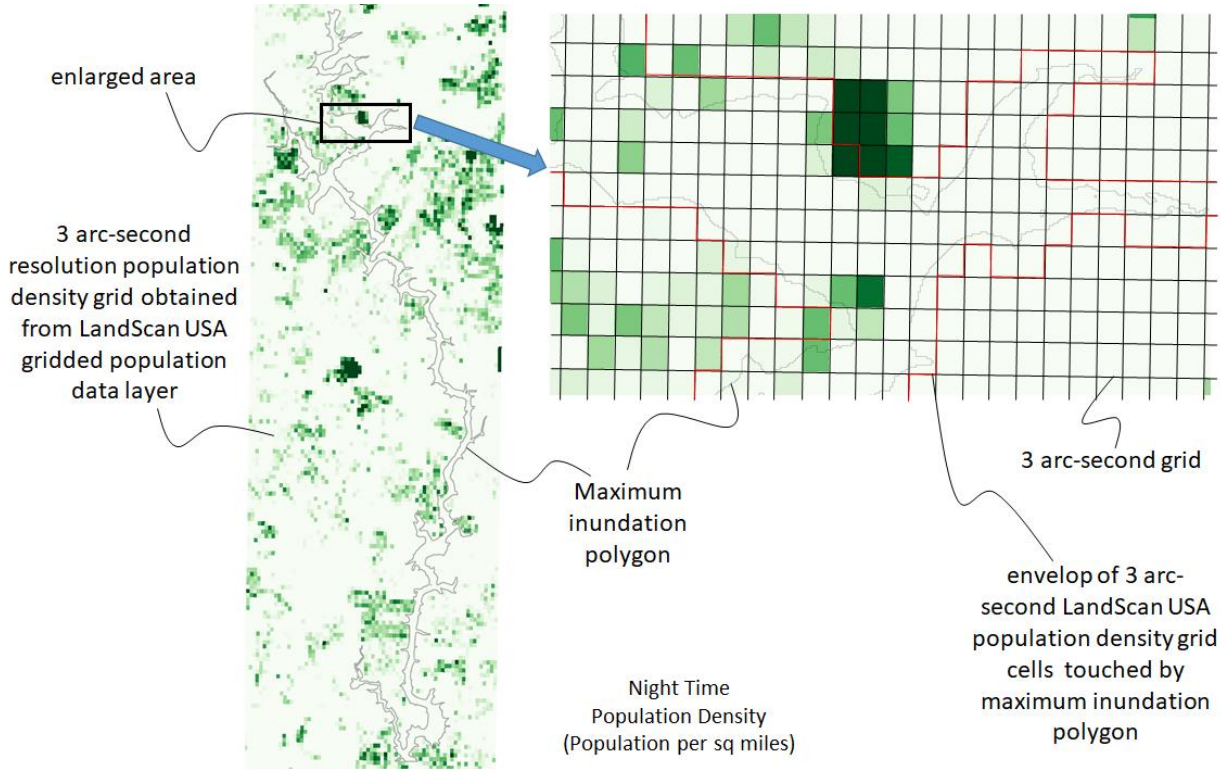

Figure 45 Superposition of maximum inundation polygon on the LandScan USA population density grid.

Note that the envelope of all the grid cells touched by the maximum inundation polygon is drawn as a red line following the cell edges. The population density cells inside this envelop are the ones that are partially or completely inundated by the flood. In Figure 46, these cells are highlighted in transparent yellow. These cells are extracted as a list for PAR calculation using the yellow polygon area as a mask.

It should be remembered that the computational cells are always smaller than the population density cells (currently the largest cell size allowed for a DSS-WISE Lite simulation is 200 feet). Some of the

extracted cells along the edge of the maximum inundation polygon are partially affected the inundation. Thus, assuming that the maximum inundation polygon is correctly computed, counting the PAR as the sum of the population of the extracted cells would lead to an overestimation. Thus the PAR counting using nighttime and daytime population densities is carried out based on the computational cells that are inundated.

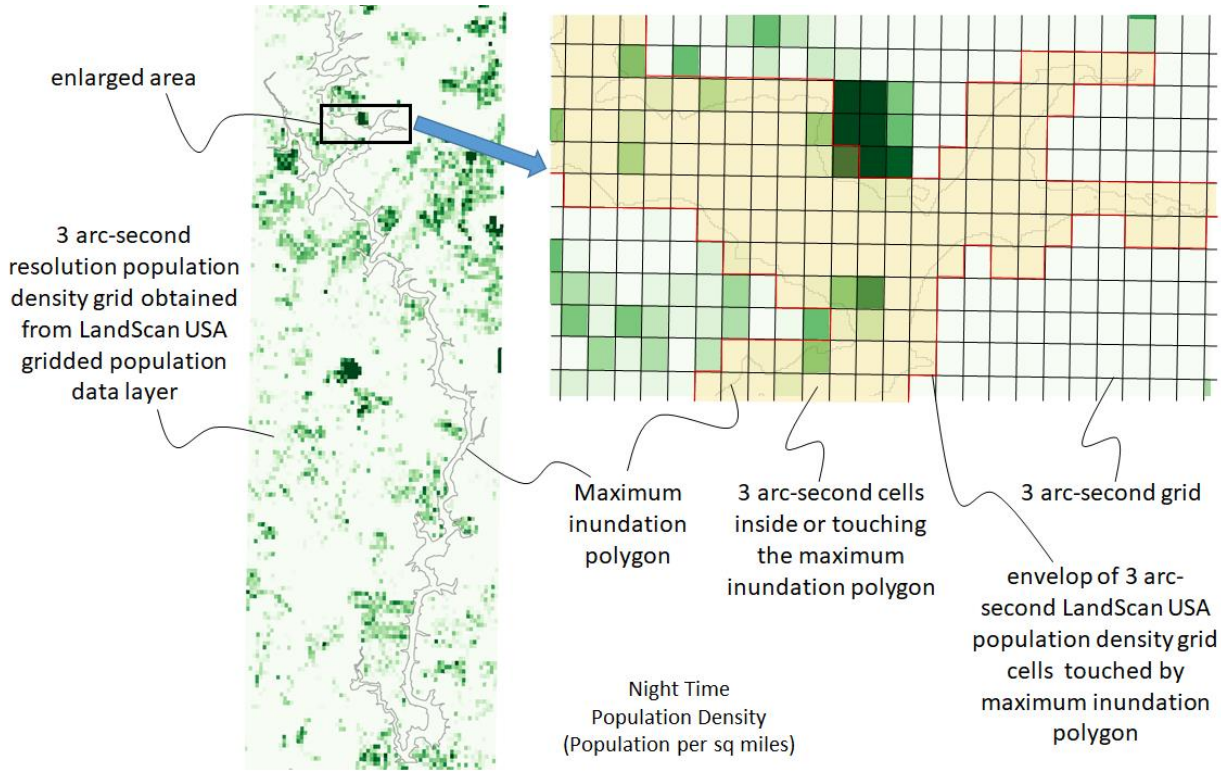

Figure 46 Extracting 3 arc-second population density grid cells to be used in PAR calculation.

Chapter 9 FORMAT AND ATTRIBUTES OF RESULTS SHAPEFILES

This section provides information on the format and structure of various shapefiles generated by DSS-WISE Lite and DSS-WISE HCOM. For each the relevant information is provided in at least two but sometimes in three tables:

1. Attribute table for the shapefile
2. Description of the attributes in the attribute table
3. Table of color codes and legends (provided only for some shapefiles).

9.1 Format and Structure of the Results Shapefiles Generated by DSS-WISE Lite

The complete list of files generated by DSS-WISE Lite is given in Table 8. Table 25 lists the tables providing information on the format and structure DSS-WISE Lite results shapefiles.

Table 25 Index for Results Shapefiles Generated by DSS-WISE Lite

DSS-WISE Lite Results Shapefile	Attributes	Description of Attributes	Color Code and Legends
X_Hmax_ft_polygons_upto_final.shp	Table 27	Table 28	Table 29
X_Flood_Arrival_Time_hr_polygons_upto_final.shp	Table 30	Table 31	Table 32
X_DVmax_ft2ps_polygons_upto_final.shp	Table 33	Table 34	Table 35
X_DVmax_Arrival_Time_hr_polygons_upto_final.shp	Table 37	Table 38	Table 39
X_Vmax_ftps_polygons_upto_final.shp	Table 39	Table 40	Table 41
X_Inundation_Extent_3_mi.shp	Table 42	Table 46	-
X_Inundation_Extent_7_mi.shp	Table 43	Table 46	-
X_Inundation_Extent_15_mi.shp	Table 44	Table 46	-
X_Inundation_Extent_60_mi.shp	Table 45	Table 46	-
X_Inundation_Extent_Final_Y_mi.shp	Table 47	Table 48	-

9.2 Format and Structure of the Results Shapefiles Generated by DSS-WISE HCOM

The complete list of files generated by DSS-WISE Lite is given in Table 9. Table 26 lists the tables providing information on the format and structure DSS-WISE Lite results shapefiles.

Table 26 Index for Results Shapefiles Generated by DSS-WISE HCOM

DSS-WISE HCOM Results Shapefile	Attributes	Description of Attributes	Color Code and Legends
X_HCOM_PLFZ_polygons.shp	Table 49	Table 50	Table 51
X_HCOM_Indoor_Hazard_Categories_polygons.shp	Table 52		Table 54
X_HCOM_Outdoor_Hazard_Categories_polygons.shp	Table 55	Table 56	Table 57
X_HCOM_Census_Block_polygons.shp	Table 20	Table 21	-
X_HCOM_NT_PopDensity_persqmi_polygons.shp	Table 58	Table 59	Table 60
X_HCOM_DT_PopDensity_persqmi_polygons.shp	Table 61	Table 62	Table 63

Table 27 Attribute table for the shapefile "X_Hmax_ft_polygons_upto_final" generated by DSS-WISE Lite.

ID	LBOUND	UBOUND	PROJNAME	SCENNAME	SCENDESCP	AREA_ACRES
5	6	30.9	Sunny Day Breach	D 4469	Sunny Day Breach, Top of Dam, Sudden Failure	968.861
9	30	30.9	Sunny Day Breach	D 4469	Sunny Day Breach, Top of Dam, Sudden Failure	2.59
4	3	30.9	Sunny Day Breach	D 4469	Sunny Day Breach, Top of Dam, Sudden Failure	1170.946
3	2	30.9	Sunny Day Breach	D 4469	Sunny Day Breach, Top of Dam, Sudden Failure	1223.581
2	1	30.9	Sunny Day Breach	D 4469	Sunny Day Breach, Top of Dam, Sudden Failure	1276.419
1	0	30.9	Sunny Day Breach	D 4469	Sunny Day Breach, Top of Dam, Sudden Failure	1329.017
8	24	30.9	Sunny Day Breach	D 4469	Sunny Day Breach, Top of Dam, Sudden Failure	48.567
7	18	30.9	Sunny Day Breach	D 4469	Sunny Day Breach, Top of Dam, Sudden Failure	138.54
6	12	30.9	Sunny Day Breach	D 4469	Sunny Day Breach, Top of Dam, Sudden Failure	380.799

Table 28 Description of the attributes for the shapefile "X_Hmax_ft_polygons_upto_final" generated by DSS-WISE Lite.

Attribute	Type	Explanation
ID	Integer	The ID number is the number for ordering the maximum depth intervals for the features (polygons): 1: 0 ft. to UBOUND 2: 1 ft. to UBOUND 3: 2 ft. to UBOUND 4: 3 ft. to UBOUND 5: 6 ft. to UBOUND 6: 12 ft. to UBOUND 7: 18 ft. to UBOUND 8: 24 ft. to UBOUND 9: 30 ft. to UBOUND Note that the lower bounds for all feature (polygon) ID numbers are different but the upper bounds are the same and equal to the maximum flood depth (which is 30.9 ft. in this example) achieved in the maximum flood extent. This is because Hmax polygons are mean to be stacked polygons and must be viewed stacked in the order of increasing ID number. The polygon with

		the smallest ID number is the bottommost polygon and the polygon with the highest ID number is the topmost polygon.
LBOUND	Real number	This is the lower bound of maximum flood depth in ft. for the feature
UBOUND	Real number	This is the upper bound of maximum flood depth in ft. for the feature. It should be noted that all polygons have the same upper bound, which is the maximum flood depth achieved in the maximum flood extent.
PROJNAME	Text	This is the project name provided by the user.
SCENNAME	Text	This is the scenario name provided by the user.
SCENDESCP	Text	This is the scenario description provided by the user.
AREA-ACRES	Real number	This is the surface area of the polygon with the specified lower and upper bounds of maximum flood depth.

Table 29 Color code and legend for the H_{max} polygons in "X_Hmax_ft_polygons_upto_final" generated by DSS-WISE Lite.

ID	LBOUND	UBOUND	R	G	B	A	Color	Legend
1	0	30.9	204	251	255	0.5		0 - 1
2	1	30.9	153	230	255	0.5		1 - 2
3	2	30.9	76	166	255	0.5		2 - 3
4	3	30.9	25	102	255	0.5		3 - 6
5	6	30.9	35	42	217	0.5		6 - 12
6	12	30.9	84	39	136	0.5		12 - 18
7	18	30.9	142	1	82	0.5		18 - 24
8	24	30.9	197	27	125	0.5		24 - 30
9	30	30.9	255	61	61	0.5		30 +

Table 30 Attribute table for the shapefile "X_Flood_Arrival_Time_hr_polygons_upto_final.shp" generated by DSS-WISE Lite.

ID	LBOUND	UBOUND	PROJNAME	SCENNAME	SCENDESCP	AREA_ACRES
4	0	1.5	Sunny Day Breach	D 4469	Sunny Day Breach, Top of Dam, Sudden Failure	358.072
1	0	0.25	Sunny Day Breach	D 4469	Sunny Day Breach, Top of Dam, Sudden Failure	80.927
2	0	0.5	Sunny Day Breach	D 4469	Sunny Day Breach, Top of Dam, Sudden Failure	140.634
7	0	12	Sunny Day Breach	D 4469	Sunny Day Breach, Top of Dam, Sudden Failure	1260.826
8	0	18.19	Sunny Day Breach	D 4469	Sunny Day Breach, Top of Dam, Sudden Failure	1329.017
5	0	3	Sunny Day Breach	D 4469	Sunny Day Breach, Top of Dam, Sudden Failure	598.659
6	0	6	Sunny Day Breach	D 4469	Sunny Day Breach, Top of Dam, Sudden Failure	852.847
3	0	1	Sunny Day Breach	D 4469	Sunny Day Breach, Top of Dam, Sudden Failure	264.711

Table 31 Description of the attributes for the shapefile "X_Flood_Arrival_Time_hr_polygons_upto_final.shp" generated by DSS-WISE Lite.

Attribute	Type	Explanation
ID	Integer	The ID number is the number for ordering the maximum depth intervals for the features (polygons): 1: 0 hrs to 0.25 hrs 2: 0 hrs to 0.5 hrs 3: 0 hrs to 1 hrs 4: 0 hrs to 1.5 hrs 5: 0 hrs to 3 hrs 6: 0 hrs to 6 hrs 7: 0 hrs to 12 hrs 8: 0 hrs to 24 hrs 9: 0 hrs to 48 hrs 10: 0 hrs to 72 hrs 11: > 72 hrs Note that the lower bounds for all feature (polygon) ID numbers are the same and equal to 0 hrs (i.e. beginning of the simulation) whereas the upper bounds are different. This is because T_{arr} polygons are meant to be stacked polygons and must be viewed stacked in the order of decreasing ID number. The polygon with the smallest ID number is the topmost polygon and the polygon with the highest ID number is the bottommost polygon. The number of polygons created depends on the simulation time achieved. If the simulation ends before 72 hrs, there

		would be less than 11 polygons. In the test case simulation, only 8 polygons have been generated. The upper bound of the 8th polygon is 18.19 hrs, which the maximum value of T_{arr} in the raster file "X_Arrival_Time_hr_upto_final.tif".
LBOUND	Real number	This is the lower bound of the flood arrival time for the feature. All features have the same lower bound.
UBOUND	Real number	This is the upper bound of the flood arrival time for the feature.
PROJNAME	Text	This is the project name provided by the user.
SCENNAME	Text	This is the scenario name provided by the user.
SCENDESCP	Text	This is the scenario description provided by the user.
AREA-ACRES	Real number	This is the surface area of the polygon with the specified lower and upper bounds of the flood arrival time.

Table 32 Color code and legend for the T_{arr} polygons in "X_Flood_Arrival_Time_hr_polygons_upto_final.shp" generated by DSS-WISE Lite.

ID	LBOUND	UBOUND	R	G	B	A	Color	Legend
1	0	0.25	103	0	31	0.5		$\leq$ 0.25 hrs
2	0	0.5	165	0	38	0.5		$\leq$ 0.5 hrs
3	0	1	217	32	48	0.5		$\leq$ 1 hrs
4	0	1.5	244	109	67	0.5		$\leq$ 1.5 hrs
5	0	3	253	174	97	0.5		$\leq$ 3 hrs
6	0	6	254	224	139	0.5		$\leq$ 6 hrs
7	0	12	255	254	204	0.5		$\leq$ 12 hrs
8	0	24	230	245	152	0.5		$\leq$ 24 hrs
9	0	48	171	221	164	0.5		$\leq$ 48 hrs
10	0	72	102	194	165	0.5		$\leq$ 72 hrs
11	72	UBOUND	50	136	189	0.5		$>$ 72 hrs

Table 33 Attribute table for the shapefile "X_DVmax_ft2ps_polygons_upto_final" generated by DSS-WISE Lite.

ID	LBOUND	UBOUND	PROJNAME	SCENNAME	SCENDESCP	AREA_ACRES
5	13	54	Sunny Day Breach	D 4469	Sunny Day Breach, Top of Dam, Sudden Failure	411.561
10	377	478.66	Sunny Day Breach	D 4469	Sunny Day Breach, Top of Dam, Sudden Failure	0.56
9	215	377	Sunny Day Breach	D 4469	Sunny Day Breach, Top of Dam, Sudden Failure	6.143
4	8.6	13	Sunny Day Breach	D 4469	Sunny Day Breach, Top of Dam, Sudden Failure	144.573
3	6.5	8.6	Sunny Day Breach	D 4469	Sunny Day Breach, Top of Dam, Sudden Failure	80.946
2	4.3	6.5	Sunny Day Breach	D 4469	Sunny Day Breach, Top of Dam, Sudden Failure	109.725
1	0	4.3	Sunny Day Breach	D 4469	Sunny Day Breach, Top of Dam, Sudden Failure	477.916
8	161	215	Sunny Day Breach	D 4469	Sunny Day Breach, Top of Dam, Sudden Failure	14.591
7	108	161	Sunny Day Breach	D 4469	Sunny Day Breach, Top of Dam, Sudden Failure	23.893
6	54	108	Sunny Day Breach	D 4469	Sunny Day Breach, Top of Dam, Sudden Failure	66.621
5	13	54	Sunny Day Breach	D 4469	Sunny Day Breach, Top of Dam, Sudden Failure	411.561

Table 34 Description of the attributes for the shapefile "X_DVmax_ft2ps_polygons_upto_final" generated by DSS-WISE Lite.

Attribute	Type	Explanation
ID	Integer	The ID number is the number for ordering the maximum velocity intervals for the features: 1: 0 ft^2/s to 4.3 ft^2/s 2: 4.3 ft^2/s to 6.5 ft^2/s 3: 6.5 ft^2/s to 8.6 ft^2/s 4: 8.6 ft^2/s to 13 ft^2/s 5: 13 ft^2/s to 54 ft^2/s 6: 54 ft^2/s to 108 ft^2/s 7: 108 ft^2/s to 161 ft^2/s 8: 161 ft^2/s to 215 ft^2/s 9: 215 ft^2/s to 377 ft^2/s 10: 377 ft^2/s to 478.66 ft^2/s Note that the feature ID numbers correspond to different lower and upper bounds. The upper bound of the last feature (ID= 8) is always the maximum velocity (which in this example is 36.95 ft/s) achieved in the maximum flood extent. The number of polygons can be less than 8.

		Their number depends on the maximum flood velocity compared to the standard intervals listed above.
LBOUND	Real number	This is the lower bound of maximum flood velocity in ft^2/s for the feature
UBOUND	Real number	This is the upper bound of maximum flood velocity in ft^2/s for the feature.
PROJNAME	Text	This is the project name provided by the user.
SCENNAME	Text	This is the scenario name provided by the user.
SCENDESCP	Text	This is the scenario description provided by the user.
AREA-ACRES	Real number	This is the surface area of the polygon with the specified lower and upper bounds of maximum flood velocity.

Table 35 Color code and legend for the DV_{max} polygons in shapefile "X_DVmax_ft2ps_polygons_upto_final" generated by DSS-WISE Lite..

ID	LBOUND	UBOUND	R	G	B	A	Color	Legend
1	0	4.3	204	254	255	0.5		0 - 4
2	4.3	6.5	100	203	255	0.5		4 - 7
3	6.5	8.6	51	153	255	0.5		7 - 9
4	8.6	13	241	60	241	0.5		9 - 13
5	13	54	188	45	188	0.5		13 - 54
6	54	108	184	225	134	0.5		54 - 108
7	108	161	77	146	33	0.5		108 - 163
8	161	215	255	238	153	0.5		163 - 217
9	215	377	255	120	87	0.5		217 - 379
10	377	478.66	217	32	48	0.5		379+

Table 36 Attribute table for the shapefile "X_DVmax_Arrival_Time_hr_polygons_upto_final.shp" generated by DSS-WISE Lite.

ID	LBOUND	UBOUND	PROJNAME	SCENNAME	SCENDESCP	AREA_ACRES
5	1.5	3	Sunny Day Breach	D 4469	Sunny Day Breach, Top of Dam, Sudden Failure	189.991
8	12	18.19	Sunny Day Breach	D 4469	Sunny Day Breach, Top of Dam, Sudden Failure	248.503
7	6	12	Sunny Day Breach	D 4469	Sunny Day Breach, Top of Dam, Sudden Failure	383.03
2	0.25	0.5	Sunny Day Breach	D 4469	Sunny Day Breach, Top of Dam, Sudden Failure	38.393
1	0	0.25	Sunny Day Breach	D 4469	Sunny Day Breach, Top of Dam, Sudden Failure	33.251
4	1	1.5	Sunny Day Breach	D 4469	Sunny Day Breach, Top of Dam, Sudden Failure	122.011
3	0.5	1	Sunny Day Breach	D 4469	Sunny Day Breach, Top of Dam, Sudden Failure	68.604
6	3	6	Sunny Day Breach	D 4469	Sunny Day Breach, Top of Dam, Sudden Failure	245.693

Table 37 Description of the attributes for the shapefile "X_DVmax_Arrival_Time_hr_polygons_upto_final.shp" generated by DSS-WISE Lite.

Attribute	Type	Explanation
ID	Integer	The ID number is the number for ordering the maximum depth intervals for the features (polygons): 1: 0 hrs to 0.25 hrs 2: 0 hrs to 0.5 hrs 3: 0 hrs to 1 hrs 4: 0 hrs to 1.5 hrs 5: 0 hrs to 3 hrs 6: 0 hrs to 6 hrs 7: 0 hrs to 12 hrs 8: 0 hrs to 24 hrs 9: 0 hrs to 48 hrs 10: 0 hrs to 72 hrs 11: > 72 hrs Note that the lower bounds for all feature (polygon) ID numbers are the same and equal to 0 hrs (i.e. beginning of the simulation) whereas the upper bounds are different. This is because Tq_{arr} polygons are meant to be stacked polygons and must be viewed stacked in the order of decreasing ID number. The polygon with the smallest ID number is the topmost polygon and the polygon with the highest ID number is the bottommost polygon. The number of polygons created depends on the simulation time achieved. If the simulation ends before 72 hrs, there

		would be less than 11 polygons. In the test case the simulation, only 8 polygons have been generated. The upper bound of the 8th polygon is 18.19 hrs, which the maximum value of Tq_{arr} in the raster file "X_DVmax_Arrival_Time_hr_upto_final.tif".
LBOUND	Real number	This is the lower bound of the arrival time of DV_{max} for the feature. All features have the same lower bound.
UBOUND	Real number	This is the upper bound of the arrival time of DV_{max} for the feature.
PROJNAME	Text	This is the project name provided by the user.
SCENNAME	Text	This is the scenario name provided by the user.
SCENDESCP	Text	This is the scenario description provided by the user.
AREA-ACRES	Real number	This is the surface area of the polygon with the specified lower and upper bounds of the arrival time of DV_{max}.

Table 38 Color code and legend for the Tq_{arr} polygons in "X_DVmax_Arrival_Time_hr_polygons_upto_final.shp" generated by DSS-WISE Lite.

ID	LBOUND	UBOUND	R	G	B	A	Color	Legend
1	0	0.25	103	0	31	0.5		$\leq$ 0.25 hrs
2	0	0.5	165	0	38	0.5		$\leq$ 0.5 hrs
3	0	1	217	32	48	0.5		$\leq$ 1 hrs
4	0	1.5	244	109	67	0.5		$\leq$ 1.5 hrs
5	0	3	253	174	97	0.5		$\leq$ 3 hrs
6	0	6	254	224	139	0.5		$\leq$ 6 hrs
7	0	12	255	254	204	0.5		$\leq$ 12 hrs
8	0	24	230	245	152	0.5		$\leq$ 24 hrs
9	0	48	171	221	164	0.5		$\leq$ 48 hrs
10	0	72	102	194	165	0.5		$\leq$ 72 hrs
11	72	UBOUND	50	136	189	0.5		$>$ 72 hrs

Table 39 Attribute table for the shapefile "X_Vmax_ftps_polygons_upto_final" generated by DSS-WISE Lite.

ID	LBOUND	UBOUND	PROJNAME	SCENNAME	SCENDESCP	AREA_ACRES
5	10	15	Sunny Day Breach	D 4469	Sunny Day Breach, Top of Dam, Sudden Failure	16.492
4	6	10	Sunny Day Breach	D 4469	Sunny Day Breach, Top of Dam, Sudden Failure	42.213
3	3	6	Sunny Day Breach	D 4469	Sunny Day Breach, Top of Dam, Sudden Failure	193.407
2	1	3	Sunny Day Breach	D 4469	Sunny Day Breach, Top of Dam, Sudden Failure	621.322
1	0	1	Sunny Day Breach	D 4469	Sunny Day Breach, Top of Dam, Sudden Failure	466.639
8	30	36.95	Sunny Day Breach	D 4469	Sunny Day Breach, Top of Dam, Sudden Failure	0.514
7	20	30	Sunny Day Breach	D 4469	Sunny Day Breach, Top of Dam, Sudden Failure	3.278
6	15	20	Sunny Day Breach	D 4469	Sunny Day Breach, Top of Dam, Sudden Failure	1.974
5	10	15	Sunny Day Breach	D 4469	Sunny Day Breach, Top of Dam, Sudden Failure	16.492

Table 40 Description of the attributes for the shapefile "X_Vmax_ftps_polygons_upto_final" generated by DSS-WISE Lite.

Attribute	Type	Explanation
ID	Integer	The ID number is the number for ordering the maximum velocity intervals for the features: 1: 0 ft/s to 1 ft/s 2: 1 ft/s to 3 ft/s 3: 3 ft/s to 6 ft/s 4: 6 ft/s to 10 ft/s 5: 10 ft/s to 15 ft/s 6: 15 ft/s to 20 ft/s 7: 20 ft/s to 30 ft/s 8: 30 ft/s to 36.95 ft/s Note that the feature ID numbers correspond to different lower and upper bounds. The upper bound of the last feature (ID= 8) is always the maximum velocity (which in this example is 36.95 ft/s) achieved in the maximum flood extent. The number of polygons can be less than 8. Their number depends on the maximum flood velocity compared to the standard intervals listed above.
LBOUND	Real number	This is the lower bound of maximum flood velocity in ft/s for the feature
UBOUND	Real number	This is the upper bound of maximum flood velocity in ft/s for the feature.

PROJNAME	Text	This is the project name provided by the user.
SCENNAME	Text	This is the scenario name provided by the user.
SCENDESCP	Text	This is the scenario description provided by the user.
AREA-ACRES	Real number	This is the surface area of the polygon with the specified lower and upper bounds of maximum flood velocity.

Table 41 Color code and legend for the DV_{max} polygons in shapefile "X_Vmax_ftps_polygons_upto_final" generated by DSS-WISE Lite.

ID	LBOUND	UBOUND	R	G	B	A	Color	Legend
1	0	1	77	146	33	0.5		0 - 1
2	1	3	102	189	99	0.5		1 - 3
3	3	6	217	239	139	0.5		3 - 6
4	6	10	255	238	153	0.5		6 - 10
5	10	15	255	204	102	0.5		10 - 15
6	15	20	255	153	51	0.5		15 - 20
7	20	30	255	102	26	0.5		20 - 30
8	30	36.95	217	32	48	0.5		30+

Table 42 Attribute table for the shapefile "X_Inundation_Extent_3_mi.shp" generated by DSS-WISE Lite.

PROJNAME	SCENNAME	SCENDESCP	AREA_ACRES	MILEMARK
Sunny Day Breach	D 4469	Sunny Day Breach, Top of Dam, Sudden Failure	414.536	3.003

Table 43 Attribute table for the shapefile "X_Inundation_Extent_7_mi.shp" generated by DSS-WISE Lite.

PROJNAME	SCENNAME	SCENDESCP	AREA_ACRES	MILEMARK
Sunny Day Breach	D 4469	Sunny Day Breach, Top of Dam, Sudden Failure	816.997	7

Table 44 Attribute table for the shapefile "X_Inundation_Extent_15_mi.shp" generated by DSS-WISE Lite.

PROJNAME	SCENNAME	SCENDESCP	AREA_ACRES	MILEMARK
Sunny Day Breach	D 4469	Sunny Day Breach, Top of Dam, Sudden Failure	?[24]	15

Table 45 Attribute table for the shapefile "X_Inundation_Extent_60_mi.shp" generated by DSS-WISE Lite.

PROJNAME	SCENNAME	SCENDESCP	AREA_ACRES	MILEMARK
Sunny Day Breach	D 4469	Sunny Day Breach, Top of Dam, Sudden Failure	?[23]	60

Table 46 Description of the attributes for the shapefiles "X_Inundation_Extent_3_mi.shp", "X_Inundation_Extent_7_mi.shp, "X_Inundation_Extent_15_mi.shp", "X_Inundation_Extent_60_mi.shp" generated by DSS-WISE Lite.

Attribute	Type	Explanation
PROJNAME	Text	This is the project name provided by the user.
SCENNAME	Text	This is the scenario name provided by the user.
SCENDESCP	Text	This is the scenario description provided by the user.
AREA-ACRES	Real number	This is the surface area of the polygon with the specified lower and upper bounds of maximum flood velocity.

[24] These files were not generated for the test case because the flood front did not travel beyond 10.215 miles from the breach center.

MILEMARK	Real number	Distance of the flood front from the breach center when the inundation extent was generated

Table 47 Attribute table for the shapefile "X_Inundation_Extent_Final_Y_mi.shp" generated by DSS-WISE Lite.

PROJNAME	SCENNAME	SCENDESCP	AREA_ACRES	MILEMARK
Sunny Day Breach	D 4469	Sunny Day Breach, Top of Dam, Sudden Failure	1329.017	10.215

Table 48 Description of the attributes for the shapefile "X_Inundation_Extent_Final_Y_mi.shp" generated by DSS-WISE Lite.

Attribute	Type	Explanation
PROJNAME	Text	This is the project name provided by the user.
SCENNAME	Text	This is the scenario name provided by the user.
SCENDESCP	Text	This is the scenario description provided by the user.
AREA-ACRES	Real number	This is the surface area of the polygon with the specified lower and upper bounds of maximum flood velocity.
MILEMARK	Real number	Distance of the flood front from the breach center when the simulation was terminated. Note that the polygon in "X_Inundation_Extent_Final_Y_mi.shp" does not represent the inundation extent at a specific time. It is the bounding polygons of all cells that received flood waters regardless of the duration.

Table 49 Attribute table for the shapefile "X_HCOM_PLFZ_polygons.shp" generated by DSS-WISE HCOM.

ID	INFO	PROJNAME	SCENNAME	SCENDESC	AREA_ACRE
2	Adults	Sunny Day Breach	D 4469	Sunny Day Breach, Top of Dam, Sudden Failure	1115.59
1	Children	Sunny Day Breach	D 4469	Sunny Day Breach, Top of Dam, Sudden Failure	1223.75

Table 50 Description of the attributes for the shapefile "X_HCOM_PLFZ_polygons.shp" generated by DSS-WISE HCOM.

Attribute	Type	Explanation
ID	Integer	The ID number corresponds to PLFZ areas for Children and Adults: 1: $D_{max} > 2\ ft.$ and $DV_{max} > 5.4\ ft^2/s$ (criteria for PLFZ for children) 2: $D_{max} > 4\ ft.$ and $DV_{max} > 6.5\ ft^2/s$ (criteria for PLFZ for adults) Based on the creteria given above, it is clear that polygon 2 is a subset of polygon 1. In other words, if an area is considered as PLFZ for adults, it is also PLFZ for children.
INFO	Text	Information about the area delineated by the polygon
PROJNAME	Text	This is the project name provided by the user.
SCENNAME	Text	This is the scenario name provided by the user.
SCENDESC	Text	This is the scenario description provided by the user.
AREA-ACRES	Real number	This is the surface area of the polygon feature.

Table 51 Color code and legend for flood hazard polygons for people caught indoors in the shapefile "X_HCOM_Outdoor_Hazard_Categories_polygons.shp" generated by DSS-WISE HCOM.

ID	INFO	R	G	B	A	Color	Legend
1	Children	255	143	51	0.5		PLFZ for Children
2	Adults	217	32	48	0.5		PLFZ for Adults

Table 52 Attribute table for the shapefile "X_HCOM_Indoor_Hazard_Categories_polygons.shp" generated by DSS-WISE HCOM.

ID	INFO	PROJNAME	SCENNAME	SCENDESC	AREA_ACRE
5	Large Concrete	Sunny Day Breach	D 4469	Sunny Day Breach, Top of Dam, Sudden Failure	0.56
1	Poorly Constructed	Sunny Day Breach	D 4469	Sunny Day Breach, Top of Dam, Sudden Failure	66.62
2	Well-built Timber	Sunny Day Breach	D 4469	Sunny Day Breach, Top of Dam, Sudden Failure	23.89
3	Well-built Masonry	Sunny Day Breach	D 4469	Sunny Day Breach, Top of Dam, Sudden Failure	14.57
4	Concrete	Sunny Day Breach	D 4469	Sunny Day Breach, Top of Dam, Sudden Failure	6.14

Table 53 Description of the attributes for the shapefile "X_HCOM_Indoor_Hazard_Categories_polygons.shp" generated by DSS-WISE HCOM.

Attribute	Type	Explanation
ID	Integer	The ID number corresponds to the DV_{max} value beyond which a certain type of structure is likely to fail; thus, causing the people in the structure to be in danger. Five hazard classes are recognized: 1: $DV_{max} > 54\ ft^2/s$ (Poorly Constructed Building) 2: $DV_{max} > 108\ ft^2/s$ (Well-built Timber Building) 3: $DV_{max} > 162\ ft^2/s$ (Well Built Masonry Building) 4: $DV_{max} > 215\ ft^2/s$ (Concrete Building) 5: $DV_{max} > 377\ ft^2/s$ (Large Concrete Building) Increasing ID number corresponds to increasing damage level to the structure; thus to the people indoors.
INFO	Text	Information about the area delineated by the polygon
PROJNAME	Text	This is the project name provided by the user.
SCENNAME	Text	This is the scenario name provided by the user.
SCENDESC	Text	This is the scenario description provided by the user.
AREA-ACRES	Real number	This is the surface area of the polygon feature.

Table 54 Color code and legend for flood hazard polygons for people caught indoors in the shapefile "X_HCOM_Outdoor_Hazard_Categories_polygons.shp" generated by DSS-WISE HCOM.

ID	INFO	AREA_ACRE	R	G	B	A	Color	Legend
1	Poorly Constructed	66.62	204	254	255	0.5		Poorly Constructed Building
2	Well-built Timber	23.89	100	203	255	0.5		Well Built Timber Building
3	Well-built Masonry	14.57	51	153	255	0.5		Well Built Masonry Building
4	Concrete	6.14	25	102	255	0.5		Concrete Building
5	Large Concrete	0.56	134	29	134	0.5		Large Concrete Building

Table 55 Attribute table for the shapefile "X_HCOM_Outdoor_Hazard_Categories_polygons.shp" generated by DSS-WISE HCOM.

ID	INFO	PROJNAME	SCENNAME	SCENDESC	AREA_ACRE
5	Extreme Hazard	Sunny Day Breach	D 4469	Sunny Day Breach, Top of Dam, Sudden Failure	521.31
1	Very Low Hazard	Sunny Day Breach	D 4469	Sunny Day Breach, Top of Dam, Sudden Failure	477.49
2	Low Hazard	Sunny Day Breach	D 4469	Sunny Day Breach, Top of Dam, Sudden Failure	109.71
3	Moderate Hazard	Sunny Day Breach	D 4469	Sunny Day Breach, Top of Dam, Sudden Failure	80.95
4	Significant Hazard	Sunny Day Breach	D 4469	Sunny Day Breach, Top of Dam, Sudden Failure	143.95

Table 56 Description of the attributes for the shapefile "X_HCOM_Outdoor_Hazard_Categories_polygons.shp" generated by DSS-WISE HCOM.

Attribute	Type	Explanation
ID	Integer	The ID number corresponds to the DV_{max} value ranges corresponding hazard level for a certain population type caught outdoors by the flood. Five hazard classes for people caught outdoors are recognized: 1: $0.0 < DV_{max} < 4.3\ ft^2/s$ (Very Low Hazard) 2: $4.3 < DV_{max} < 6.5\ ft^2/s$ (Low Hazard) 3: $6.5 < DV_{max} < 8.6\ ft^2/s$ (Moderate Hazard 4: $8.6 < DV_{max} < 13\ ft^2/s$ (Significant Hazard) 5: $DV_{max} > 13\ ft^2/s$ (Extreme Hazard) Increasing ID number corresponds to increasing hazard level for people caught outdoors.
INFO	Text	Information about the area delineated by the polygon
PROJNAME	Text	This is the project name provided by the user.
SCENNAME	Text	This is the scenario name provided by the user.
SCENDESC	Text	This is the scenario description provided by the user.
AREA-ACRES	Real number	This is the surface area of the polygon feature.

Table 57 Color code and legend for flood hazard polygons for people caught outdoors in the shapefile "X_HCOM_Outdoor_Hazard_Categories_polygons.shp" generated by DSS-WISE HCOM.

ID	INFO	AREA_ACRE	R	G	B	A	Color	Legend
1	Very Low Hazard	477.49	0	176	80	0.5		Very Low Hazard
2	Low Hazard	109.71	153	255	102	0.5		Low Hazard
3	Moderate Hazard	80.95	255	255	0	0.5		Moderate Hazard
4	Significant Hazard	143.95	255	192	0	0.5		Significant Hazard
5	Extreme Hazard	521.31	255	55	55	0.5		Extreme Hazard

Table 58 Attribute table for the shapefile "X_HCOM_NT_PopDensity_persqmi_polygons.shp" generated by DSS-WISE HCOM.

ID	LBOUND	UBOUND	PROJNAME	SCENNAME	SCENDESCP	AREA_ACRES
5	8000	8819.4	Sunny Day Breach	D 4469	Sunny Day Breach, Top of Dam, Sudden Failure	1.747
1	0	1000	Sunny Day Breach	D 4469	Sunny Day Breach, Top of Dam, Sudden Failure	117.099
2	1000	2000	Sunny Day Breach	D 4469	Sunny Day Breach, Top of Dam, Sudden Failure	71.649
3	2000	4000	Sunny Day Breach	D 4469	Sunny Day Breach, Top of Dam, Sudden Failure	85.631
4	4000	8000	Sunny Day Breach	D 4469	Sunny Day Breach, Top of Dam, Sudden Failure	20.975

Table 59 Description of the attributes for the shapefile "X_HCOM_NT_PopDensity_persqmi_polygons.shp" generated by DSS-WISE HCOM.

Attribute	Type	Explanation
ID	Integer	The ID number is the number for ordering the maximum velocity intervals for the features:
LBOUND	Real number	This is the lower bound of the feature representing a nighttime population density range. Considering that a single person in a 3 arc-second cell (which is the resolution of the original LandScan USA data layers) corresponds to about 319 people per square mile, the LBOUND of the feature no 1 is set to this value.
UBOUND	Real number	This is the lower bound of the feature representing a nighttime population density range.
PROJNAME	Text	This is the project name provided by the user.
SCENNAME	Text	This is the scenario name provided by the user.
SCENDESCP	Text	This is the scenario description provided by the user.
AREA-ACRES	Real number	This is the total surface area of the polygons with the specified lower and upper bounds of nighttime population density.

Table 60 Color code and legend for flood hazard polygons for people caught outdoors in the shapefile "X_HCOM_NT_PopDensity_persqmi_polygons.shp" generated by DSS-WISE HCOM.

ID	LBOUND	UBOUND	AREA_ACRES	R	G	B	A	Color	Legend
1	0	1000	117.099	65	182	196	0.5		319 - 1000
2	1000	2000	71.649	65	160	210	0.5		1000 - 2000
3	2000	4000	85.631	33	97	175	0.5		2000 - 4000
4	4000	8000	20.975	130	26	158	0.5		4000 - 8000
5	8000	8819.4(*)	1.747	184	0	149	0.5		8000 - 8819.4
(*) UBOUND of the 5th and last feature reflects the highest nighttime population density in the inundated area.									

Table 61 Attribute table for the shapefile "X_HCOM_DT_PopDensity_persqmi_polygons.shp" generated by DSS-WISE HCOM.

ID	LBOUND	UBOUND	PROJNAME	SCENNAME	SCENDESCP	AREA_ACRES
5	8000	15795.35	Sunny Day Breach	D 4469	Sunny Day Breach, Top of Dam, Sudden Failure	1.748
2	1000	2000	Sunny Day Breach	D 4469	Sunny Day Breach, Top of Dam, Sudden Failure	50.683
1	0	1000	Sunny Day Breach	D 4469	Sunny Day Breach, Top of Dam, Sudden Failure	186.99
4	4000	8000	Sunny Day Breach	D 4469	Sunny Day Breach, Top of Dam, Sudden Failure	1.747
3	2000	4000	Sunny Day Breach	D 4469	Sunny Day Breach, Top of Dam, Sudden Failure	6.989

Table 62 Description of the attributes for the shapefile "X_HCOM_DT_PopDensity_persqmi_polygons.shp" generated by DSS-WISE HCOM.

Attribute	Type	Explanation
ID	Integer	The ID number is the number for ordering the maximum velocity intervals for the features:
LBOUND	Real number	This is the lower bound of the feature representing a daytime population density range. Considering that a single person in a 3 arc-second cell (which is the resolution of the original LandScan USA data layers) corresponds to about 319 people per square mile, the LBOUND of the feature no 1 is set to this value.
UBOUND	Real number	This is the lower bound of the feature representing a daytime population density range.
PROJNAME	Text	This is the project name provided by the user.
SCENNAME	Text	This is the scenario name provided by the user.
SCENDESCP	Text	This is the scenario description provided by the user.
AREA-ACRES	Real number	This is the total surface area of the polygons with the specified lower and upper bounds of daytime population density.

Table 63 Color code and legend for flood hazard polygons for people caught outdoors in the shapefile "X_HCOM_DT_PopDensity_persqmi_polygons.shp" generated by DSS-WISE HCOM.

ID	LBOUND	UBOUND	AREA_ACRES	R	G	B	A	Color	Legend
1	0	1000	186.99	65	182	196	0.5		319 - 1000
2	1000	2000	50.683	65	160	210	0.5		1000 - 2000
3	2000	4000	6.989	33	97	175	0.5		2000 - 4000
4	4000	8000	1.747	130	26	158	0.5		4000 - 8000
5	8000	15795.35(*)	1.748	184	0	149	0.5		8000 - 8819.4
(*) UBOUND of the 5th and last feature reflects the highest daytime population density in the inundated area.									

REFERENCES

Adams, Oscar S. (1921). Latitude Developments Connected With Geodesy and Cartography, (with tables, including a table for Lambert equal area meridional projection). Special Publication No. 67 of the US Coast and Geodetic Survey.

Altinakar, M.S., McGrath, M.Z., Matheu, E.E., Ramalingam, V.P., Seda-Sanabria, Y. Breitkreutz, W., Oktay, S., Zou, J.Z., Yezierski, M. (2012). Validation of Automated Dam-Break Flood Simulation and Assessment of Computational Performance. Proceedings of the Dam Safety 2012, ASDSO Annual Conference, September 16-20, Colorado Convention Center, Denver, CO.

Altinakar, M.S., McGrath, M.Z., Ramalingam, V.P. and Omari, H. (2010). 2D Modeling of Big Bay Dam Failure in Mississippi: Comparison with Field Data and 1D Model Results. Proc. of the Int. Conference on Fluvial Hydraulics (River Flow 2010), September 8-10, Braunschweig, Germany.

Altinakar, M.S. and McGrath, M.Z., 2012. Parallelized Two-Dimensional Dam-Break Flood Analysis with Dynamic Data Structures. ASCE-EWRI, 2012 World Environmental & Water Resources Congress, Albuquerque, New Mexico, May 20-24, 2012.

Altinakar, M.S., McGrath, M.Z., Ramalingam, V.P., Demby, J.E. Jr., and Inci, G. (2018). "Two-Dimensional Dam-Break Flood Modeling and Mapping for the USA." Proc. of the 5th International Symposium on Dam Safety. Oct. 27-31, 2018. Istanbul, Turkey.

Altinakar, M.S., McGrath, M.Z., Ramalingam, V.P., and Demby, J.E. Jr. (2017). "Web-Based, Automated Two-Dimensional Dam and Levee Failure Flood Modeling and Mapping." Proc. of the ASDSO 2017 Southeast Regional Conference, April 18-20, 2017, the Music City Center, Nashville, TN.

Altinakar, M.S., McGrath, M.Z., Matheu, E.E., Ramalingam, V.P., Seda-Sanabria, Y. Breitkreutz, W., Oktay, S., Zou, J.Z., Yezierski, M. (2012). Validation of Automated Dam-Break Flood Simulation and Assessment of Computational Performance. Proceedings of the Dam Safety 2012, ASDSO Annual Conference, September 16-20, Colorado Convention Center, Denver, CO.

Altinakar, M.S. and McGrath, M.Z. (2012). Parallelized Two-Dimensional Dam-Break Flood Analysis with Dynamic Data Structures. ASCE-EWRI, 2012 World Environmental & Water Resources Congress, Albuquerque, New Mexico, May 20-24, 2012.

Altinakar, M.S., McGrath, M.Z., Ramalingam, V.P. and Omari, H. (2010). 2D Modeling of Big Bay Dam Failure in Mississippi: Comparison with Field Data and 1D Model Results. Proc. of the Int. Conference on Fluvial Hydraulics (River Flow 2010), September 8-10, Braunschweig, Germany ftp://ftp.library.noaa.gov/docs.lib/htdocs/rescue/cgs_specpubs/QB275U35no671921.pdf

Bhaduri, B., Bright, E., Coleman, Ph., Urban, M.L. 2007. "LandScan USA: a high-resolution geospatial and temporal modeling approach for population distribution and dynamics." GeoJournal (2007) 69:103–117. DOI 10.1007/s10708-007-9105-9

Bhaduri, B. 2007. Workshop Presentation. https://www.csm.ornl.gov/workshops/RAMSworkshop07/presentations/bhaduri.ppt

British Columbia Hydro (BCH) 2006. "Life Safety Model System V1.0, Guidelines, Procedures, Calibration and Support Manual." Technical Report Engineering Report E310, British Columbia Hydro (BCH).

BCH (2006). Life Safety Model System V1.0, Guidelines, Procedures, Calibration and Support Manual. Technical Report Engineering Report E310, British Columbia Hydro (BCH).

Bhaduri, B., Bright, E., Coleman, Ph., Urban, M.L. (2007). LandScan USA: a high-resolution geospatial and temporal modeling approach for population distribution and dynamics. GeoJournal (2007) 69:103–117. DOI 10.1007/s10708-007-9105-9

Burkholder, E.F. 2017. The 3-D Global Spatial Data Model: Principles and Applications. CRC Press. 2nd Ed. ISBN 9781498722162.

Cox, R.J., Yee, M. and Ball, J.E. 2004. “Safety of People in Flooded Streets and Floodways.” 8th National Conference on Hydraulics in Water Engineering, Gold Coast. The Institution of Engineers, Australia.

Cox, R.J., Shand, T.D., and Blacka, M.J. 2010. “Australian Rainfall and Runoff, Revision Project 10: Appropriate Criteria for People.” AR&R Report Number P10/S1/006. Engineers Australia, Water Engineering. ISBN 978-085825-9454. http://arr.ga.gov.au/revision-projects/project-list/projects/project-10

Cox, R.J., Yee, M. and Ball, J.E. (2004). Safety of People in Flooded Streets and Floodways. 8th National Conference on Hydraulics in Water Engineering, Gold Coast. The Institution of Engineers, Australia.

Cox, R.J., Shand, T.D., and Blacka, M.J. (2010). Australian Rainfall and Runoff, Revision Project 10: Appropriate Criteria for People. AR&R Report Number P10/S1/006. Engineers Australia, Water Engineering. ISBN 978-085825-9454. http://arr.ga.gov.au/revision-projects/project-list/projects/project-10

Dobson, J.E., Bright, E.A., Coleman, Ph.R., Durfee, R.C., and Worley, B.A. (2000). LandScan: A Global Population Database for Estimating Populations at Risk. Photogrammetric Engineering & Remote Sensing, Vol. 66, NO. 7, July 2000, pp. 849-857. https://www.asprs.org/wp-content/uploads/pers/2000journal/july/2000_jul_849-857.pdf

Dobson, J.E., Bright, E.A., Coleman, Ph.R., Durfee, R.C., and Worley, B.A. 2000. “LandScan: A Global Population Database for Estimating Populations at Risk.” Photogrammetric Engineering & Remote Sensing, Vol. 66, NO. 7, July 2000, pp. 849-857. https://www.asprs.org/wp-content/uploads/pers/2000journal/july/2000_jul_849-857.pdf

Feinberg, B. (2017). Using Potentially Lethal Flood Zones to Assess Downstream Impacts from Dam Failure. Presentation at National Dam Safety Training Seminar.

Federal Emergency Management Agency (FEMA). (2011). “Estimating Loss of Life for Dam Failure Scenarios.” Draft version.

FEMA. (2004). Federal Guidelines for Dam Safety: Hazard Potential Classification System for Dams. Prepared by the Interagency Committee on Dam Safety. U.S. Federal Emergency Management Agency, Report No: FEMA 333, April, 2004.

FEMA/FIA. (2013). “Non-Residential Floodproofing – Requirements and Certification – for Buildings Located in Special Flood Hazard Areas.” Federal Emergency Management Agency (FEMA) and Federal Insurance Administration (FIA), Technical Bulletin 3-93 (FIA-TB-3), https://www.fema.gov/media-library-data/20130726-1511-20490-5294/job6.pdf.

FEMA. (2011) Estimating Loss of Life for Dam Failure Scenarios. Draft version.

Godunov, S.K., 1959. A Difference Scheme for Numerical Solution of Discontinuous Solution of Hydrodynamic Equations. Math. Sbornik, 47, 271–306, transl. US Joint Publ. Res. Service, JPRS 7226, 1969.

Godunov, S.K., Zabrodine, A., Ivanov, A., 1976. Résolution numérique des problèmes multidimensionnels de la dynamique des gaz. Editions MIR de Moscou, 1976.

Harten, A., Lax, P., van Leer, D., 1983. On Upstream Differencing and Godunov-type Methods for Hyperbolic Conservation Laws. SIAM Review 25, pp. 35–61.

Homer, C.G., Dewitz, J.A., Yang, L., Jin, S., Danielson, P., Xian, G., Coulston, J., Herold, N.D., Wickham, J.D., and Megown, K. (2015). Completion of the 2011 National Land Cover Database for the conterminous United States-Representing a decade of land cover change information. Photogrammetric Engineering and Remote Sensing, v. 81, no. 5, p. 345-354.

HSPD-7 (2007). Homeland Security Presidential Directive 7 on “Critical Infrastructure Identification, Prioritization, and Protection”. December 17, 2003.
https://www.energy.gov/sites/prod/files/HSPD-7.pdf

PPD-21 (2013). Presidential Policy Directive 21 on Critical Infrastructure Security and Resilience. February 12, 2013.

https://www.dhs.gov/sites/default/files/publications/PPD-21-Critical-Infrastructure-and-Resilience-508.pdf.

McKee, J.J., Rose, A.N., Bright, E.A., Huynh, T., and Bhaduri, B.L. (2014). Locally adaptive, spatially explicit projection of US population for 2030 and 2050. PNAS, 112(5), 1344-1349. http://www.pnas.org/content/pnas/112/5/1344.full.pdf

McKenzie, B., Koerber, W., Fields, A., Benetsky, M., Rapino, M. 2013. Commuter-Adjusted Population Estimates: ACS 2006-10. A working paper by "A Journey to Work and Migration Statistics Branch" of the USCB published to accompany the USCB's release of the first commuter-adjusted population estimates based on the American Community Survey (ACS). https://www.census.gov/library/working-papers/2013/acs/2013_McKenzie_02.html https://www.census.gov//content/dam/Census/library/working-papers/2013/acs/2013_McKenzie_02.pdf

McKee, J.J., Rose, A.N., Bright, E.A., Huynh, T., and Bhaduri, B.L. (2014). "Locally adaptive, spatially explicit projection of US population for 2030 and 2050." PNAS, 112(5), 1344-1349. http://www.pnas.org/content/pnas/112/5/1344.full.pdf

Moritz, H. 1980. Geodetic Reference System. Bulletin Geodesique, Vol 54:3, 1980 http://geoweb.mit.edu/~tah/12.221_2005/grs80_corr.pdf ftp://athena.fsv.cvut.cz/ZFG/grs80-Moritz.pdf

NIMA (1997). Department of Defense World Geodetic System 1984, Its Definition and Relationships with Local Geodetic Systems. National Imagery and Mapping Agency, NIMA TR 8350.2. Third Ed., July 4, 1997. http://kom.aau.dk/~borre/geodesy/wgs84rpt.pdf

Rapp, Richard H. (1991). "Chapter 3". Geometric Geodesy, Part I. Columbus, OH: Dept. of Geodetic Science and Surveying, Ohio State Univ. https://kb.osu.edu/handle/1811/24333. https://kb.osu.edu/bitstream/handle/1811/24333/Rapp_Geom_Geod_Vol_I.pdf?sequence=1&isAllowed=y.

Robinson, A. H., Morrison, J. L., Muehrcke, P. C., Jon Kimerling, A. and Guptill, S. C. 2002. Elements of Cartography. John Wiley, 2002, 6th edn.

Santini M., Taramelli A. and Sorichetta A. 2010. ASPHAA: A GIS-based algorithm to calculate cell area on a latitude-longitude (geographic) regular grid. Trans. in GIS 14, 351–377 (2010). https://pdfs.semanticscholar.org/e57c/3b3d464ac78af696e3f02c0f8b4d83d94591.pdf

Snyder, J. P. 1987. Map Projections--A Working Manual. U. S. Geological Survey Professional Paper 1395. Washington, DC: U. S. Government Printing Office, p. 13, 1987 https://pubs.usgs.gov/pp/1395/report.pdf

Tobler W.R. and Chen Z. (1986). A quadtree for global information storage. Geographical Analysis 18: 4

Toro, Eleuterio F., 1999. Riemann Solvers and Numerical Methods for Fluid Dynamics. Berlin: Springer Verlag.

Toro, E.F. (2001). Shock-Capturing Methods for Free-Surface Shallow Flows. Wiley and Sons Ltd., Chichester, U.K.

Toro, E.F., Spruce, M., Speares, W. (1992). Restoration of the Contact Surface in the HLL–Riemann Solver, Technical Report CoA–9204, Department of Aerospace Science, College of Aeronautics, Cranfield Institute of Technology, UK.

Toro, E.F., Spruce, M., Speares, W. (1994). Restoration of the contact surface in the HLL-Riemann Solver. Shock Waves, Volume 4, No 1, pp. 25-34.

APPENDIX A: State FIPS Codes and Abbreviations

Table 64 List of (taken from https://www2.census.gov/geo/docs/reference/state.txt)

STATE	STUSAB	STATE_NAME	STATENS
1	AL	Alabama	1779775
2	AK	Alaska	1785533
4	AZ	Arizona	1779777
5	AR	Arkansas	68085
6	CA	California	1779778
8	CO	Colorado	1779779
9	CT	Connecticut	1779780
10	DE	Delaware	1779781
11	DC	District of Columbia	1702382
12	FL	Florida	294478
13	GA	Georgia	1705317
15	HI	Hawaii	1779782
16	ID	Idaho	1779783
17	IL	Illinois	1779784
18	IN	Indiana	448508
19	IA	Iowa	1779785
20	KS	Kansas	481813
21	KY	Kentucky	1779786
22	LA	Louisiana	1629543
23	ME	Maine	1779787
24	MD	Maryland	1714934
25	MA	Massachusetts	606926
26	MI	Michigan	1779789
27	MN	Minnesota	662849
28	MS	Mississippi	1779790
29	MO	Missouri	1779791
30	MT	Montana	767982
31	NE	Nebraska	1779792
32	NV	Nevada	1779793
33	NH	New Hampshire	1779794
34	NJ	New Jersey	1779795
35	NM	New Mexico	897535
36	NY	New York	1779796
37	NC	North Carolina	1027616
38	ND	North Dakota	1779797
39	OH	Ohio	1085497
40	OK	Oklahoma	1102857
41	OR	Oregon	1155107
42	PA	Pennsylvania	1779798
44	RI	Rhode Island	1219835

45	SC	South Carolina	1779799
46	SD	South Dakota	1785534
47	TN	Tennessee	1325873
48	TX	Texas	1779801
49	UT	Utah	1455989
50	VT	Vermont	1779802
51	VA	Virginia	1779803
53	WA	Washington	1779804
54	WV	West Virginia	1779805
55	WI	Wisconsin	1779806
56	WY	Wyoming	1779807
60	AS	American Samoa	1802701
66	GU	Guam	1802705
69	MP	Northern Mariana Islands	1779809
72	PR	Puerto Rico	1779808
74	UM	U.S. Minor Outlying Islands	1878752
78	VI	U.S. Virgin Islands	1802710

Explanations of the columns of the table are as follows:

STATE FIPS (Federal Information Processing Series) code of the state
STUSAB Abbreviation of the state name
STATE-NAME Official name of the state
STATENS Eight digit GNIS (Geographic Names Information System)[25] code of the state

[25] The Geographic Names Information System (GNIS) is a database that contains name and locative information about more than two million physical and cultural features located throughout the United States of America and its territories (https://geonames.usgs.gov/apex/f?p=138:1:0:::::).

APPENXID B: Flood Hazard for People Caught Outdoors

DEFRA (2006) defines flood hazard as conditions in which people are likely to be swept or drown in a flood due to a combination of flood depth, velocity and presence of debris. They state that the results are classified in "hazard classes". A flood hazard map is defined as a map of the location of different hazard classes in the inundation area generated by a specific flood. This document also defines various other concepts:
People vulnerability
Flood vulnerability map
Flood risks to people
Average annual risk
Average annual individual risk
Average annual societal risk
Acceptable risk

The variables for defining flood hazard class of a specific location uses three variables:

1) Flood hazard
    a) Flood characteristics
        i) Depth of flood (m)
        ii) Velocity of flood flow (m/s)
        iii) Debris factor (index value)
2) Area vulnerability
    a) Nature of terrain
        i) Slope of the terrain
        ii) Texture of the terrain (smooth or uneven with potholes, depressions, ditches, obstacles)
        iii) Frictional characteristics of the terrain (slippery or not)
        iv) Presence of buildings
        v) Presence of features to hold on to
3) Environmental factors
    a) Weather
        i) Wind
        ii) Rain
        iii) Temperature
        iv) etc.
    b) Time of the day
        i) Visibility (darkness or light)
4) People vulnerability (ability of people to respond to flood)
    a) Physical characteristics of the individual
        i) Age
        ii) Physical fitness (which may be related to age)
        iii) Height and mass
        iv) Disabilities
    b) Clothing
        i) Clothes
        ii) Shoes
    c) Psychological characteristics of the individual
        i) State of fear and/or panic

ii) Training level and preparedness

In addition, presence of sediments, animals, contaminants in the water may also create additional factors that increase hazard level.

According to DEFRA (2006) the following observations can be made:

1) An average adult is unable to stand in still water with depth of about 1.5 m or greater.
2) For flowing water, the depth at which a person can stand still is much less
   a) For example, some people will be at risk when the water depth is only 0.5m if the velocity is 1m/s (about 2 mph).
   b) If the velocity increases to 2m/s (about 4mph), some people will be unable to stand in a depth of water of only 0.3m.
   c) Most people will be unable to stand when the velocity is 2m/s and the depth is 0.6m.

The flood hazard is defined as

$$FH = D(V + 0.5) + DF \tag{49}$$

Where FH is the flood-hazard index value, D and V are flood flow depth and velocity, and DF is debris factor, which depends on the dominant land use in the area as well as the flow depth and velocity.

Table 65 Debris factor values for different land types and flood velocities (DEFRA 2006).

Criteria based on flood depth and velocity	Dominant land-use type		
	Pasture/Arable	Woodland	Urban
$0 \leq D\ (m) \leq 0.25$	0	0	0
$0.25 \leq D\ (m) \leq 0.75$	0	0.5	1
$D > 0.75\ m$ and/or $V > 2\ m/s$	0.5	1	1

Table 66 Flood hazard classes according to DEFRA (2006).

Hazard Class	FH		Explanation
	From	To	
Class 1	0.75	1.50	Danger for some
Class 2	1.50	2.50	Danger for most
Class 2	2.50	20.00	Danger for all

Table 67 Flood hazard (FH) for $DF = 0$. Colors correspond to flood hazard classes listed in Table 66.

V (m/s)	D (m)									
	0.25	0.50	0.75	1.00	1.25	1.50	1.75	2.00	2.25	2.50
0.00	0.13	0.25	0.38	0.50	0.63	0.75	0.88	1.00	1.13	1.25
0.50	0.25	0.50	0.75	1.00	1.25	1.50	1.75	2.00	2.25	2.50
1.00	0.38	0.75	1.13	1.50	1.88	2.25	2.63	3.00	3.38	3.75
1.50	0.50	1.00	1.50	2.00	2.50	3.00	3.50	4.00	4.50	5.00
2.00	0.63	1.25	1.88	2.50	3.13	3.75	4.38	5.00	5.63	6.25
2.50	0.75	1.50	2.25	3.00	3.75	4.50	5.25	6.00	6.75	7.50
3.00	0.88	1.75	2.63	3.50	4.38	5.25	6.13	7.00	7.88	8.75
3.50	1.00	2.00	3.00	4.00	5.00	6.00	7.00	8.00	9.00	10.00
4.00	1.13	2.25	3.38	4.50	5.63	6.75	7.88	9.00	10.13	11.25
4.50	1.25	2.50	3.75	5.00	6.25	7.50	8.75	10.00	11.25	12.50
5.00	1.38	2.75	4.13	5.50	6.88	8.25	9.63	11.00	12.38	13.75

Numerous deaths occur when people attempt to drive through flood waters. DEFRA (2006) mentions that most cars and vans become unstable in 0.5 m still water and this depth reduces as velocity increases. Even large vehicles, such as fire engines, become unstable in 0.9 m still water.

References for APPENDIX B:

Abt, S.R., Wittler, R.J., Taylor, A., and Love, D.J. (1989). Human Stability in a High Flood Hazard Zone. American Water Resources Association (AWRA). Water Resources Bulletin. Vol 25, No. 4. August, 1989. j.1752-1688.1989.tb05404.x.pdf

DEFRA. (2006). Flood Risks to People: Phase 2. FD2321/TR2 Guidance Document. Defra /Environment Agency Flood and Coastal Defence R&D Programme. Authored by HR Wallingford, Flood Hazard Research Centre, Middlesex University, Risk & Policy Analysts Ltd.

FEMA. (2015). Asessing the Consequences of Dam Failure: a How-To Guide. Document prepared by AECOM. Draft version of September 2015.
AssessingConsequences BOR final edits 6_9_2017-gi.docx

Jonkman, S.N. and Penning-Rowsel, E. 2008. Human Instability in Flood Flows. Journal of the American Water Resources Association (JAWRA) 44(5):1208-1218. DOI: 10.1111/j.1752-1688.2008.00217.x j.1752-1688.2008.00217.x.pdf

Martı´nez-Gomariz, E. and Go´mez, M. 2016. Experimental study of the stability of pedestrians exposed to urban pluvial flooding. Nat Hazards (2016) 82:1259–1278. DOI 10.1007/s11069-016-2242-z. s11069-016-2242-z.pdf

Russo, B., Gomez, M., and Macchione, F. 2013. Pedestrian Hazard Criteria for Flooded Urban Areas. Natural Hazards (2013) 69:251–265. DOI 10.1007/s11069-013-0702-2.s11069-013-0702-2.pdf

Sayers, P. and Meadowcroft, I. . RASP – A Hirerarchy of Risk-Based Methods and their Application. Proceedings of the 40th Defra Flood Control and Coastal management Conference. University of York, UK. July 7-5, 2005.

Wang, Z., Lai, C., Chen X., Yang, B., Zhao, S., and Bai, X. 2015. Flood hazard risk assessment model based on random forest. Journal of Hydrology 527 (2015) 1130–1141.
1-s2.0-S0022169415004217-main.pdf

Wade, S., Ramsbottom, D., Floyd, P., Penning-Rowsel, E. and Surendran, S. 2005. Risks to people: Developing New approaches for Flood Hazard and Vulnerability Mapping. Proceedings of the 40th Defra Flood Control and Coastal management Conference. University of York, UK. July 7-5, 2005.

Xia, J., Falconer, R.A., Lin, Binliang, and Tan G. 2011. Numerical assessment of flood hazard risk to people and vehicles in flash floods. Environmental Modelling & Software 26 (2011) 987-998.
1-s2.0-S1364815211000648-main.pdf

Xia, J., Falconer, R., Wang, Y. and Xiao, X. 2014. New criterion for the stability of a human body in floodwaters, Journal of Hydraulic Research, 52:1, 93-104, DOI: 10.1080/00221686.2013.875073
New criterion for the stability of a human body in floodwaters.pdf
New criterion for the stability of a human body in floodwaters_discussion.pdf

Xia, J., Falconer, R., Guo, P., and Gu, A. 2014. Stability Criterion For A Flooded Human Body Under Various Ground Slopes. Proceedings of the 11th International Conference on Hydroinformatics HIC 2014, New York City, USA.
Stability Criterion For A Flooded Human Body Under Various Ground.pdf

APPENDIX C: Flood Hazard for People Caught Indoors

FEMA (2015) draft document on assessing consequences recommends the following stability thresholds

1. Typical residential structures - depths > 4 ft and/or DV >75 ft2/s
2. Mobile homes - depths > 2 ft and/or DV > 30 ft2/s
3. Persons caught out of doors (tent camping, fishing, hiking, etc.) –
    a. Adults: DV > 6.5 ft2/s and/or depths > 4 ft
    b. Children: DV > 5.4 ft2/s and/or depths > 2 ft
4. Motor vehicle (compact car) floating: depths > 1 ft and DV > 4.3 ft2/s
5. Motor vehicle (compact car) sliding/toppling: DV > 5.4 ft2/2s

Flood depth and velocity relationship for danger level for houses built on foundations (ACER):

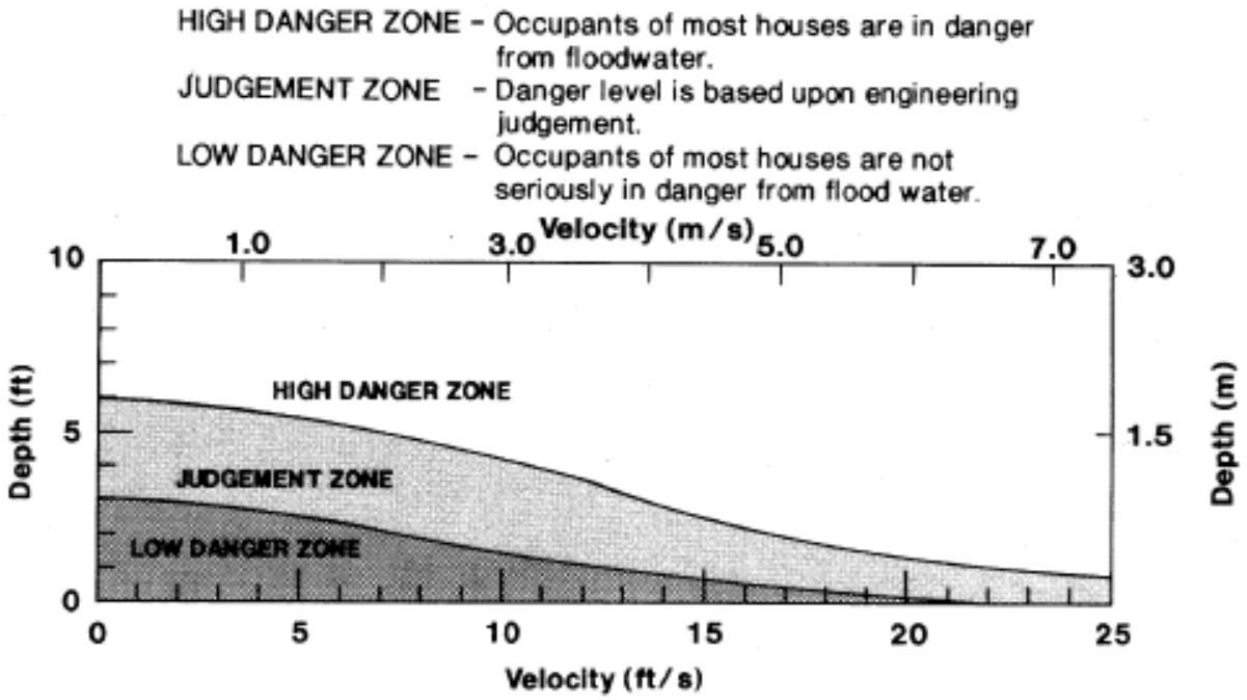

Figure 2. – Depth–velocity flood danger level relationship for houses built on foundations.

For mobile homes

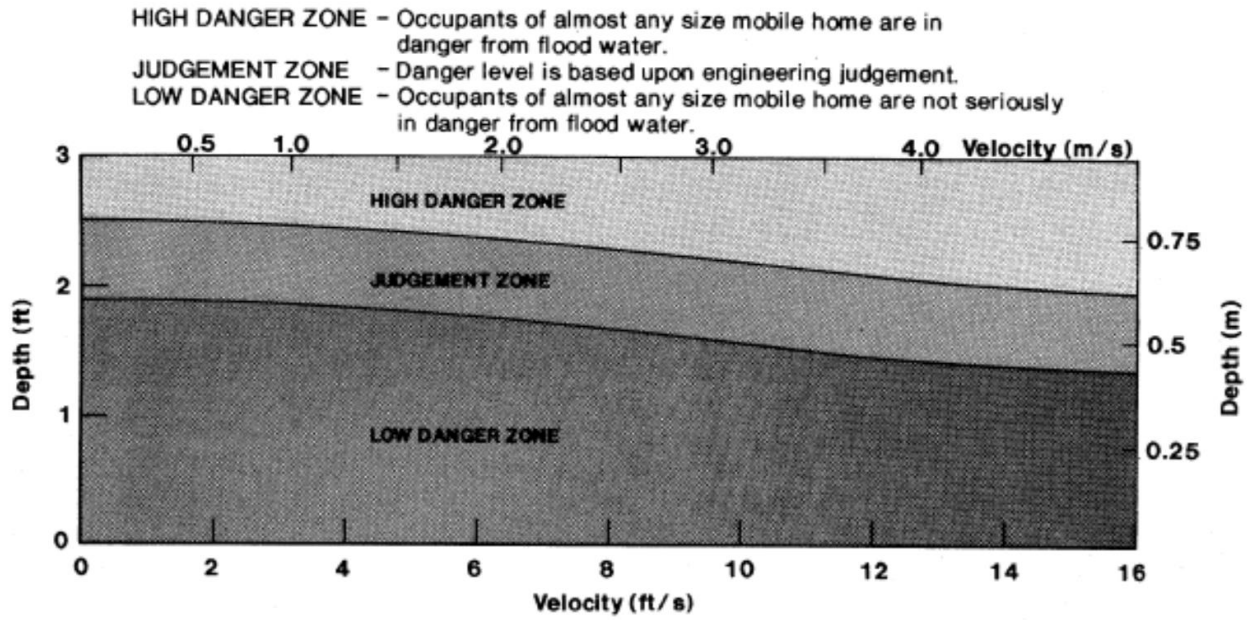

Figure 3. – Depth–velocity flood danger level relationship for mobile homes.

Passenger Vehicles

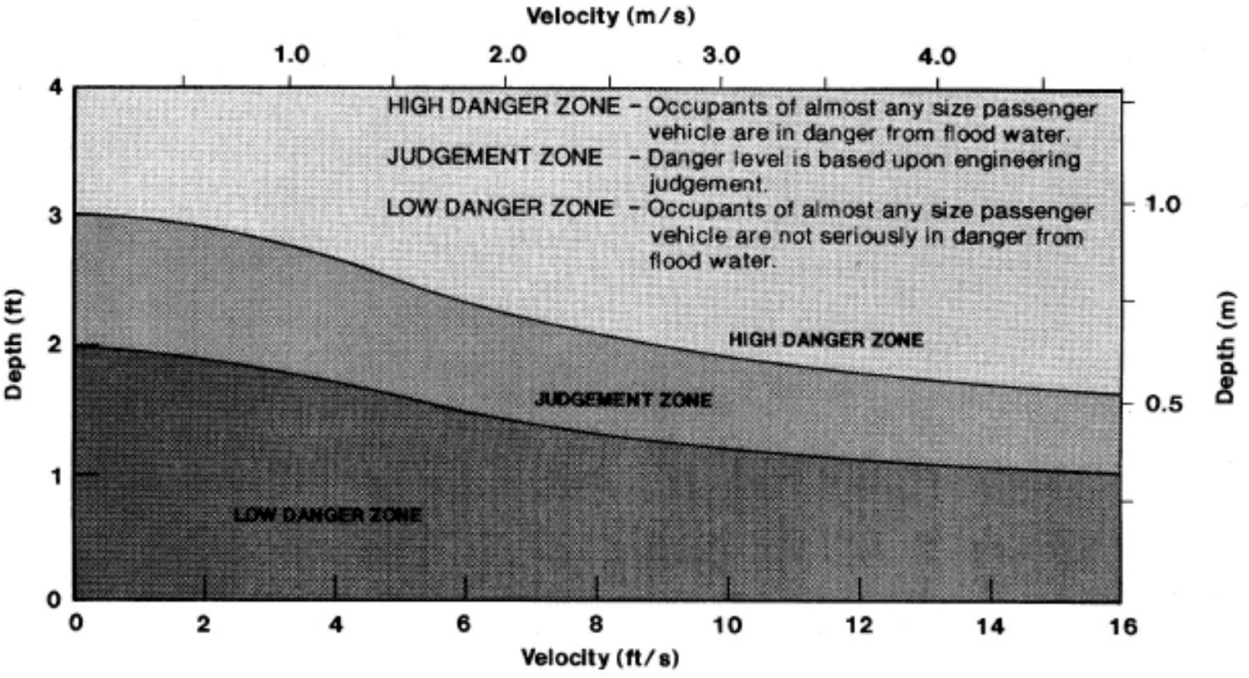

Figure 4. – Depth–velocity flood danger level relationship for passenger vehicles.

For adults

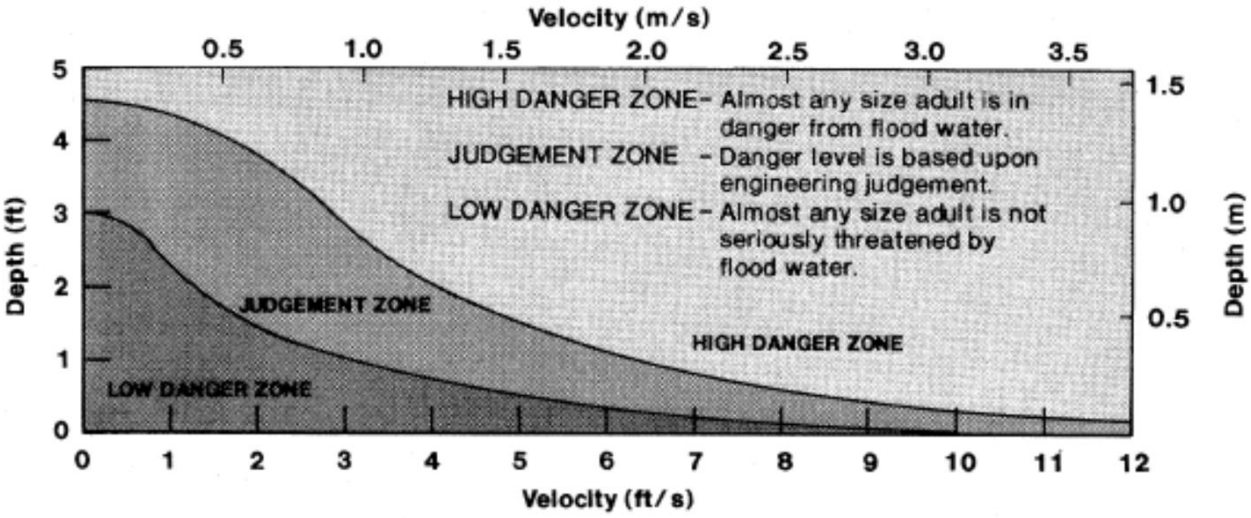

Figure 5. – Depth–velocity flood danger level relationship for adults.

Children

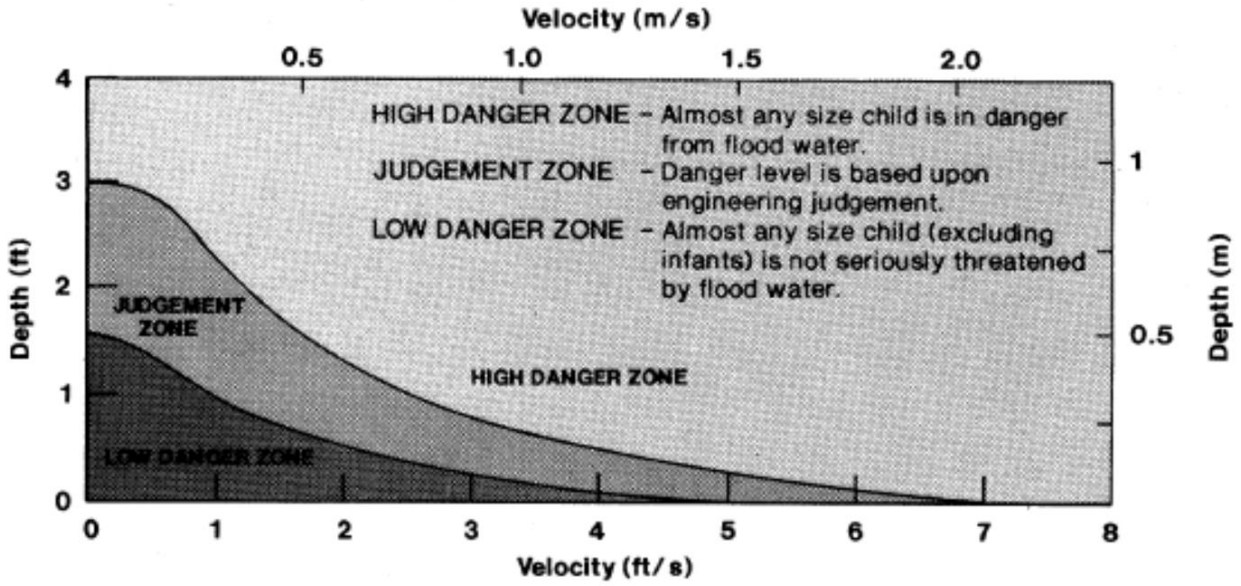

Figure 6. – Depth–velocity flood danger level relationship for children.

References for APPENDIX C

Australian Rainfall and Runoff, Book 9, Chapter 6, Safety Design Criteria, by Grantley Smith and Ron Cox, http://arr.ga.gov.au/arr-guideline/books-and-chapters

BC Hydro Life Safety Model System V 1.0, Guidelines, Procedures, Calibration and Support Manual, Engineering Report E310, August 2006

RESCDAM, Final Report of Helsinki University of Technology, The Use of Physical Models in Dam-Break Flood Analysis, Appendix 2, December 11, 2000

APPENDIX D: Guidelines for Dam-Break Flood Simulation

ACER

For earthen dam

$$B_{avg} = 3\ (HDE - BME) \tag{50}$$

For arch dam

$$B_{avg} = 0.45\ (CL - BL) \tag{51}$$

For concrete gravity dam

$$B_{avg} = 0.375\ (CL - BL) \tag{52}$$

For stone-masonry dam

$$B_{avg} = 0.3\ (CL - BL) \tag{53}$$

For rock-placed dam

$$B_{avg} = 2.5\ (HDE - BME) \tag{54}$$

HDE is the elevation of the crest of the dam or the failure elevation, BME is the final breach invert elevation.

For sunny day simulation, BME is taken as the normal pool elevation

For overtopping dam failure, it is assumed that the dam fails when the water depth on the crest is one foot. Thus, HDE is taken as the crest elevation plus one foot.

http://rivermechanics.net/images/models/SDB%20Input%20Summary020519.pdf

Table 2. Estimation of Breach Parameters
(Dr. Danny Fread's Rule of Thumb Recommendations)

Dam Type	Codes	Rule of Thumb		SMPDBK	
		TFH (hrs)	BW	TFH (min)	BW
Earth	ER	0.1-0.5	2HD-5HD	HD/10	3HD < CL
Concrete Gravity	PG	0.0-0.2	≤ 0.5CL	HD/40	5HD < CL
Concrete Arch	VA	0.0-0.1	≥ 0.8CL	HD/50	0.9CL
Rock Fill	RE			HD/5	4HD < CL
Buttress	CB			HD/40	5HD < CL
Multi-Arch	MV			HD/50	0.9CL
Other	OT			HD/10	CL
Slag Pile		0.0-0.1	≥ 0.8CL	HD/10	Min(CL,10HD)
Concrete	CN			HD/50	0.9CL
Masonry	MS			HD/5	4HD
Stone	ST			HD/5	4HD
Timber Crib	TC			HD/5	CL
TFH = time of failure BW = average rectangular breach width				HD = dam height CL = dam crest length	